

**Measuring Fluorine in Human Bone Using *In vivo* Neutron Activation Analysis
(IVNAA)**

**Measuring Fluorine in Human Bone Using *In vivo* Neutron Activation Analysis
(IVNAA)**

By

Farshad Mostafaei, M.Sc.

A Thesis
Submitted to the School of Graduate Studies
in Partial Fulfilment of the Requirements
for the degree
Doctor of Philosophy

McMaster University

© Copyright by Farshad Mostafaei, December, 2014

DOCTOR OF PHILOSOPHY (2014)
(Medical Physics)

McMaster University
Hamilton, Ontario

**TITLE: MESURING FLUORINE IN HUMAN BONE USING INVIVO NEUTRON
ACTIVATION ANALYSIS (IVNAA)**

AUTHOR: Farshad Mostafaei, M.Sc.

SUPERVISOR: Dr. Fiona E. McNeill

NUMBER OF PAGES: xi, 135

Abstract

The subject of whether fluorine (F) is detrimental to human health has been controversial for many years. Much of the discussion focusses on the known benefits and known detriments to dental care and problems that fluorine causes in bone structure at high doses.

It is therefore desirable to have the means to monitor fluorine concentrations in the human body as a means to directly assess exposure. A monitoring tool could be applied in studies of human health and perhaps answer some of the questions regarding levels at which fluorine has protective effects and negative health consequences. This thesis presents work in the further development of a low risk non-invasive method for the monitoring of fluorine in human bone. The work was based on the technique of neutron activation analysis (NAA). Fluorine accumulates in bone as a long term storage site following exposure. In this thesis, the McMaster Tandem accelerator was used to produce neutrons through the ${}^7\text{Li}(p,n){}^7\text{Be}$ reaction, measuring F levels in the human hand bone using IVNAA. The gamma rays emitted through the ${}^{19}\text{F}(n,\gamma){}^{20}\text{F}$ reaction are measured using nine NaI(Tl) detectors with 4π geometry.

Four published papers are presented in this thesis. The main outcome of the first publication was the development of a new phantom. This was needed to reduce the aluminum contamination. The main outcome of the second publication was a series of improvements to the method for the *in vivo* measurement of bone fluorine using NAA of the new phantoms. In the third publication the best hand position and neutron flux map in the irradiation cavity were determined through both Monte Carlo simulation (FLUKA) and experimental methods. Finally, the fourth publication describes the utility of the improved technique in a pilot study of environmentally exposed people.

The overall conclusion from this thesis work is that a low risk monitoring tool, based on an NAA technique, has been developed which is capable of monitoring fluorine in urban Canadians. The technique can now be applied in studies of human health.

Acknowledgments

My supervisor

I would like to express my sincere gratitude to Dr. Fiona McNeill for the continuous support throughout the process of my PhD research, for her motivation, enthusiasm, and immense knowledge.

My supervisory committee

Dr. David Chettle, Dr. Bill Prestwich and Dr. Soo-Hyun Byun provided invaluable advice on statistics and data analysis, and who always thoroughly evaluated my work.

Yasaman

I could not have finished this project without your kindnesses, support and patience. With your encouraging care and love this process was much easier.

My parents

I am sure that without all your prayers I could not have achieved anything. I am very grateful for having such wonderful support in all stages of my life.

Friends

I appreciate your continuous support and care in all that was involved in my project.

Contents

Acknowledgment	iii
1 Introduction	1
1.1 Fluorine	1
1.1.1 Sources of fluoride	5
1.1.2 Fluoride in humans	11
1.1.3 Consequences of fluoride exposure	15
1.1.4 Fluorine measurements	21
1.2 Neutron activation analysis	23
1.3 Irradiation facility	26
1.4 Detection system.....	28
1.5 Fluorine phantom	30
Thesis outline	32
2 Design of a phantom equivalent to measure bone-fluorine in a human's hand via delayed neutron activation analysis (Article I)	34
2.1 Introduction to Article I	34
2.2 Contents of Article I.....	34

3 Improvements in an <i>in vivo</i> neutron activation analysis (NAA) method for the measurement of fluorine in human bone (Article II)	45
.....	
3.1 Introduction to Article II.....	45
3.2 Contents of Article II.....	45
4 An investigation of the neutron flux in bone-fluorine phantoms comparing accelerator based <i>in vivo</i> neutron activation analysis and FLUKA simulation data (Article III)	59
.....	
4.1 Introduction to Article III.....	59
4.2 Contents of Article III.....	59
5 Measuring fluorine in human bone using <i>in vivo</i> and <i>ex vivo</i> neutron activation analysis (Article IV)	69
.....	
5.1 Introduction to Article IV	69
5.2 Contents of Article IV.....	69
5.1 Abstarct.....	70
5.2 Introduction.....	72
5.3 Matherials and Method	74

5.3.1 In vivo measurements	74
5.4 Ex vivo measurements	80
5.5 Results.....	81
5.6 Discussion	102
5.7 Conclusion	105
5.8 Acknowledgments	106
5.9 References.....	107
6 Coclusions and Future work.....	111
6.1 Thesis conclusions	111
6.1.1 Development of a new Bone-Fluorine phantom.....	111
6.1.2 Improvements in the IVNAA Method for Measurement of Fluoride.....	113
6.1.3 Monte Carlo Modelling of the Bone Fluoride System.....	114
6.1.4 Measurements of Fluoride in Bone in Urban Canadians: a Study of Volunteers from the City of Hamilton	116
6.2 Future work.....	120
6.2.1 Transfer times.....	120
6.2.2 Future <i>in vivo</i> studies	121
References.....	125

List of Figures

Figure 1.1 Dental and skeletal fluorosis	19
Figure 1.2 Fluorine phantom spectrum.....	25
Figure 1.3 Layout of irradiation cavity.....	27
Figure 1.4 Tandatron accelerator at the McMaster Accelerator Labs (MAL).....	27
Figure 1.5 Irradiation cavity	28
Figure 1.6 The detection system at MAL	29
Figure 1.7 Nine NaI(Tl) digram withtheir high voltage unit number	29
Figure 1.8 Fluorine calibration line	32
Figure 5.1 a) Experiment layout during the previously published phantom study, b) Experiment layout during this <i>in vivo</i> study	75
Figure 5.2 A volunteer photographed while being irradiated during a fluorine measurement	75
Figure 5.3 Comparison of the first five second and the 300 second spectrum from a fluoride-doped phantom.....	77
Figure 5.4 Frequency distribution of the precisions observed in 2008 and 2013	82
Figure 5.5 Background differences, old and new location	84

Figure 5.6 Fluoride concentration with age measured in the human hand from 35 participants.....	89
Figure 5.7 Comparison of the 2013 and 2008 data.....	90
Figure 5.8 The 2013 data for a) men and b) women.....	91
Figure 5.9 Fluoride versus age for women and men using the combined 2013 and 2008 data.....	93
Figure 5.10 Bone fluorine content versus age in women (for the 2008 and 2013 data combined) with women age less than 50 years, and age 50 and older	94
Figure 5.11 Comparison of bone-fluorine concentration in tea-drinkers, and non-tea-drinkers	96
Figure 5.12 Comparison of tea drinkers and non-tea drinkers with data from 2008 and 2013 combined.....	97
Figure 5.13 Comparison between 2008 & 2013 fluorine measurements.....	99
Figure 5.14 Phantom calibration line.....	100
Figure 5.15 Fluorine concentration with age measured in the twelve bone biopsy samples.....	101
Figure 5.16 A comparison of <i>in vivo</i> and <i>ex vivo</i> measurement data	101
Figure 6.1 The detection system best position beside the irradiation cavity	115
Figure 6.2 Volunteer's hand irradiation at MAL for IVNAA measurements	119

List of Tables

Table 1.1 Summary of fluorine measurements	22
Table 5.1 Mean and median <i>in vivo</i> precisions.....	81
Table 5.2 The precisions for phantoms measured with the detection system in the beam hall beside the irradiation cavity and in the control room area.....	85
Table 5.3 The precision data of mean and median transfer times	86
Table 5.4 Comparison of different bone-fluoride published studies	104
Table 6.1 Measured levels of fluoride in tea as reported by researchers from different countries.....	118

1. Introduction

1.1. Fluorine

The naturally occurring widely distributed element and the thirteenth most common element in the earth's crust is fluorine. It is considered the most reactive element in the halogen family (Glock et al., 1941). It is found in rocks, clay, coal, water and air, and substitutes for hydrogen in inorganic salts and organic compounds. Examples found in nature include the combination of fluorine with other rock-forming minerals to form fluorspar or fluorite (CaF_2); rock phosphates (e.g. fluorapatite: $(\text{Ca}_5(\text{PO}_4)_3\text{F})$); cryolite (Na_3AlF_6); micas and hornblende (WHO 2006; Edmunds et al., 2005).

The concentrations of fluorine observed in soil range between 20-1000 mg kg^{-1} . The levels can vary based on the characteristics of the environment. For instance, the concentration can be higher in mineralized areas, or in regions that use fertilizers, or areas with volcanic and industrial emissions. High fluoride environments occur in many areas of the globe and are directly associated with marine sediments, volcanic, gneissic and granite rocks. These areas include the Mediterranean; southern Europe and Russia, the Middle East, the East African Rift from Jordan to Tanzania, West and southern Africa, India, Pakistan, Thailand, China and the southern USA (WHO 2006; Edmunds et al., 2005).

These higher concentrations of fluorine that are found in natural resources can become highly poisonous and hazardous to people and the environment (Chachra et al., 2008; Yildiz et al., 2003). Fluoride is not distributed uniformly in the environment, the presence

of fluoride minerals and geogenic processes can influence its formation. The solubility of the mineral fluorite (CaF_2) limits the concentration of F^- element in water. Therefore high-fluoride waters are commonly associated with calcium-poor conditions and where substitution of calcium by sodium occurs. High pH thermal waters also tend to be rich in the element. Based on the rock that water flows through therefore, the fluorine concentration can vary in groundwater. This variation generally does not exceed 10 mg/L in North America (Sastri et al., 2001; EPA, 1985). In addition, concentrations in surface water (< 0.5 mg/L) and seawater (1.2-1.5 mg/L) tend to be lower than those in groundwater (1-10 mg/L) due to longer residence times for rock-water interactions. However, in the volcanic regions of East Africa, depending on local conditions, values of 2800 mg/L can be found in sodic lakes and 50 mg/L in groundwater indicate concentrations of fluorine in water are highly variable. Fluoride can therefore be a major cause of morbidity in Africa and the Far East, where concentrations of fluorine in drinking water (sourced from groundwater) can exceed 10 mg/L (Saleh et al., 2001). In the groundwater of many villages in China the fluorine concentrations are greater than 8 mg/L (Drinking Water Atlas of China, 1990).

As a result of exposure to high-fluoride drinking waters, human dental and skeletal fluorosis affects millions of people in many of these areas (WHO 2006; Edmunds et al., 2005).

Several studies have demonstrated that fluorine in certain amounts (0.5-1.5 mg F/L) can be useful for dental care (preventing tooth decay) and bone formation (Bryson 2004). At the same time, studies also demonstrate individuals who have been exposed to higher levels of fluoride through drinking water, food and air for a certain time period suffered from dental and skeletal fluorosis (Ando et al., 1998 ; Dinman et al 1976). The risk-benefit of fluoride is therefore highly dependent on exposure level.

Large numbers of people around the world are adversely affected by fluoride exposure. For example, among the twenty six districts of the west coast of India, twenty four are reported to have high fluorine content in their water sources (Susheela 2007). Over all, due to high water-borne fluoride over 66 million individuals in India are estimated to be at high risk for fluorosis (Vasant et al., 2013).

The harmful health effects of fluoride such as black teeth and eroded dental enamel were noted as early as the late 1800s and early 1900s in populations in Mexico, Italy and the USA. Studies done by Smith et al. in the 1930s established fluoride in drinking water as a cause of dental fluorosis. Based on estimates 1.7 million people in China and 1 million people in India suffer from fluorosis (WHO, 2006). Dental fluorosis has since been reported from all around the globe and latest estimates suggest that it may affect 70 million people in the future (WHO, 2006).

As a result of industrial process fluorine concentrations fluctuate (0.2-1.3 mg/L) in Meuse, (Slooff, 1988;Wright et al., 2013). The fluorine levels in drinking water in

Canada are generally low compared to levels worldwide. They have been reported to be in the range 0.05-0.2 mg/L for non-fluoridated water supplies and in the range 0.6-1.1 mg/L for fluoridated water systems (Health Canada, 2010). Some areas of the world have very low levels of fluorine, for example, in the Netherlands, levels are below 0.2 mg/L (Whelton et al., 2004). Also, in Finland, the fluorine concentrations in drinking water are generally low (<0.1mg/liter) (Kurttio et al., 1999). However, because of high fluorine concentrations in soil and bedrock in the southern parts of the country, some fluorine concentrations in Finland exceed the drinking water quality guideline value of 1.5 mg/liter (Kurttio et al., 1999). Since houses are not connected to municipal drinking water supply systems fluorine concentrations in drinking water are especially high in rural areas (Burt, 2002). This example shows that because fluorine levels in water are so dependent on geology and thus geography that countries have to be careful in interpreting data and basing risk estimates on average drinking water exposures.

Early epidemiological investigations were performed by Dean during the 1930s and 1940s and confirmed a relationship between dental fluorosis and increasing fluorine content in USA's drinking water (Kaminsky et al., 1990). However, this study also confirmed an association, and thus interpreted beneficial consequence of fluoride, in the prevention of dental caries. The number of decayed or missing teeth was reduced in areas with fluorine in the water. As a result of Dean's study, fluoridation programs have been implemented in many countries in the world. Based on the estimations performed in the census conducted in 1985, 121 million Americans receive supplementary fluoride via public water supplies (Fluoridation Census, 1988; Kaminsky et al., 1990).

Many individuals around the globe are familiar with fluoride as an ingredient of dental-care products. Today water fluoridation programs are often questioned. While it improves oral hygiene in many parts of the world, at the same time some concerns remain in lay populations about the potential harmful impacts of the element. People exposed to high fluorine intakes can have health consequences (which will be discussed further later in this chapter). Since the relationship between fluoride exposure and health is non-linear, and in fact potentially U-shaped, it becomes important to have knowledge about the different sources of fluoride to which individuals can be exposed in order to build a complete picture of the potential for harm.

1.1.1. Sources of fluoride

Even though fluorine has had a major role in caries prevention over the past five decades, ingestion of too much fluoride means people can develop dental fluorosis (Wright et al., 2013). This is not completely uncommon, even in North America, where people are exposed via a number of routes. Sources of fluoride include, but are not limited to, fluoridated toothpaste, fluoridated mouthwash, marine products, tea and drinking water (Johnson et al 2007; Yadav et al 2007; Kurland et al 2007). Overall, the main sources of fluoride exposure in Canada include, food, beverages, water and many dental products. Of these, water and dental products are considered the major sources for fluoride

exposure for Canadians. For example, toothpastes generally contain high levels of fluorine. In fact, it is hard to find non-fluoridated toothpastes in most grocery store aisles. The foam from toothpastes is likely to be swallowed by consumers (Health Canada, 2010). There are some known reports of fluoridosis resulting from toothpaste ingestion (Levy et al., 2006).

Another source that could have significant amounts of fluorine concentration is water: in 2005, fluoridated drinking water was provided for 43% of Canadians. Generally, the municipal water in North America contains about 1 ppm (1 mg/L) fluorine. On average each adult consumes approximately 1.5 L of water per day. Also, only 0.2% of the American population is exposed to more than 2.0 mg/L (EPA, 1985) other than water, fluorine is found in a lesser amount of concentrations in Canadian atmosphere and soil. Surveys conducted in the late 1980s demonstrated that the mean concentration of fluorine in non-fluoridate drinking water was $<50 \mu\text{g/L}$ (Health Canada, 2009).

Among all provinces in Canada, Ontario, Alberta and Manitoba indicate a percentage of 76%, 75%, and 70% of fluoridated drinking water for people (compare to the 43% average), this is the highest concentration of fluoridated drinking water in Canada (Health Canada, 2009).

Some European countries have decided to deliver fluoride at an optimal level for dental health, in many forms, to their residents. This includes fluoridation of water, toothpaste, salt and milk. For example, in addition to consuming fluoride through water the school

system provides fluoridated milk to about 20,000 children in the UK (Burt, 1985). Most commonly, however, active fluoridation programs focus on drinking water. It should be noted that fluoridation of the water supply is not universal as some areas, e.g., in France, Mouscron in Belgium and Hartlepool in the UK, already have naturally optimally fluoridated water supplies (0.7-1.5 ppm F). However, in areas of low naturally occurring fluoride, governments provide supplementary fluoride and this includes other areas of Europe such as Spain, Switzerland and many parts of the UK. In those areas they are currently operating water fluoridation schemes (Whelton et al., 2004; Health Canada, 2010).

There are many by-laws mandating water fluoridation in Europe. In Ireland about 74% of population consumes fluoridated water (0.8-1.0 ppm F) from a program starting in 1964 (Brown, 2000). In 1986 the fluoridation of water in Spain meant that more than 3.3 million people (Kiritsy, 1996) received added fluoride in drinking water. In 1985, the UK made an assessment and decided to provide fluoridated water to 10% of the population (Vargas, 1998).

However, fluoridation of the water supply is controversial. In Holland water fluoridation began in 1953 and ended in 1973. This was due to perceived problems with the legislation and anti-fluoridation campaign activities (Kaplan, 1996). The natural level of fluorine in the Netherlands is low, so the average level in drinking water for Netherlands population is below 0.2 mg/L (Slooff, 1988).

The concerns about fluoridation include, in part, concerns about the potential for over-exposure. Even research performed as early as in the 1930s, 1950s and 1960s revealed the fact that 7-16% of children who were exposed to fluoride illustrate mild fluorosis in their permanent dentition (Burt, 2002). Surveys performed in 1984 for Children's Dental Health in Ireland revealed the fact that fluoridated areas showed a questionable or concerning level of fluorosis in children: 5% of 8-year-olds and 4% of 15-year-olds (Burt, 2002).

Kenya is considered the African country with the highest level of naturally occurring fluoride in ground water. This is based on samples which showed that twelve out of seventeen groundwater systems in the Kisumu area were proven to have fluorine levels greater than 1.1 mg/L (Nair et al. 1984). (The sea water in Egypt has been reported to have a concentration of 1.3 mg/L fluorine (Slooff, 1988), but our interest here is in drinking water supplies). Fluorine levels are found to be up to 3.3 mg/L in drinking water extracted from well water in Kenya. The fluorine levels in well water can reach levels up to 8 mg/L in the next-door country of Tanzania, since the soil contains fluoride minerals (EPA, 1985).

Tea is known to be a significant source of fluoride exposure. Due to its comforting and calming effect, tea has been enjoyed around the globe for centuries. On the basis of several studies, tea is considered the second most consumed drink amongst the people of the world (Duckworth et al., 1978). When it is consumed regularly, it can lead to an excess exposure to fluoride, which eventually can cause negative health effects. Tea

contains up to 4.97 $\mu\text{g/g}$ of fluorine, it is known as the highest concentration of fluorine in food (Health Canada 2010). Raw tea leaves can contain fluorine levels up to 400 mg/kg (Duckworth et al., 1978). Generally, tea itself can contain fluorine levels in a range from 0.1 to 4.2 mg/L. This level can increase to 3 mg/L when brewed with deionized water (Duckworth et al., 1978). The most common way of consuming tea is brewing tea leaves, but it is marketed in three different ways: tea leaves, tea bags and tea beverages. The tea marketed in Taiwan has been shown to contain high levels of fluorine: 7.04, 7.79, 5.37, and 25.7 mg/ L. The mean concentration of fluorine in black tea is known to be 1.97– 8.64 mg/L. Among all types of tea, packaged tea, specifically black tea, had the highest fluorine concentrations (Lung et al., 2003). Brewing tea in different containers such as glass or pottery does not affect the fluorine intake concentrations (Lung et al., 2003).

Other studies performed in Taiwan demonstrate that consuming high amounts (≥ 5 L/week) of tea can result in excessive exposure to fluoride causing dental or skeletal fluorosis (Lung et al., 2003). The conclusion of this study notes that fluoride intake can be reduced when individuals select teas with curved leaves, rinsing the tea leaves before making tea, and drinking black tea without adding sugar (Lung et al., 2008). Several case reports demonstrate the negative effect fluorine can have on skeletal health when tea is consumed regularly and excessively. For example, a 40-year-old woman who consumed a daily average of 4.2 mg/day fluorine from tea developed skeletal fluorosis (Fisher et al.,

1981). In another case, a 52-year old woman who regularly drank 4–8 L/week of double-strength instant tea was reported to develop skeletal fluorosis (Whyte et al., 2005).

In addition to tea, bottled waters can also contain fluorine in significant concentrations. Usually bottled water contains less than 0.3 mg F/L, but in some cases, some imported mineral water can contain higher levels of fluorine (Flaitz et al., 1989; Levy, 1994; Tate and Chan, 1994; Van Winkle et al., 1995). For instance, a series of studies done in Iowa in the early 1990`s on 78 bottles revealed the fact that 83% contained <0.3 mg/L, 7% contained 0.3–0.7 mg/L, 1% contained 0.71–1.00 mg/L, and 9% contained >1 mg/L (Van Winkle et al., 1995). So, roughly one in ten bottled waters had fluorine concentrations higher than fluoridated tap water.

Finally, fluoride can be used in various industrial methods and processes. It is used, for example, for pipe linings, cable installation, refrigerants and in polymers used in plastic. Fluoride can be used as a separation element to produce uranium, beryllium and aluminum isotopes (Kaminsky et al., 1990) . The elemental form of fluoride, which is an irritating gas with a sharp odor, is so chemically reactive that it rarely occurs naturally in the elemental state. It has the ability to react with most substances, and when combined with metals it produces fluoride and forms hydrofluoric acid when combined with water. Although fluoride can be useful in many industrial applications, it can be a source of occupational exposure risk. For example, fluoride is used in the aluminum smelting

process, during which it releases fluoride-containing vapors, a hazardous gas which workers may inhale (Dinman et al 1976).

Fluoride can be consumed in different dosages through different sources by each individual. It is important to know what happens to fluoride when it is absorbed by the body.

1.1.2. Fluorine in humans

It has been believed for a long time that fluoridated drinking water has a positive effect on dental caries (Limeback, 1999). Based on this assumption, there have been recommendations made to add fluorine supplements in approximate level of 1 mg/L (1 mg fluoride ion per liter of drinking water) to drinking water. Adults consume 2-3 liters per day, so consume 2–3 mg F from drinking water per day. In addition, individuals over the age of twelve roughly ingest 0.4 mg of fluoride from food per day (Burt, 1992). This comes from food cooked in fluoridated water and also from uptake of fluoride in plants and animals (Burt, 1992).

In 2010, water fluoridation was considered to be among the ten major achievements of 20th century by the Centers for Disease Control and Prevention (Burt, 2002). This was considered in first world nations such as USA, Britain, Australia, New Zealand and World Health Organization (WHO 2003).

Most individuals consume some fluoride from oral care products. Children are most likely to swallow tooth paste while brushing their teeth (Simard et al., 1989). Generally, when brushing teeth the average person uses 1g of toothpaste, and it is suggested that adults ingest 25% of that (Whitford 1994). Overall, in North America toothpastes contain approximately 1000 to 1100 ppm fluorine, so that means that by this estimate, every person ingests 0.25 to 0.75 mg/day of fluorine from dental products (Whitford 1994).

North American adults, in total, take in 1.2 to 2.2 mg F/day from all sources (food, beverages, toothpaste) in addition to fluoridated water (Whitford 1994). The fluorine ingested is absorbed in the body, in some cases this takes place in the mouth but the majority of the time this occurs by diffusion, mainly in the stomach and the small intestine (Whitford, 1989). Studies suggest that half of ingested fluoride is absorbed within thirty minutes. The plasma peak concentration is therefore reached in the first hour (Phipps, 1996). Overall, 90% of the consumed fluorine is retained in the body and the remaining 10% is discharged through the feces.

When fluorine reaches the stomach, half of the amount is absorbed and linked to tissue and the other half continues through the body (Ludlow et al 2007; Spencer et al 1970). Based on the strong bonding characteristics of fluorine to tissue, over time, and with aging, fluorine accumulates in the body (Parkins *et al* 1974). Many studies prove a direct relationship between the concentration of fluorine in the bone and age (Alhava 1980; Charen et al 1979; Eble et al 1992; Richards et al 1994; Torra et al 1998).

Fluorine is tightly bound and stored in the skeleton because it displaces the hydroxide (OH^-) functional group in the hydroxyapatite matrix in the bone (Whitford 1994). Also, studies demonstrate that the typical bone fluorine concentration in people is in a linear relationship with water concentration (Turner et al 1995; Zipkin et al 1960). Therefore, bone is a perfect location in the human body to measure fluorine. It accumulates over time in bone and since 99% of the fluorine mass is linked with calcified tissues, concentrations are expected to be highest in bone (Whitford 1994).

Based on studies by Trautner and Einwag, when fluorine is co-absorbed with food, levels of peak plasma can be reduced. For example, milk can reduce fluorine's bioavailability by 30% (Trautner & Einwag, 1989). Studies performed by Shulman et al. to calculate the effects of milk and solid foods on fluorine absorption in humans also show interesting results: they determined that milk has the ability to reduce fluorine absorption by 13%, while the presence of food reduced the absorption by 47% (Shulman et al., 1990). Research by Yadav et al. demonstrates that the bioavailability of fluorine can vary from different food sources anywhere from 2-7% (Yadav et al., 2007). In different studies, there have been different explanations as to why dietary sources can reduce the bioavailability of fluoride (Rao, 1984). It is suggested that the absorption of fluorine can be influenced based on the water solubility of fluoride compounds. For example, sodium fluoride is absorbed faster than the less soluble calcium fluoride (CaF_2) and disodium monofluorophosphate (McIvor, 1990; IPCS, 2002). In addition, the fluoride compounds that are found naturally in water produce fluoride ions that will be absorbed fully by the gastrointestinal tract.

Fluoride in drinking water is thus generally considered fully bioavailable (IPCS, 2002). In order to investigate the difference between the bioavailability of fluoride in naturally fluoridated water and in artificially fluoridated water a study was performed. This study in particular was designed to determine the effect of water hardness on the bioavailability of fluoride in drinking water. The conclusions of this study demonstrate that there was no major difference between the absorption of fluoride consumed from fluoridated drinking water and natural drinking water. There was also no difference found among the absorption of fluorine from hard and soft waters, at fluorine concentrations close to 1 mg/L (Maguire et al., 2004).

Within the first 24 hours of fluoride ingestion, about 50–75% of the oral dose appears in human adult urine (Spencer et al., 1970, 1981; Ekstrand et al., 1977). In a study performed by Haftenberger et al. the proportion of fluoride discharged in preschool children (3–6 years old) urine was examined (Haftenberger et al., 2001). The results showed that 51.5% of the fluoride ingested was excreted in the urine, and that the total daily fluoride intake excreted in the urine was measured to be an average of 35.5% (Villa et al., 2000). In other studies, of young children, a much higher value of 80% excretion of ingested fluoride was found in the first 24 hours after ingestion in 4-year-old children (Zohouri et al., 2000). This may suggest different retention/metabolism characterises in adults and children.

The excess fluorine not absorbed by the skeleton is discharged into the urine by the kidneys. As a result, individuals who experience reduced renal function are at a greater risk to develop skeletal fluorosis (Boivin et al., 1986). In most cases, fluorine returns

from tissue to the circulatory system more slowly, resulting in calcified tissues (Phipps et al., 1996). As a result, in many cases the half-life of fluorine in bone has been estimated to be 8 to 9 years (Hodge et al., 1963). As the bone fluorine levels increase to 4500 ppm in the mineral phase, the bone strength decreases (Turner et al., 1993), and if calcium intake is 'normal', the bone strength can decrease by 13% when the fluorine content in the mineral phase reaches 10,000 ppm (Turner et al., 1993). In some cases bone strength has been found to decrease by 45% when fluorine intake is connected to calcium deficiency (Turner et al., 1993). Excess dosage and accumulation of fluoride is therefore potentially detrimental, especially when concurrent with disease or malnourishment, and requires further investigation to be properly understood.

1.1.3. Consequences of fluoride exposure

Fluoride can cause different effects in the body based on the amount ingested. It has an apparently useful effect at low dosages. When the dosage of fluoride is approximately 1ppm it can have a positive preventative quality in terms of controlling dental caries (Boivin et al 1989; Khandare et al 2005). This level of dosing is that usually performed on municipally fluoridated water supplies. Studies performed on six different groups of individuals in China have demonstrated that when the fluorine concentration of their drinking water is in the dosage range 0.25 to 7.79 ppm, it can have a protective effect on bone fracture risk (Li et al 2001, Vestergaard et al 2008).

At the next level of dosage, fluoride has the ability to modify the tissue structure, altering the interface between the collagen and mineral. This was thought to be helpful for osteoporosis treatment. Studies suggest, however, that when, osteoporosis is ‘treated’ with sodium fluoride, the risk of hip fracture increases after sodium fluoride therapy (Inkovaara et al., 1975; Mamell et al., 1988; Hedlund et al., 1989; Riggs et al., 1990). An increase in bone fragility can be a direct result of the increase in bone mass caused by fluoride. This was an important finding. Raising the risk of hip fracture can be dangerous. Hip fractures are known to be a major cause of morbidity, disability, and mortality in the elderly (Lindsay 1990).

It is known that fluoride can create damage to the body when it is ingested excessively and in high dosages. It has the ability to weaken the skeleton and discolor teeth, eventually increasing wear of the enamel. These levels of fluorine toxicity are usually seen in communities where the local drinking water has naturally high fluorine levels (Burt, 2002).

Excess levels of fluorine have the ability to increase the risk of dental skeletal fluorosis and brown mottling of teeth. It is also likely these high levels will create skeletal fluorosis (Shashi et al., 2008; Wilson 1993). Christiani & Gautier first used the term fluorosis (fluorine toxicity) in 1925. Fluorosis is a disease commonly related to high fluoride intakes from drinking water, tea, and inhalation from coal-based fuels which causes bone deformities. Skeletal fluorosis increases bone density, which ultimately creates skeletal deformity and fractures. The cause of skeletal fluorosis is because of fluorine's long retention half-life in bone and thus the tendency to build up over time. Skeletal and bone

fluorosis is a disabling condition that causes harsh pain for the patient (Shashi et al., 2008; Wilson 1993).

Fluorine toxicity can cause osteosclerosis, osteopenia and/or osteomalacia in an individual's bone mass (Tamer et al 2007; Wang et al 2007). This fluorine toxicity can also cause a thyroid hormone imbalance in children (Susheela et al 2005), and in addition it results in joint aches, deformation, calcification of ligaments and impairment in range of motion (Shashi et al., 2008; Wilson 1993)

It has been shown that regular intake of 14 mg fluorine per day will cause bone fractures, and overall the risk of bone effects increase when fluorine intake per day is over 6 mg (Fawell, 2003; Kurttio et al., 1999; Sampaio et al., 1999). Fluorine toxicity can become apparent in any age. Other than being fatal, it may result in physical and economic disability in and thus hardship for individuals.

The risk of fluorine toxicity can increase due to various factors. This may include drinking water and the individual's nutritional status (Fawell, 2003). Fluorosis is more common in areas such as China and India which have higher fluorine concentrations in their water (Boivin et al 1989; Khandare et al 2005). In the 1930s, human skeletal fluorosis was reported in France and Denmark, the cause was directly related to mineral processing and cryolite (Na_3AlF_6) mines exposure. In the late 1930s, skeletal fluorosis was identified as a widespread disease in India, Africa, and China and many parts of the globe in individuals who consumed drinking water with fluorine concentrations in the range of 3 to >20 mg/L (Krishnamachari, 1987; Kaminsky et al., 1990; Ad Hoc

Subcommittee on Fluoride, 1991; Wang et al., 1999; Shivashankara et al., 2000; IPCS, 2002; Boivin et al 1989; Khandare et al 2005). The concentration of fluorine in drinking water is known to be anywhere from 7-14 ppm in these areas. A study in Brazil on 650 children aged 6-11 years old showed low (below 0.7 ppm F), medium (between 0.7-1.0 ppm F) and high (above 1.0 ppm F) dental fluorosis in 30.5, 61.1 and 71.4% of the children respectively (Sampaio et al., 1999).

In addition to effects on bones and teeth, severe consumption of fluoride can cause abdominal pain, diarrhoea, fatigue, drowsiness, coma, cardiac arrest, and eventually be fatal for humans (Kaminsky et al., 1990; Whitford, 1990; Augenstein et al., 1991; ATSDR, 2003). It has been shown that when the more soluble fluoride salts (e.g., sodium fluoride) are ingested, the effects can be harsher (WHO, 1984). This was seen in an incident when seven elementary students drank water with a fluorine concentration of 92 mg/L. They experienced severe nausea and vomiting (Sidhu et al., 2002). A minimum of 5 mg F/kg body weight can lead to extremely harmful health issues (Whitford, 1996).



Figure 1.1. Dental and skeletal fluorosis (Fordyce et al. 2007; Shashi 1992)

Exposure to fluoride may also cause hyperglycemia, hypercholesterolemia, hyperphospholipidemia and hypertriacylglycerolemia (Shashi 1992; Chlubek et al. 2003; Grucka-Mamaczar et al. 2004; Rupal et al. 2010). Also, when an individual is exposed to fluoride over a long period of time during their early developmental stages, the oxidative stress in their blood can increase, while the antioxidant defence systems in liver decreases. This can cause a reduction of non-enzymatic and enzymatic antioxidants such as SOD, CAT, GPX, GSH, GST and TAA (Shivarajashankara et al. 2003; Shanthakumari et al. 2004). Although fluoride can have effects on multiple systems, it is the effect on bone which has raised public health concerns. The question for municipalities is whether in an attempt to protect teeth, they may be increasing risk of fractures. To examine the effect of fluoridation of drinking water and hip fracture rates, two different Canadian cities, Edmonton and Calgary in the province of Alberta have been compared. The city of Edmonton has been fluoridating its water to a level of 1 mg/L since 1967, while the

natural fluoride levels of Calgary's drinking water are one third of Edmonton. The two cities are only 300 km apart. There was found to be no significant difference in the hip fracture health of these two cities' citizens (Suarez-Almazor et al., 1993).

Despite recommendations it had made in the past, Health Canada is now only recommending water fluoridation for health benefits regarding dental caries, and notes that fluoridation was not successful for experiments performed for growth and reproduction goals (Department of National Health and Welfare, 1983; Department of National Health and Welfare, 1990). This is also true in the United States. The National Research Council considers fluoridation as a beneficial factor for human health (NRC, 1993). This is because it improves dental health, while there appears to be little evidence of detrimental effects on bone at the levels of water fluoridation that are currently used. The majority of studies on excessive fluoride ingestion and non-neoplastic effects on human health have been on skeletal fluorosis and fractures. These have generally shown no evidence of skeletal fluorosis in individuals who consumed fluoridated water in the concentration of 1.2 and 3.3–6.2 mg/L for a time period of more than 10 years (McCauley and McClure, 1954; Schlesinger et al., 1956; Hodge and Smith, 1981; Sowers et al., 1986). Additionally, radiographic data on individual in the USA demonstrated that consumers who drank water that contained fluorine at levels of 4.0 mg/L, did not experience any level of skeletal changes caused by skeletal fluorosis (Kaminsky et al, 1990).

In conclusion, when fluoride is used moderately, it can benefit dental health while avoiding dental fluorosis. Since dental fluorosis it is not a health hazard, it is not

considered to be a toxicological end-point. It can be linked to cosmetic issues, so is considered a rather significant social issue. Overall, however, when fluorine levels are an average of 0.9 mg/L in drinking water, there will be no negative health effects for humans (Health Canada 2010). Currently the level of 1.5 mg/L F in water is considered to be protective against all potential harmful health effects, including cancer, bone fracture, immunotoxicity, reproductive/developmental toxicity, genotoxicity, and/or neurotoxicity.

1.1.4. Fluorine measurements

Since it is difficult to attain bone samples from healthy living individuals, samples are generally gathered from autopsies for studies about toxic metal exposures in the environment. Bone biopsies are not only inconvenient, they do pose a risk, and patients are unlikely to volunteer for bone biopsy because of concerns about pain. However some studies have been performed on both autopsy and biopsy data. In at least one study, the fluorine concentration in bone was measured *ex vivo* using reactor-based neutron activation analysis (NAA) (Krishnan et al 1985). The measured bones in that study were collected through the biopsy of both deceased and living subjects (Krishnan et al 1985). A summary of bone-fluorine measurements (mostly on autopsy data) with different methods is shown in table 1.1.

Table 1.1. Summary of fluorine measurements

Studies	Location	Bone site	Age	Technique	mg F/g dry bone	mg F/g Ca
Glock et al., 1941	England	Rib bone	0-68	Chemical method	0.24-3.1	0.88-11.4*
Mernagh et al., 1977	Canada	Biopsy sample (osteodystrophy)	N/A	NAA	0.5-1.2	3.2-8.5 (7.6-48.8)
Krishnan et al., 1985	Canada	Biopsy sample (fluorosis patients)	N/A	NAA	N/A	13.4±2.9 (21.5±3.2)
Ebifegha et al., 1986	Canada	Index Finger	N/A	NMR	2.17-5.1	8-18.7*
Fraser Code et al., 1990	Canada	Index Finger	N/A	NMR	0.47-1.1	1.7-4*
McNeill et al., 1991	Canada	Trabecular and cortical bone of the rat	N/A	NMR	N/A	N/A
Ishiguro et al., 1993	Japan	Cortical bone (Human rib)	20-93	Fluoride electrode	0.125-0.75	0.46-2.76*
Samudralwar et al., 1993	USA	Rib (Cortical bone & Trabecular bone)		PIGE (p,p'γ)***	2.074±0.652 1.71±0.632	7.63* 6.29*
Richards et al., 1994	Denmark	Vertebral trabecular	20-91	Fluoride electrode	0.91*	3.34†
Ishiguro et al., 1996	Japan	Trabecular bone Periosteal cortical Endosteal cortical	21-76	Chemical method	0.2-0.6 0.27-1.1 0.23-0.7	0.74-2.21* 0.99-4.05* 0.85-2.58*
Sastri et al., 2001	Turkey and Russia	Iliac crest, rib		PIGE (p,p'γ)***	0.5-1.999	1.84-7.36*
Yildiz et al., 2003	Turkey	vertebra, femur neck, femur trochanter, and Ward's triangle	45-54	DXA**	1.0761±0.179 0.8603±0.1166 0.6821±0.107 0.6527±0.1355	3.96* 3.17* 2.51* 2.4*
Chamberlain et al., 2012	Canada	Hand	20-87	IVNAA	0.3-2.4*	1.1-8.8
This study, 2013	Canada	Hand	23-75	IVNAA	0.3-3.15*	1.1-11.6

* Determined using a conversion factor of 3.68 g dry bone/g Ca (Woodard, 1964)

** Dual X-ray absorbtometry

*** Particle induced gamma-ray emission

† Determined using a conversion factor of 2.5 g bone ash/g Ca (ICRP 1975)

The table shows that fluoride accumulates in calcified tissues and as discussed earlier, it has been shown that fluorine levels correlate with age, suggesting that the level of fluorine in an individual could be a measure of the person's long term exposure to fluoride. As bone biopsies are unlikely to be approved for studies of volunteers, a low risk and painless method of assessing fluorine levels could be extremely useful for

population health studies. The objective of this PhD thesis, therefore, is to develop a painless non-invasive method for measuring F *in vivo* by NAA.

1.2. Neutron activation analysis

The most generally applied techniques for the non-invasive assessment of body and tissue composition studies have been x-ray fluorescence (XRF) and neutron activation analysis (NAA) (Chettle 2006). XRF is challenging for fluorine as the x-ray energy would be 0.677 keV, too low energy to be measureable outside of the body. NAA, although challenging, is the technique that has been pursued.

In NAA studies of people, in order to measure the activated element of interest in the detector, we need to irradiate the tissue with a radioactive source or accelerator while keeping the radiation dose to reasonably low levels (Chettle & Fremlin, 1984). In previous work, prior to this thesis, the technique showed that a reasonably low detection limit, 0.66 mg F/g Ca, could be achieved for an equivalent dose of 30 mSv: a dose comparable to the dose received by patients during clinical examinations (Chamberlain et al., 2012a). The main focus of this thesis has been to further development of the technique of *in vivo* NAA for the measurement of fluorine by investigating better phantom preparation and different detection regimes.

The technique of using neutron activation analysis in medical applications is generally called *in vivo* neutron activation analysis (IVNAA). The detection of the element is

performed in this case by measuring the radioactive daughter of the element of interest. The target nuclei of the sample are irradiated by a neutron source. A scintillation or semiconductor detector measures the γ -rays from the uniquely identified element, in this case fluorine. The level of the element can be quantified by comparing the signals between the person and appropriate calibration standards.

Fluorine was measured in this thesis by neutron activation analysis via the $^{19}\text{F}(n,\gamma)^{20}\text{F}$ reaction. ^{20}F β^- decays (100%) to an excited state of ^{20}Ne , which de-excites 99.1% of the time by the emission of a 1.63 MeV gamma ray (Tilley et al 1998).



This gamma-ray is detected and compared to the signal from calibration standards. One of the issues discussed in this thesis is that during measurements and data analysis there was found to be an overlap between the gamma-ray signals of fluorine (^{20}F), chlorine (^{38}Cl) and aluminum (^{28}Al). Figure 1.2 shows the overlap between ^{20}F , ^{38}Cl and ^{28}Al in a phantom spectrum. This thesis work describes attempts, during measurements and data analysis, to reduce or eliminate the signal from the interfering ^{38}Cl gamma-ray (E=1.64 MeV, half-life=37.2 min) by using anti-coincidence counting methods instead of summing data from nine NaI(Tl) detectors and delaying the start of a second count for 120 seconds after irradiating phantom and/or subject in order to subtract chlorine. The thesis also describes a program of work to find a phantom material that was aluminum free. Figure 1.2 showing the spectrum of the phantom.

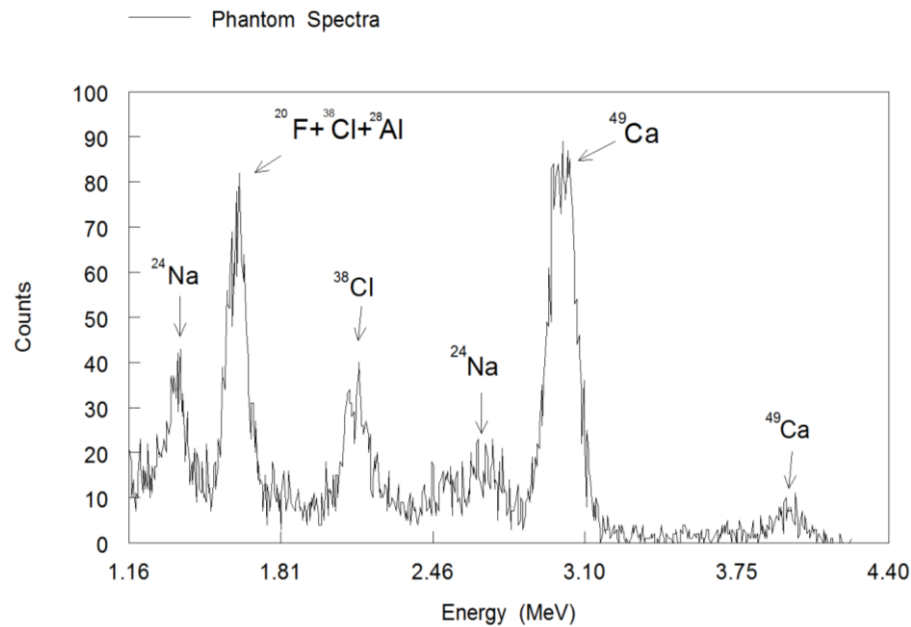


Figure 1.2. Fluorine Phantom spectrum

In our studies, the bones of the hand were chosen as a suitable site for non-invasive F measurements for several reasons. First, the neutron beam cannot easily be confined to a small area and because a hand can be extended away from the body, the torso can be kept out of the neutron beam as much as possible. This reduces the radiation dose to the more radiosensitive organs of the body which are located in the torso. Additionally, no active bone marrow is contained in the adult hand bone, thus also reducing radiation risk (ICRP 2002). Another consideration is that it is easy to position a hand inside an irradiation cavity or detection chamber. Finally, people find it psychologically acceptable to have their hand irradiated while they do not, for example, find the idea of a skull irradiation to be equally acceptable.

The hand bone is largely composed of cortical bone (95% (ICRP 2002)). Although the uptake of F^- is expected to be higher in trabecular bone (Jenkins 1990), having a site that is largely uniform in one type of bone is more desirable to obtain reproducible results (Jenkins 1990).

1.3. Irradiation facility

In this thesis work, all irradiations were performed using a hand irradiation system located at the McMaster University Tandatron Accelerator at the McMaster Accelerator Labs (MAL). The accelerator produces neutrons via the ${}^7\text{Li}(p,n){}^7\text{Be}$ reaction by irradiating a metal lithium target with protons. This facility was initially designed and used for studies of manganese, aluminum and magnesium which are described extensively in the literature (Aslam et al 2008; Byun et al 2007; Pejović–Milić et al 2006; Aslam et al 2003; Davis et al 2008). Full details regarding the irradiation cavity are discussed in Chapter 4. To describe the cavity simply, it is a large box on the end of the beam line and there is an access hole large enough so that the hand can be centered in the cavity. To reduce the participant's whole body dose due to neutrons streaming along the access hole cavity opening (Byun et al 2006), a water bag is used to shield the torso. The water thickness could be adjusted by increasing or decreasing the volume of water in the bag.

Figure 1.3 showing the layout of the irradiation box while Tandatron accelerator and irradiation cavity are shown with Figure 1.4 and 1.5.

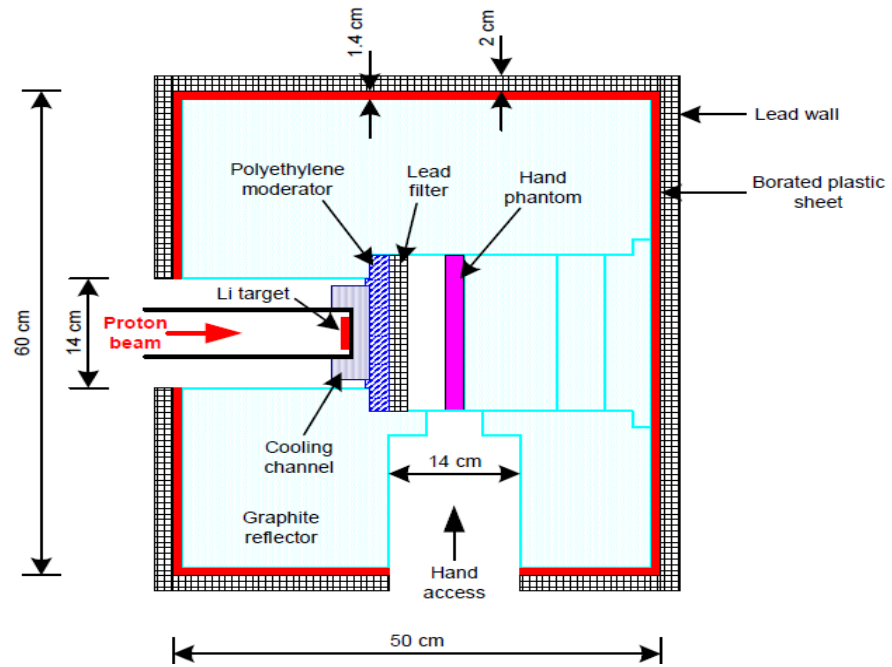


Figure 1.3: Layout of irradiation cavity (Byun *et al* 2007).



Figure 1.4. Tandatron accelerator at the McMaster Accelerator Labs (MAL)



Figure 1.5. Irradiation cavity

1.4. Detection system

The detection system used in this thesis is comprised eight $10.2 \times 10.2 \times 40.6 \text{ cm}^3$ plus one $10.2 \times 10.2 \times 10.2 \text{ cm}^3$ NaI(Tl) detectors arranged in an array with a close to 4π geometry. Figure 1.6 shows the detection system. The detection system is surrounded by a box composed of borax, polyethylene and polyester resin to reduce the neutron fluence at the outer surface. The detection system was placed near the irradiation cavity during the measurement of people because of the short half life (11.2 s) of fluorine. During the subject measurements the detection system was covered with an additional layer of concrete blocks in order to reduce the in-system activation. Without these blocks, the

fluorine peak was not observable after short runs of the accelerator due to a signal from activated iodine in the detectors. Figure 1.7 shows the alignment of detectors and voltage unit numbers.



Figure 1.6. The detection system at MAL

8 Power Designs Bottom Unit	3 Surface Concept Unit 3	7 Power Designs Top Unit
4 Hewlett Packard Standalone	9 Surface Concept Unit 4	2 Surface Concept Unit 2
5 Surface Concept Unit 5	1 Surface Concept Unit 1	6 Surface Concept Unit 6

Figure 1.7. Nine NaI(Tl) diagram with their high voltage unit number

1.5. Fluorine phantom

Calibration of the system is performed against ‘anthropomorphic’ hand phantoms. Hand bone phantoms with varying amounts of F concentrations were created and the process to describe the creation of a new phantom is thoroughly described in Chapter 2. Dry powder phantoms were chosen instead of water phantoms because experience in the laboratory has shown that water phantoms leak and can, over time, evaporate, thus changing concentrations, although not element mass. Additionally, due to an observed reaction between calcium and fluorine, we found making homogenous liquid phantoms to be almost impossible.

Phantoms with various concentrations of fluorine were created in order to construct a calibration line. In order to show system reproducibility, three sets of fluorine phantoms were made, and measured under the same conditions. Again, this will be discussed in chapter 3. Figure 1.8 shows an example of a fluorine calibration line of fluorine gamma-ray peak area versus fluorine concentration.

A fitting function was used to extract the F peak areas from each phantom spectrum. The peaks were modelled by Gaussian functions and the background by a linear function. Matlab, using the Levenberg-Marquardt fitting algorithm, was used for curve fitting. The fitting function had a total of five parameters (three for the Gaussian peak and two for the linear background) and took the form:

$$y = mx + B + \frac{A}{\sigma_1 \sqrt{2\pi}} \exp\left(-\frac{1}{2} \left(\frac{x - x_a}{\sigma_1}\right)^2\right)$$

Where, y represents the count rate (s^{-1}) and m represents the slope of the linear background, B the intercept of linear background, A the peak areas, σ_1 the peak width (standard deviation), x_a the peak centroid. To maintain stability of all the fits for the spectra obtained from the detectors, the peak widths and centroid positions were constrained to fall within 0.5 standard deviations of the values determined from the highest concentration peaks.

In the literature, there is more than one definition of minimum detectable limit. In our laboratory, we calculate minimum detectable limit (MDL) in the following manner:

$MDL = 2. \sigma F$, where σF is calculated from

$$\left(\frac{\sigma F}{F}\right)^2 \approx \left(\frac{\sigma A^2 + \sigma C^2}{(A-C)^2}\right) + \left(\frac{\sigma B}{B}\right)^2 - 2 \frac{\sigma A \sigma B}{AB} \rho_{AB} ,$$

where σF is measurement uncertainty of the zero concentration phantom , A is the zero concentration phantom peak area, B is the slope and C is the intercept of the calibration line, σA , σB and σC are standard deviations of A , B and C respectfully, and ρ_{AB} is the covariance between A and B (Bevington, 2003).

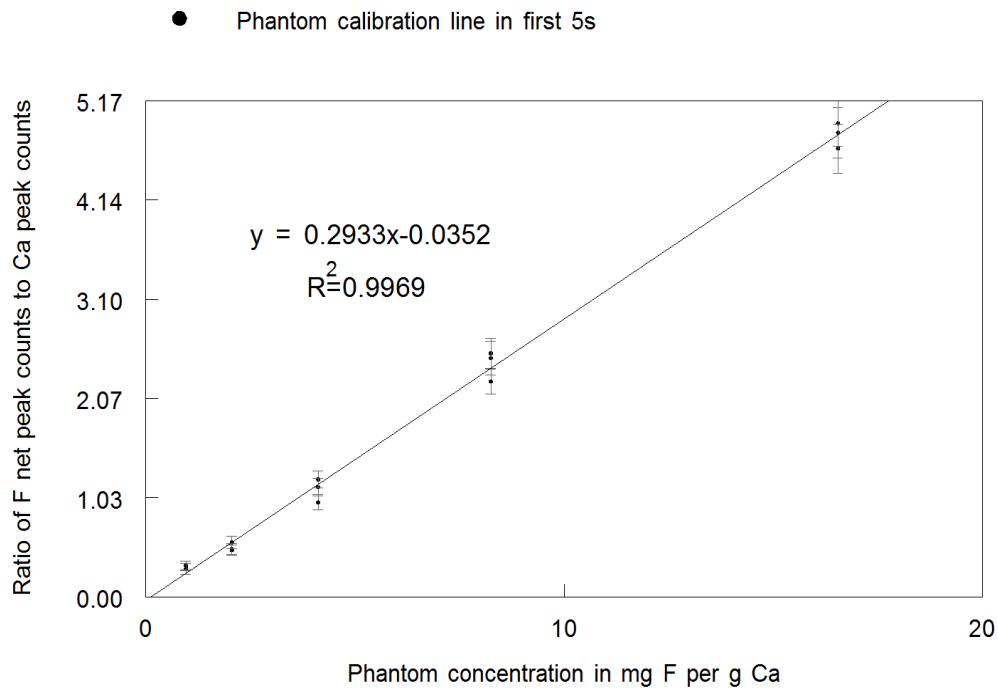


Figure 1.8. Fluorine calibration line

Thesis Outline

This chapter, Chapter 1, is intended to give an introduction to Fluorine, the known health effects and metabolism. These are presented because they describe the motivation for this thesis work. This chapter discusses the basic technique of NAA, and describes the method for fluorine NAA *in vivo*.

Chapter 2 presents article I, which describes the design of a phantom equivalent to measure bone-fluorine in a human hand via delayed neutron activation analysis. The introduction section of article I describes in detail the project motivation and the choice of phantoms for the target tissues of F retention.

Chapter 3 presents article II which demonstrates improvements to an *in vivo* neutron activation analysis (NAA) method for the measurement of fluorine in human bone. Several improvements to the methodology are described and the resultant overall improvement of detection in phantoms is presented.

Chapter 4 presents article III which describes an investigation of the neutron flux distribution in bone-fluorine phantoms comparing accelerator based *in vivo* neutron activation analysis and FLUKA simulation data. The purpose of this work was to investigate the effects of hand position in the cavity on the ability to detect fluorine.

Chapter 5 presents article IV which describes a small pilot study of volunteers from the Hamilton community measuring fluorine in human bone using *in vivo* neutron activation analysis. Fluorine could be measured in all volunteers, and factors which may explain fluoride exposure are discussed.

Finally, suggestions for future work and overall conclusions are discussed in Chapter 6.

Chapter 2

Design of a phantom equivalent to measure bone-fluorine in a human's hand via delayed neutron activation analysis (Article I)

2.1 Introduction to Article I

Article I describes a phantom equivalent to measure bone-fluorine in the human hand. This first published paper demonstrated the development of a new type of bone-fluorine phantom. This was essential to reduce the aluminum contamination observed in phantoms which were used in previous studies. The aluminum gamma peak interferes with the fluorine peak due to overlapping energies within the resolution of the detector system. The new phantom eliminates the interference and improves the measurement uncertainty. The experimental work presented in Article I was performed by the author of this thesis under the supervision of Dr. Fiona McNeill, and with the additional guidance of Dr. David Chettle and Dr. William Prestwich. Mr. Mike Inskip provided access to the lab for the Mowiol preparations.

2.2 Contents of Article I

The following article is reproduced with permission. Copyright © 2013 Institute of Physics and Engineering in Medicine.

Design of a phantom equivalent to measure bone-fluorine in a human's hand via delayed neutron activation analysis

F Mostafaei, F E McNeill, D R Chettle, W V Prestwich and M Inskip

Medical Physics and Applied Radiation Sciences, McMaster University, Hamilton, ON L8S 4K1, Canada

E-mail: mostaf@mcmaster.ca

Received 12 February 2013, accepted for publication 28 March 2013

Published 15 April 2013

Online at stacks.iop.org/PM/34/503

Abstract

Fluorine is an element that can be either beneficial or harmful, depending on the total amount accumulated in the teeth or bones. In our laboratory, we have developed a non-invasive technique for the *in vivo* measurement of fluoride in bone using neutron activation analysis and performed the first pilot human study. Fluoride in humans is quantified by comparing the γ -ray signal from a person to the γ -ray signal obtained from appropriate anthropomorphic calibration phantoms. An identified problem with existing fluoride phantoms is contamination with aluminum. Aluminum creates an interfering γ -ray signal which, although it can be subtracted out, increases the uncertainty in the measurement and worsens the detection limit. This paper outlines a series of studies undertaken to develop a better calibration phantom for fluorine measurement, which does not have aluminum contamination.

Keywords: phantom, bone-fluorine, delayed neutron activation analysis

(Some figures may appear in colour only in the online journal)

Introduction

A common naturally-occurring contaminant and sometimes also additive of water and many foods is fluorine, which is an element associated with both benefits and problems in teeth and bone. Water, tea and some *foods* are the major sources of intake for fluoride (F^-) (Yadav *et al* 2007, Johnson *et al* 2007). In North America and some other countries, there is still controversy as to whether fluorine should be added to drinking water (Ludlow *et al* 2007, Chamberlain *et al* 2012a). It is established that addition of about 1 ppm to water can be useful for the purpose of improved dental care (such as reduced caries), and at certain concentrations, fluoride has long been shown to reduce bone fracture risks (Chamberlain *et al* 2012b, Kurland *et al* 2007).

However, in some cases of high exposure, fluoride has been found to be toxic and harmful for consumers. Examples include people who have been found to have unusual habits such as swallowing fluoride containing toothpaste (Kurland *et al* 2007). Bone deformities, and changes in children's thyroid hormone levels are some of the health consequences that have been observed through ingestion of high doses of fluoride (Susheela *et al* 2005). Another occasionally observed condition (due to the long half-life of fluoride in bone) for individuals exposed to elevated fluoride intake, is fluorosis (Tamer *et al* 2007, Wang *et al* 2007). Different approaches by nations to the issues surrounding fluoride in drinking water have been described (Khandare *et al* 2005, Li *et al* 2001, Vestergaard *et al* 2008).

Fluorine accumulated in the skeleton interacts with bone by displacing the hydroxide content of the bone mineral. Bone is therefore potentially a useful site for measuring the fluoride concentration as a result of long term accumulation (Clarke *et al* 1994, Chamberlain *et al* 2012a). The concentration of fluorine in the skeleton has previously been measured using a reactor-based *ex vivo* technique, but obtaining a bone sample *via* biopsy is rarely possible (Krishnan *et al* 1985). Our laboratory recently conducted the first series of *in vivo* measurements of bone fluoride using neutron activation analysis (NAA). The volunteers' fluoride concentration was assessed non-invasively (Chamberlain *et al* 2012b) and the measurement relied on the comparison of *in vivo* fluoride signals to those from anthropomorphic standard addition calibration phantoms.

Limitations with the phantoms used in our earlier studies were identified, including contamination by aluminum. This paper describes work that was undertaken to develop an improved anthropomorphic phantom that could be used for studies of fluoride in bone and potentially other elements as well. In total, eleven different possible phantom types were investigated, with one phantom type identified as being best for future studies.

Irradiation materials and methods

Sample (and in vivo) irradiation

An irradiation cavity was created for the *in vivo* analysis of toxic elements in a human hand using the accelerator-based ${}^7\text{Li}(p,n){}^7\text{Be}$ neutron source at the McMaster Accelerator Laboratory (Aslam *et al* 2008a). The irradiation facility has been previously described in the literature (Byun *et al* 2007). Those elements whose neutron capture cross sections are sufficiently large can be analyzed by measuring the emission of γ -rays following neutron irradiation (Byun *et al* 2007, Pejović-Milić *et al* 2006). Measurement of the *in vivo* γ -ray signal, when compared with the γ -ray signal from an appropriate calibration standard, permits the level of the element in a person to be quantified.

The irradiation geometry means that the sample is totally enclosed within a cavity which has a port which allows hand access. This irradiation cavity setup has been used (Aslam *et al* 2008a, 2008b, Davis *et al* 2008) for the successful non-invasive measurement of several trace and minor elements in a series of studies of human volunteers. Elements studied have included magnesium, aluminum, manganese and fluorine (Davis *et al* 2008, Aslam *et al* 2008a, 2008b, Chamberlain *et al* 2012a). This irradiation cavity and method was used to irradiate the phantoms described in this paper. In this set up the equivalent dose to the phantoms was determined to be 30 mSv (Chamberlain *et al* 2012a).

Sample detection

Two methods were used to measure the samples described in this paper. Firstly, a system of eight $10.2 \times 10.2 \times 40.6 \text{ cm}^3$ plus one $10.2 \times 10.2 \times 10.2 \text{ cm}^3$ NaI(Tl) detectors

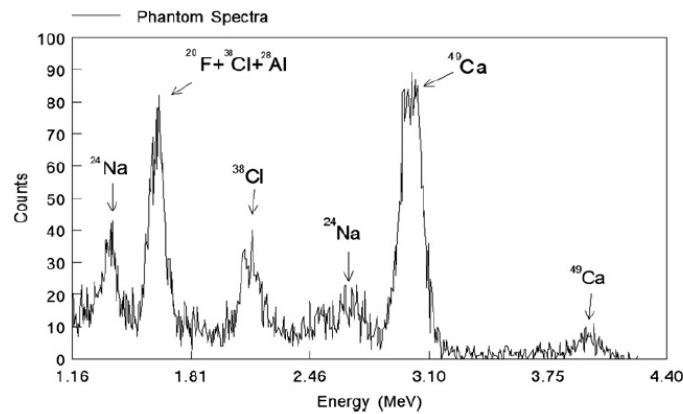


Figure 1. Phantom measurement spectrum.

arranged in an array with close to a 4π geometry were used. Samples were placed inside the 4π cavity in order for the γ -ray signal to be counted. Signals from each of the nine detectors, in anti-coincidence mode, were gathered and directed through a pre-amplifier and recorded by a multichannel analyzer (Byun *et al* 2006).

Secondly, some samples were measured using a hyper-pure germanium detector. This was used to measure γ -ray signal from small samples of materials that were irradiated in the pneumatic activation system at the McMaster Nuclear Reactor (MNR).

Phantoms

Eleven different types of phantom in total were studied

For the original fluoride *in vivo* study, hand bone phantoms with different concentrations of F had been fabricated in 125 ml cylindrical Nalgene (polyethylene) containers. However, subsequent work determined that the presence of aluminum contamination within the plastic of the bottles made the determination of fluoride more challenging. Figure 1 shows a phantom measurement spectrum and it can be seen that there are a number of γ -ray signals that either overlap or are in close proximity to one another. In particular, the ^{28}Al peak overlaps with the ^{20}F signal. Subtracting the ^{28}Al signal from the ^{20}F increases the uncertainty in the estimation of the fluorine signal. It is therefore preferable to try and eradicate the Al contamination from the phantoms.

Phantom type 1. Initially, we tried water-based phantoms in Nalgene bottles. However, the masses of powder, and the volumes of water required, meant that the materials did not mix well. It was not possible readily to obtain a homogenous solution of fluorine and calcium, and post-irradiation settling was found to occur.

Phantom type 2, 3 and 4. We next eliminated the water and used dry powder phantoms. These consisted of NaNO_3 (1.25 g of Na), NH_4Cl (1.19 g of Cl), CaCO_3 (14.9 g of Ca) and varying masses of NH_4F with a fluorine content that varied between 0.03 to 0.5 g (as per ICRP 1975).

Table 1 shows the elements which were added to the phantom in the specified concentrations so as to match a 'reference' man (ICRP 1975). Detection was of micrograms

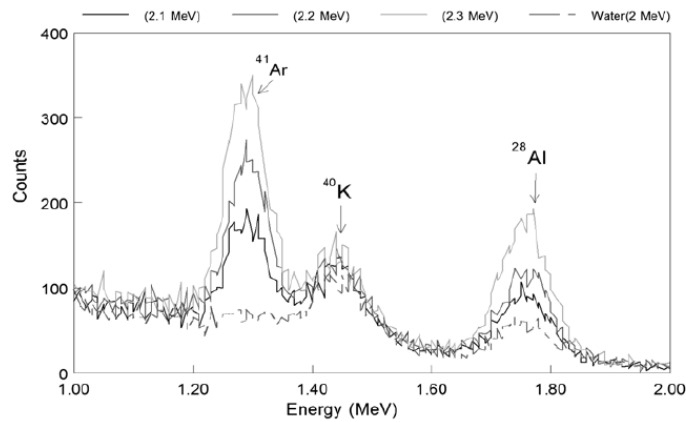


Figure 2. Comparison of HDPE Nalgene bottles with different proton energies.

Table 1. Elemental composition of hand bone (ICRP 1975).

	Elements		
	Ca(⁴⁸ Ca)	Na(²³ Na)	Cl(³⁷ Cl)
Expected amount (ICRP)	14.9 g	1.25 g	1.19 g
Compound added	Ca(NO ₃) ₂	NaNO ₃	NH ₄ Cl
Amount of compound (g)	88.06 ± 0.05	4.6 ± 0.01	1.80 ± 0.01

(μg) of F per gram (g) of Ca. Chlorine was required because of a spectral interference with the fluorine signal. Sodium is required because γ -rays from the $^{23}\text{Na}(n,\gamma)^{24}\text{Na}$ reaction contribute significantly to the γ -ray background signal (Chamberlain *et al* 2012a).

‘Phantom type 2’ were powder within high density polyethylene (HDPE) Nalgene bottles.

‘Phantom type 3’ were powder within low density polyethylene (LDPE) Nalgene bottles.

‘Phantom type 4’ were powder contained within Adanac Polyethylene bottles.

Analysis and results for phantoms type 2, 3 and 4

Bottles

In order to determine the level of aluminum in phantom type 2, empty 250 ml Nalgene bottles were irradiated with different neutron beam energies produced from proton energies of (2, 2.1, 2.2, 2.3 MeV respectively) with a proton current of 400 μA for 60 s (Byun *et al* 2006) as performed in earlier studies (Chamberlain *et al* 2012a, 2012b). The bottles and materials were measured for 300 seconds in anti-coincidence mode in the 4π detection system. Figure 2 shows the resulting spectra.

The lowest Al signal resulted from irradiation with the lowest proton energy. This is to be expected as the neutron yield is lower for lower energies. However, an important finding was that having a bottle filled with water did not show any significant difference in signal in comparison with the empty bottles. The extra moderation within the sample would appear to result in a negligible effect on the signal, probably because the scattering and pre-moderation within the cavity dominate the effect on the neutron flux at low energies. The bottle that showed

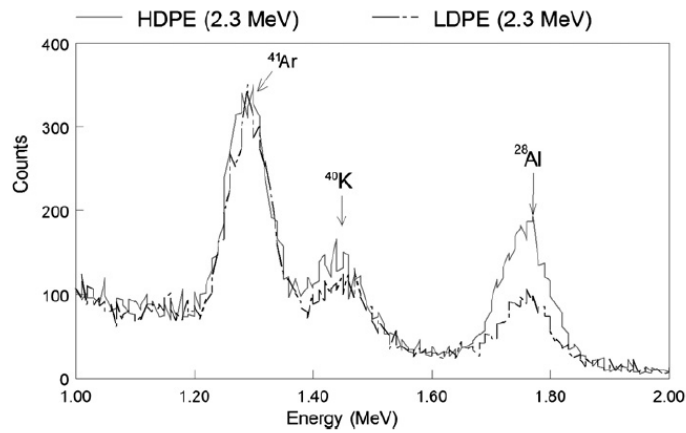


Figure 3. Comparison of HDPE and LDPE Nalgene bottles impinged with 2.3 MeV proton energy.

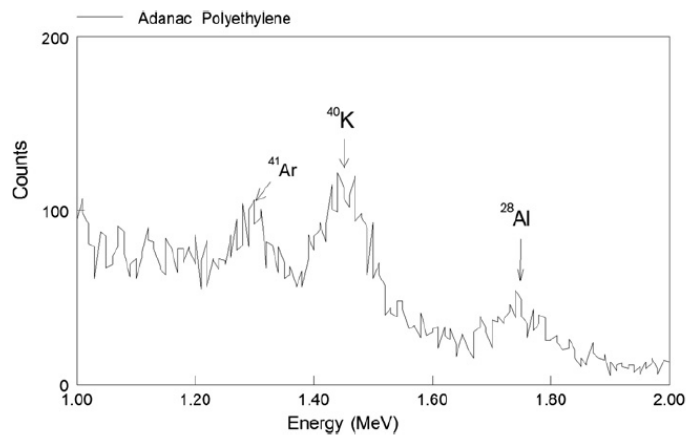


Figure 4. Adanac polyethylene in 2.3 MeV proton energy.

the most difference, in comparison to the one filled with water, was due to the activation of argon (Ar) in air. Less water meant there was more air in the bottle.

Figure 3 illustrates a comparison between phantom type 2 and phantom type 3 irradiated with a neutron beam produced by a 2.3 MeV proton energy on lithium (Chamberlain *et al* 2012a). The amount of aluminum inside the LDPE phantom is significantly lower than in the HDPE, but it is still a clear signal. LDPE is a better and more appropriate choice for creating a phantom, but is still not perfect. A further test of polyethylene phantoms (Phantom type 4) was performed to see if the Al signal could be completely eliminated. Adanac polyethylene was therefore examined through irradiation and activation, and the results from this test are shown in figure 4. Note that these bottles had a much lower volume than the previously used bottles.

The Adanac polyethylene shows a lower amount of aluminum than the previous two types of plastic container, and could be considered the best candidate for the phantoms. However, Adanac was not available in containers of sufficient volume for our studies of the human hand.

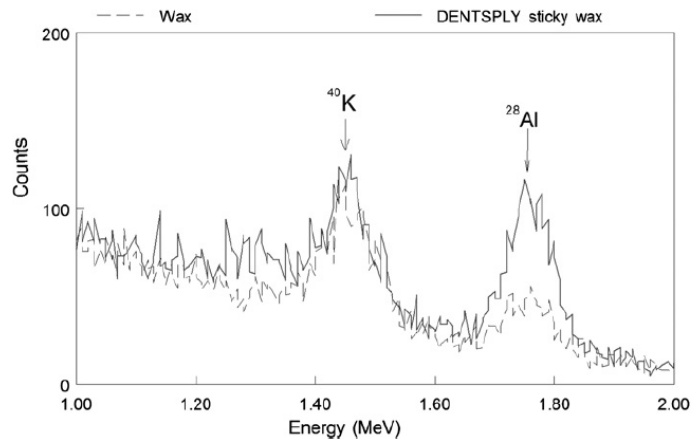


Figure 5. Comparison of Wax and DENTSPLY sticky wax in 2.3 MeV proton energy.

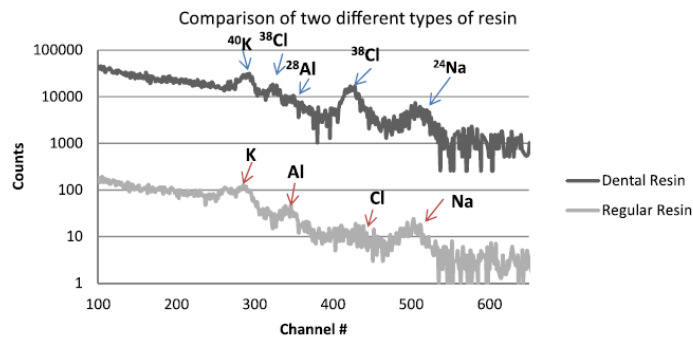


Figure 6. Comparison of dental resin and regular resin in 2.3 MeV proton energy.

Non-contained phantoms

The possible use of phantoms without containers was studied

Phantom type 5. It was suggested that using pressure on the powdered elements used in the fluorine phantom could lead to a compressed stable phantom. However, a solid pellet could not be manufactured with the systems available, and the pressed powder was found to fall apart after approximately 5 min..

Phantom type 6. An attempt was made to heat the phantom materials to melting point, to then mix and cool to a solid. Unfortunately, calcium carbonate has a melting point of 825 °C. In our attempts, the compound disassociated, rather than melting.

Two attempts were made to create phantoms using wax as a binding agent. Similarly, two attempts were made using resin as a 'binder' to keep all fluorine phantom components together. Each binder needed to be tested for aluminum contamination. Phantom 7 tested DENTSPLY sticky paraffin wax. Phantom 8 tested regular paraffin wax. Phantom 9 was a test of dental resin. Phantom 10 was a test of polyethylene resin commonly used for car repair. Figure 5 shows the results for the two waxes. Figure 6 shows the results for the two resins. Irradiations were performed as before.

Design of a phantom equivalent to measure bone-fluorine in a human's hand

509

Table 2. Aluminum net counts for finding best composition of hand bone phantom. Materials were activated at MNR.

Material name	Mass (g)	Irradiation time (s)	Aluminum net count	Al counts per g material
Wax (regular paraffin)	1.83	10	205 ± 14.3	112 ± 5.8
Adanac polyethylene	1.62	10	1028 ± 32	634 ± 16
Nalgene polyethylene	1.77	10	2904 ± 53.9	1640 ± 24.7
Regular resin	1.65	10	12 599 ± 112.2	7635 ± 70.3
Quartz (silicon dioxide)	1.58	10	19 060 ± 138	12 063 ± 103.3

The amount of aluminum inside the DENTSPLY wax was lower than the paraffin wax, however, the aluminum concentration in both forms of wax binder was measurable and therefore still not fully acceptable.

Figure 6 illustrates that the aluminum level in regular resin is comparable with wax, while the aluminum levels in dental resin are substantially lower. However, other elements in the dental resin meant that, as can be seen in the figure, the dental resin's background signal is orders of magnitude higher at the energies of interest. This makes this material unsuitable for fluorine phantoms. The background signal is much higher so the detection limit in the calibration standards would be worse.

Signal comparison using the MNR

In order to quantify the differences in aluminum signal between phantom materials more accurately, the MNR pneumatic small-sample activation system was used to irradiate the following samples: Wax, Adanac Polyethylene, Nalgene Polyethylene, and regular resin. In addition, a quartz (silicon dioxide) sample was analyzed to test whether such a container would reduce the aluminum signal. A hyperpure germanium detector was used for γ -ray detection. Table 2 illustrated the number of aluminum 1.779 MeV γ -ray net peak counts for each of these samples.

As can be seen, paraffin wax provided the lowest level of contamination per gram of material by far. However, as previously discussed this signal, although low, is still observable.

Phantom type 11(Mowiol 4-88)

Mowiol 4-88 is a high quality organic anti-fade medium that is used for immunofluorescence, as well as other molecular biological and geological applications. It is a material which hardens and which has the same refractive index as immersion oil. If used for immunofluorescence applications the addition of glycerin is recommended (Polysciences Inc. 2008). Mowiol 4-88 was prepared by following the manufacturer instructions in the following series of steps:

1. 4.8 g Mowiol 4-88 and 12 g glycerol were added to a 100 ml beaker.
2. The material was mixed well using a stir bar.
3. 12 ml of double distilled H₂O was added and the stirring continued for several hours at room temperature.
4. 24 ml 0.2 M Tris HCl (ph 8.5) was added and stirring continued. The mixture was heated occasionally to 50 °C in a water bath for approximately 10 min and stirring continued until the Mowiol 4-88 was dissolved.
5. Once dissolved, the solution was centrifuged at 500 × g for 15 min to clarify the solution.
6. The supernatant was carefully removed and aliquots stored at -20 °C (Polysciences Inc. 2008).

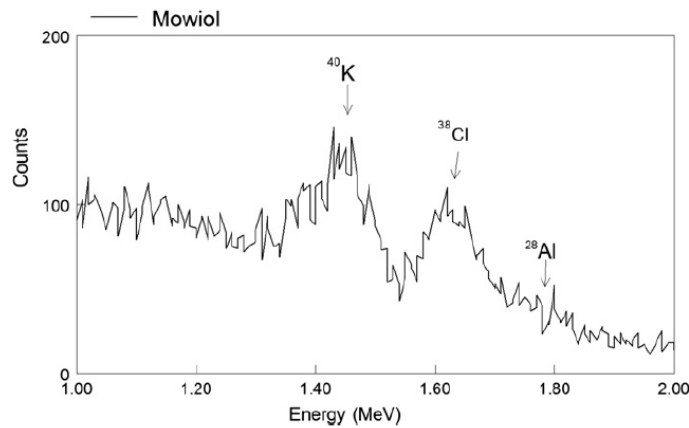


Figure 7. Mowiol 4-88 in 2.3 MeV proton energy (see arrow where Al peak would be).

After preparation, the Mowiol 4-88 material was tested as previously described, using a proton energy of 2.3 MeV with 400 μ A current. Irradiations were performed for 60 seconds, and the detection time in the 4π NaI(Tl) detector was 300 seconds in anticoincidence mode.

Mowiol was found to be the most successful material for use as a phantom binding agent in terms of limited aluminum contamination as can be seen in figure 7. The Mowiol 4-88 was found to be effectively aluminum free, which thus makes it appropriate for making fluoride bone phantoms.

Phantoms were then created using the Mowiol 4-88 as the binding agent. The Mowiol 4-88 was mixed with NaNO_3 , NH_4Cl , CaCO_3 and NH_4F . In order to obtain solid fluorine phantoms, the Mowiol 4-88 and additives were left to sit and harden at room temperature for three weeks.

Calibration data

In order to determine whether robust homogeneous fluoride-doped Mowiol phantoms could be created that produced calibration data that were comparable with the previously used phantom set, a new set of five phantoms with different masses of fluoride, 0.03–0.25 g F, was created. The phantoms were found to have remained very robust three weeks after adding the Mowiol to the components, and they showed sufficient hardening and stability to be irradiated.

The new phantoms were irradiated and measured as per the previously described method. On the same day, phantoms in the same mass range from the previously used ‘old’ phantom set (phantom type 2) were also irradiated and measured. Both sets of phantoms were made as standard addition phantoms from the same batch of ammonium fluoride, but were made several years apart. As ammonium fluoride is a compound that is hygroscopic, a drying experiment was performed to determine how much water had been absorbed by the compound. A small sample was weighed out, then placed in a relatively low temperature oven at 63 °C for several hours. The sample was found to have reduced in mass to 95.9% of the original mass. The masses, and hence concentrations, of fluoride in the new phantoms were therefore corrected by this factor.

Figure 8 shows the calibration lines of fluoride signal normalized to Ca signal versus mg of F per gram of Ca obtained from both the new fluorine phantoms and the old fluorine phantoms. The phantoms were compared over a concentration range from approximately 1–17 mg F per

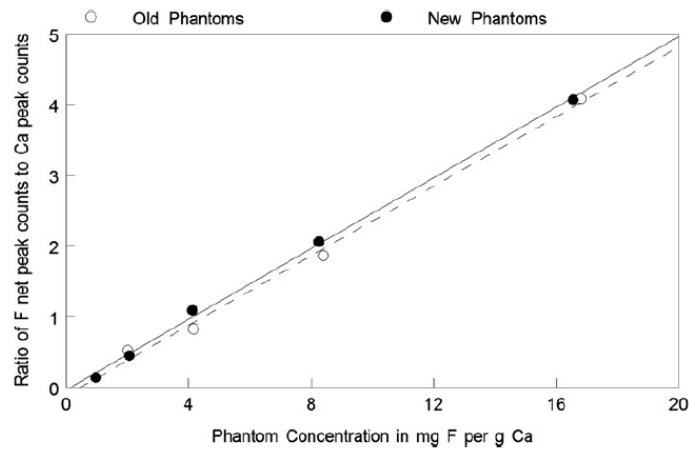


Figure 8. Fluorine calibration line comparing the new and old phantoms.

gram Ca. Previous studies in our laboratory had measured levels in environmentally exposed volunteers from Southern Ontario in the range from 0 to 10 mg F per g Ca: this phantom calibration range therefore encompasses this range of *in vivo* data.

The new and old phantoms were found to have the same calibration slope and intercept to within uncertainties.

For the 'old' phantoms, the slope of the regression was 0.246 ± 0.012 ($r^2 = 0.995$, $p = 0.002$)

For the 'new' phantoms, the slope of the regression was 0.250 ± 0.006 ($r^2 = 0.998$, $p < 0.001$)

For the 'old' phantoms, the intercept was found to be -0.10 ± 0.12

For the 'new' phantoms, the intercept was found to be -0.04 ± 0.05

The slopes and intercepts of the two sets of phantoms were found to be the same to within uncertainties, as would be expected. The measured fluorine signals from the phantoms are normalized to the calcium signals. This should mean that the accuracy of the measurement is independent of factors such as target quality, variation in beam current or positioning of the phantom in the cavity. (The precision of the measurement will however depend on these factors.) The reason for the creation of these new phantoms was to eliminate the aluminum signal and thus reduce the uncertainty on the measurement. This seems to be borne out by these data, as the slope and intercept uncertainties are less for the new phantoms than the old.

Conclusion

We have developed a new type of hand-bone phantom for the determination of fluorine concentration by *in vivo* NAA. Previously used phantoms contained a small level of aluminum contamination, which contributed to the uncertainty on the fluorine measurement. A new phantom that uses Mowiol 4-88 as the binder has been developed and found to have non-detectable levels of aluminum. The phantom has more involved preparation requirements, but is robust, and produces a linear calibration signal that is comparable with the previously used phantoms. It eliminates the problem of aluminum contamination and thus appears to reduce measurement uncertainties. This phantom is suitable for NAA studies of fluoride in bone, and may also be a suitable phantom material for *in vivo* studies of other elements.

Acknowledgments

Thanks are extended to Bonnie Kahlon of the Department of Anthropology, McMaster University, for her kind assistance, loaning of the equipment, and the preparing of Mowiol, the binder used for the phantoms in this study. The authors would also like to thank Justin Bennett, accelerator operator, for his assistance. Funding was provided by the Natural Sciences and Engineering Research Council of Canada.

References

- Aslam Pejović-Milić A, Chettle D R, McNeill F E, Pysklywec M W and Oudyk J 2008a A preliminary study for non-invasive quantification of manganese in human hand bones *Phys. Med. Biol.* **53** N371–6
- Aslam, Pejović-Milić A, McNeill F E, Byun S H, Prestwich W V and Chettle D R 2008b *In vivo* assessment of magnesium status in human body using accelerator-based neutron activation measurement of hands: a pilot study *Med. Phys.* **35** 608
- Byun S H, Pejović-Milić A, McMaster S, Matysiak W, Aslam, Liu Z, Watters L M, Prestwich W V, McNeill F E and Chettle D R 2007 Dosimetric characterization of the irradiation cavity for accelerator-based *in vivo* neutron activation analysis *Phys. Med. Biol.* **52** 1693–703
- Byun S H, Pejović-Milić A, Prestwich W V, Chettle D R and McNeill F E 2006 Improvement of *in vivo* neutron activation analysis of MN using a 4π NaI (TI) detector array *Radioanal. Nucl. Chem.* **269** 615–8
- Chamberlain M, Grafe J L, Aslam, Byun S H, Chettle D R, Egden L M, Orchard G M, Webber C E and McNeill F E 2012a The feasibility of *in vivo* quantification of bone-fluorine in humans by delayed neutron activation analysis: a pilot study *Physiol. Meas.* **33** 243–57
- Chamberlain M, Grafe J L, Aslam, Byun S H, Chettle D R, Egden L M, Webber C E and McNeill F E 2012b *In vivo* quantification of bone-fluorine by delayed neutron activation analysis: a pilot study of hand-bone-fluorine levels in a Canadian population *Physiol. Meas.* **33** 375–84
- Clarke A J, Evans J A, Truscott J G, Milner R and Smith M A 1994 A phantom for quantitative ultrasound of trabecular bone *Phys. Med. Biol.* **39** 1677–87
- Davis K, Pejović-Milić A and Chettle D R 2008 *In vivo* measurement of bone aluminum in population living in Southern Ontario, Canada *Med. Phys.* **35** 5115
- ICRP 1975 Report of the Task Group on Reference Man: A Report *ICRP Publication 23* (Oxford: Pergamon)
- Johnson H J E, Kearns A E, Doran P M, Khoo T K and Wermers R A 2007 Fluoride-related bone disease associated with habitual tea consumption *Mayo Clin. Proc.* **82** 719–24
- Khandare A L, Harikumar R and Sivakumar B 2005 Severe bone deformities in young children from vitamin D deficiency *Calcif. Tissue* **76** 412–8
- Krishnan S S, Mernagh J R, Hitchman A J W, McNeill K G and Harrison J E 1985 Measurements of fluoride in bone biopsies by neutron activation analysis for the clinical study of osteoporosis *Nucl. Chem.* **95** 119–25
- Kurland E S, Schulman R C, Zerwekh J E, Reinus W R, Dempster D W and Whyte M P 2007 Case report *J. Bone Miner. Res.* **22** 163–70
- Li Y *et al* 2001 Effect of long-term exposure to fluoride in drinking water on risks of bone fractures *J. Bone Miner. Res.* **16** 932–9
- Ludlow M, Luxton G and Mathew T 2007 Effects of fluoridation of community water supplies for people with chronic kidney disease *Nephrol. Dial. Transplant.* **22** 2763–7
- Pejović-Milić A, Byun S H, Chettle D R, McNeill F E and Prestwich W V 2006 Development of an irradiation/shielding cavity for *in vivo* neutron activation analysis of manganese in human bone *Radioanal. Nucl. Chem.* **269** 417–20
- Polysciences Inc. 2008 Data sheet 777 Mowiol® 4-88
- Susheela A K, Bhatnagar M and Vig K 2005 Excess fluoride ingestion and thyroid hormone derangements in children living in Delhi, India *Int. Soc. Fluoride Res.* **38** 98–108
- Tamer M N, Kale Köroğlu B, Arslan C, Akdoğan M, Köroğlu M, Cam H and Yildiz M 2007 Osteosclerosis due to endemic fluorosis *Sci. Total Environ.* **373** 43–8
- Vestergaard P, Jorgensen N R, Schwarz P and Mosekilde L 2008 Effects of treatment with fluoride on bone mineral density and fracture risk—a meta-analysis *Osteoporos. Int.* **19** 257–68
- Wang W *et al* 2007 Thoracic ossification of ligamentum flavum caused by skeletal fluorosis *Eur. Spine J.* **16** 1119–28
- Yadav A K, Kaushik C P, Haritash A K, Singh B, Raghuvanshi S P and Kansal A 2007 Determination of exposure and probable ingestion of fluoride through tea, toothpaste, tobacco and pan masala *J. Hazard. Mater.* **142** 77–80

Chapter 3

Improvements in an *in vivo* neutron activation analysis (NAA) method for the measurement of fluorine in human bone (Article II)

3.1 Introduction to Article II

Article II describes a series of incremental improvements to the *in vivo* fluorine measurement by NAA as tested on the new phantoms presented in Chapter 2. Overall the data demonstrated a significant improvement in detection limit of fluoride in phantoms compared to earlier work published by Chamberlain et al., 2012.

The experimental work presented in Article II was performed by the author of this thesis under the supervision of Dr. Fiona McNeill, and with the additional guidance of Dr. David Chettle and Dr. William Prestwich.

3.2 Contents of Article II

The following article is reproduced with permission. Copyright © 2013 Institute of Physics and Engineering in Medicine.

Improvements in an *in vivo* neutron activation analysis (NAA) method for the measurement of fluorine in human bone

F Mostafaei, F E McNeill, D R Chettle and W V Prestwich

Medical Physics and Applied Radiation Sciences, McMaster University, Hamilton, ON, L8S 4K1, Canada

E-mail: mostaf@mcmaster.ca

Received 3 July 2013, accepted for publication 2 September 2013

Published 18 September 2013

Online at stacks.iop.org/PM/34/1329

Abstract

We previously published a method for the *in vivo* measurement of bone fluoride using neutron activation analysis (NAA) and demonstrated the utility of the technique in a pilot study of environmentally exposed people. The method involved activation of the hand in an irradiation cavity at the McMaster University Accelerator Laboratory and acquisition of the resultant γ -ray signals in a '4 π ' NaI(Tl) detector array of nine detectors. In this paper we describe a series of improvements to the method. This was investigated via measurement of hand simulating phantoms doped with varying levels of fluorine and fixed amounts of sodium, chlorine and calcium. Four improvements to the technique were tested since our first publication. The previously published detection limit for phantom measurements using this system was 0.66 mg F/g Ca. The accelerator irradiation and detection facilities were relocated to a new section of the laboratory and one more detector was added to the detection system. This was found to reduce the detection limit (possibly because of better detection shielding and additional detector) to 0.59 mg F/g Ca, a factor of 1.12. A new set of phantoms was developed and in this work we show that they improved the minimum detectable limit for fluoride in phantoms irradiated using neutrons produced by 2.15 MeV protons on lithium by a factor of 1.55. We compared the detection limits previously obtained using a summed signal from the nine detectors with the detection limit obtained by acquiring the spectra in anticoincidence mode for reduction of the disturbing signal from chlorine in bone. This was found to improve the ratio of the detection of fluorine to chlorine (an interfering signal) by a factor of 2.8 and the resultant minimum detection limit was found to be reduced by a factor of 1.2. We studied the effects of changing the timing of γ -ray acquisition. Our previously published data used a series of three 10 s acquisitions followed by a 300 s count. Changing the acquisition to a series of six 5 s acquisitions was found to further improve the detection limit by a factor of 1.4. We also present data showing that if the neutron dose is delivered to the phantom in a shorter time period, i.e. the dose rate is

increased and irradiation shortened then the detection limit can be reduced by a further factor of 1.35. The overall improvement in detection limit by employing all of these changes was found to be a factor of 3.9. The technique now has an in phantom detection limit of 0.17 mg F/g Ca compared to a previous detection limit of 0.66 mg F/g Ca. The system can now be tested on human volunteers to see if individuals with diagnosed fluorosis can be distinguished from the general Canadian population using this technique.

Keywords: *in vivo*, neutron activation analysis, fluorine, bone

Introduction

Fluorine (F) is an essential element in bone structure. However, when the concentration of F exceeds normal values due to occupational or environmental exposures, there is evidence to suggest that significant bone damage can be induced (Johnson *et al* 2007, Yadav *et al* 2007). This strongly motivates the development of a reliable technique to analyze fluorine content in human bone *in vivo* in order to understand its toxic effects more clearly (Ludlow *et al* 2007). *In vivo* neutron activation analysis (IVNAA) has been shown to be a promising method, in part due to a feasibility study carried out at McMaster University using an accelerator-based ${}^7\text{Li}(p,n)$ neutron source (Chamberlain *et al* 2012a). The bone was selected as the target organ for measurement by IVNAA as this is both the storage site of fluoride and target organ for potential health effects (Clarke *et al* 1994, Kurland *et al* 2007). The previous feasibility study published a set of irradiation conditions designed to maximize the radioactivity of ${}^{20}\text{F}$ while minimizing the dose to the hand (Chamberlain *et al* 2012b). The achieved detection limit by Chamberlain *et al* (2012a, 2012b) of F was 0.66 mg F/g Ca for a hand dose (equivalent dose) of 30 mSv and effective dose of 35 μSv . The γ -ray signal acquisition time used was three sets of 10 s followed by a further 300 s acquisition (Chamberlain *et al* 2012a). This detection limit is acceptable, as it was found to be able to measure fluoride levels in the majority of people in an urban Canadian population. The radiation dose is significantly lower than most diagnostic procedures. In addition, while the analytical performance in the previous feasibility study is possibly able to discriminate populations of patients with excess fluoride, which the literature predicts may have a fluoride content of 1.1 mg F/g Ca (Chamberlain *et al* 2012b), it is possibly not yet sufficient to permit discrimination of whether an individual person has a fluoride level that is significantly different from the population average for their age. A clinically useful system needs to be able to identify an individual measurement which is above the norm. We decided, therefore, to investigate factors that could result in an improvement in system performance.

Method

Accelerator-based IVNAA for fluorine consists of two steps. A hand (or phantom) is irradiated in the accelerator neutron beam for a short period of time. The hand (or phantom) is then placed inside a 4π γ -ray spectrometer and the γ -ray spectrum from the activated hand is acquired for a relatively short counting period.

In order to simulate a hand bone, solid phantoms with a fluorine content of 0.0–257 mg were made using NH_4F as the fluoride doping agent. Elements important for neutron activation, Na, Cl and Ca, were also included in the phantoms in order to maintain an elemental

composition consistent with the hand of Reference Man (ICRP 1975). The phantoms were made using Mowiol to avoid aluminum contamination inside the Nalgene bottles as has been described in a previous publication (Mostafaei *et al* 2013). The aluminum gamma peak interferes with the fluorine peak due to overlapping energies and the new phantoms eliminate the interference and improve the measurement uncertainty (Mostafaei *et al* 2013).

The base line for the system measurement parameters were as follows. Each phantom was irradiated at the central sample position of the cavity developed for accelerator-based IVNAA at McMaster (Byun *et al* 2007, Pejović-Milić *et al* 2006). The incident proton energy was set at 2.15 MeV with a proton current of 370 μA . For an incident proton energy of 2.15 MeV on a thick lithium target, the resultant neutrons have maximum energies less than 400 keV. These energies are well below the threshold of the interfering $^{23}\text{Na}(n,\alpha)^{20}\text{F}$ reaction, which is approximately 4 MeV (Aslam *et al* 2003). The thermal neutron fluence rate at the center of the irradiation position is $4.8 \times 10^8 \text{ n}\cdot\text{cm}^{-2} \text{ s}^{-1}$ for these conditions (Aslam *et al* 2008a, Byun *et al* 2006). The irradiation time was set at 10 s, which corresponds to 30 mSv equivalent dose for a Li target in normal condition. The effective dose is predicted to be 35 μSv which is predominantly due to the tissue weighting factor of bone which ICRP suggests be used for the calculation of effective dose (Chamberlain *et al* 2012a). After completion of irradiation, the γ -ray spectrum was measured by a system of eight $10.2 \times 10.2 \times 40.6 \text{ cm}^3$ plus one $10.2 \times 10.2 \times 10.2 \text{ cm}^3$ NaI(Tl) detectors arranged in an array with a close to 4π geometry. The characteristics of this spectrometer were described in detail in previous publications (Aslam *et al* 2008a, 2008b, Byun *et al* 2006). The spectrum can be acquired in singles, coincidence, or anticoincidence modes. For baseline studies, the acquisition was performed in 'singles' mode with the output from all detectors directly summed together. This single signal is then amplified, digitized and recorded.

Phantoms were transferred to the detection system with an average transfer time of 9 s, and spectra were acquired for three 10 s periods using a multichannel analyzer (MCA). This was followed by a 120 s waiting period and then a further 300 s count. The purpose of the three 10 s segments was to collect information pertaining to fluorine and chlorine, while the 120 s waiting period allowed sufficient time for the fluorine to decay. The 300 s segment collected information pertaining to chlorine and calcium.

Results

Comparison of old and new phantoms

For the original fluoride *in vivo* study, hand bone phantoms with different concentrations of fluorine had been fabricated in 125 ml cylindrical Nalgene (polyethylene) containers (Chamberlain *et al* 2012a). We describe these as the 'old' phantoms. However, subsequent work determined that the presence of aluminum contamination within the plastic of the bottles made the determination of fluoride more challenging. A new phantom that uses Mowiol 4–88 as the binder has been developed and found to have non-detectable levels of aluminum (Mostafaei *et al* 2013). In that publication, data was presented for neutrons produced by a proton energy of 2.3 MeV. Our first publication which presented an minimum detection limit (MDL) for the measurement of fluorine in phantoms, and our previous *in vivo* work, employed a proton energy of 2.15 MeV with eight NaI detectors as a detection system. We therefore conducted a new series of measurements which we present here. The new and old sets of phantoms were measured one after the other on the same day using neutrons produced from 2.15 MeV protons incident on lithium to allow us to conduct a side-by-side comparison of the MDL improvement. Three sets of six phantoms were irradiated and the measurements

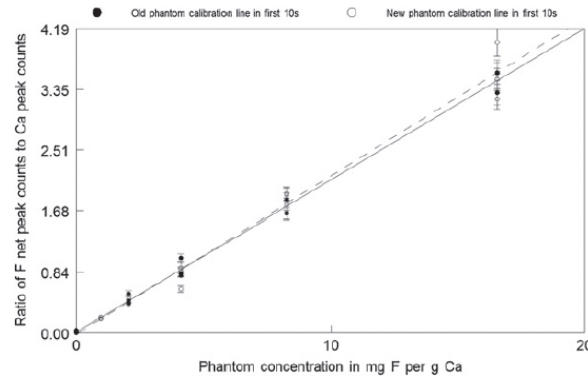


Figure 1. Comparison of old and new phantoms calibration lines in first 10 s.

Table 1. Phantom detection limits of new and old phantoms.

Timing segment (s)	New phantoms, M_{DL} (mg F/g Ca)	Old phantoms, M_{DL} (mg F/g Ca)
0–10	0.43	0.81
10–20	0.97	1.02
20–30	1.42	1.57
M_{DL} inverse variance weighted	0.38	0.59

of the new and old phantoms compared. The calibration lines are shown in figure 1. For measurements of both new and old phantoms the baseline system i.e. summing nine NaI(Tl) detectors was used.

In our laboratory we calculate the MDL in the following manner.

$\left(\frac{\sigma_f}{f}\right)^2 \approx \left(\frac{\sigma_A}{A}\right)^2 + \left(\frac{\sigma_B}{B}\right)^2 - 2\frac{\sigma_A\sigma_B}{AB}\rho_{AB}$, where $(\sigma_f)^2$ is the variance, A is the intercept, B is the slope, σ_A and σ_B are the standard deviation of A and B , and ρ_{AB} is the covariance between A and B (Lee 1999).

Then the MDL is calculated as two times of standard deviation calculated from the variance.

More detail on the MDLs for the old and new phantoms for each acquisition period is provided in table 1.

We obtained an MDL of 0.59 mg F/g Ca for the old phantoms and an MDL of 0.38 mg F/g Ca for the new phantoms. The new phantoms therefore have an improved MDL of a factor of 1.55. However, this old phantom MDL of 0.59 mg F/g Ca is also an improvement by a factor of 1.12 over our previously obtained measurement of 0.66 mg F/g Ca (Chamberlain *et al* 2012). Between the two sets of MDL measurements of the old phantoms, our whole accelerator facility was moved. This included moving of the accelerator itself, the irradiation cavity, and the 4π detection system. Everything was disassembled, moved, and reassembled and some old parts were replaced. New shielding walls were built and the detection system was placed outside of (rather than inside) the accelerator beam hall. Also, in this study one more detector was added to the detection system. It would appear that all of these changes resulted in a moderate improvement (12%) in detection limit.

Anticoincidence mode versus summing single detectors

In order to determine any potential improvement from using different acquisition modes, the ^{20}F spectra from irradiated phantoms containing different fluorine concentrations were measured

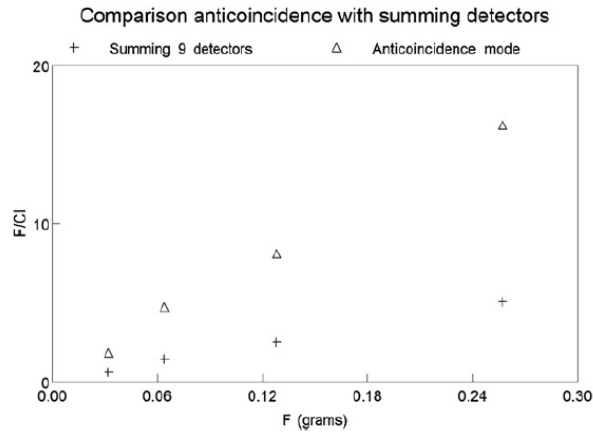


Figure 2. Comparison of different modes, anticoincidence with summing nine detectors.

in different modes. Phantoms were measured as previously described, using a proton energy of 2.15 MeV with a $370 \mu\text{A}$ proton current. Irradiations were performed for 10 s, and the detection time in the 4π NaI(Tl) detector was three 10 s followed by a 120 s wait period and then a 300 s count. Measurements were performed simultaneously using both anticoincidence mode and the summing of nine detectors.

Anticoincidence mode was hypothesized as a potential improvement because the human hand, and our phantoms, both contain both fluorine and chlorine. These two elements emit γ -rays which interfere with each other in our measurement system; the fluorine peak energy being 1.63 MeV while the chlorine peak energy is 1.64 MeV. These energies are not resolved when measured with these NaI(Tl) detectors. In the previously published system (Chamberlain *et al* 2012a), we described a method whereby the chlorine interference is subtracted from the fluorine signal. Chlorine has a longer half-life, so the chlorine signal can be measured after the fluoride signal has decayed. The measured chlorine signal can be corrected for decay over time and then subtracted from the measured combined fluorine plus chlorine signal to obtain the fluorine signal. Our data suggest that this can be performed accurately, but using a subtraction method introduces, of course, uncertainties into the measurement. If the chlorine signal can be eliminated or reduced from the outset, then the measurement uncertainties may be reduced and the detection limit improved. Fortunately, fluorine emits a single γ -ray, while chlorine emits two γ -rays in a cascade which are emitted in coincidence with each other. By counting in anticoincidence mode, in a perfect system, the fluorine counts should remain in the spectrum while the chlorine counts are eliminated or reduced. We compared anti-coincidence counting and summing to test whether in practice an overall improvement is achieved.

Figure 2 shows the comparison of the ratio of F/Cl in the single detector summing and anticoincidence modes. The ratio of F/Cl in the anticoincidence mode can be seen to have been improved by a factor of 2.8 over the same ratio in the summing mode at a typical proton energy of 2.15 MeV. Using anticoincidence mode was found to improve the MDL by factor of 1.2.

Proton energy

A test was performed to determine if better system performance could be obtained by increasing the energy of protons incident on the lithium target. It is known that there is a higher yield

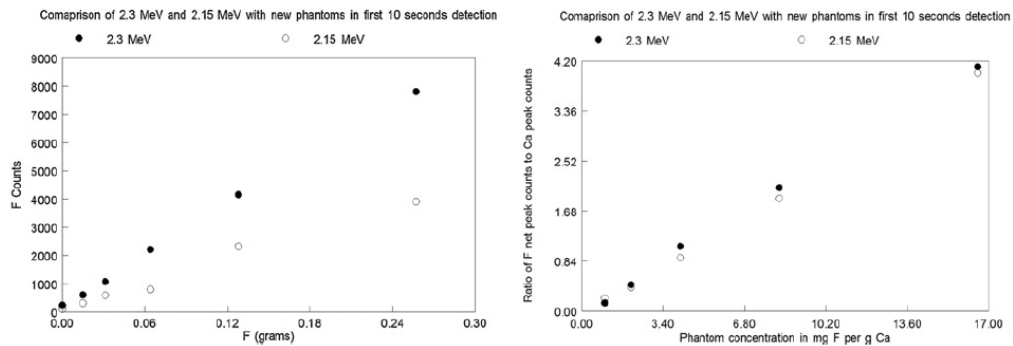


Figure 3. Comparison of calibration lines between different proton energies (2.3 and 2.15 MeV).

of neutrons per proton as the energy is increased. However, increasing the proton energy, of course, also increases the energy of neutrons that enter the irradiation cavity. Irradiations were performed at two proton energies, 2.15 and 2.3 MeV with a proton current of $370 \mu\text{A}$ for 10 s to determine if the additional activation that results from the higher neutron yield is balanced by the neutron dose.

Figure 3 illustrates that a higher proton energy does indeed result in a higher number of fluorine counts. As expected the F/Ca calibration lines for both energies are almost identical as activation of both calcium and fluorine is increased.

The minimum detectable limit for a proton energy of 2.3 MeV was found to be 0.28 mg F/g Ca as compared to the 0.32 mg F/g Ca determined for a proton energy of 2.15 MeV. This is a significant improvement. However, the equivalent dose increases from 30 to 125 mSv (Aslam *et al* 2003, Chamberlain *et al* 2012a).

The MDL improves only by approximately 14% while the dose increases by a factor of 4.17. Using a higher proton energy can increase the fluorine count by improving total neutron flux, but the dose increases dramatically more than the detection limit improves. This is not an advantage and it was therefore determined that for fluorine it is better to irradiate at the lower proton, and thus neutron, energy.

Acquisition sequence

After considering the relatively short half-life of ^{20}F , ($T_{1/2} = 11.2 \text{ s}$), the total acquisition time for fluorine for each phantom was set in the original study at 30 s (Chamberlain *et al* 2012a). In the previous study, this was performed for three acquisitions of 10 s each. The standard timing protocol discussed earlier is used both for calibration phantoms and actual human volunteers. We wished to determine whether this acquisition sequence could be improved upon. We had noted when we published the previous data that the signal to background was significantly better in the two earlier time periods. We hypothesized that performing even shorter acquisitions would result in an improved signal to background ratio, which would improve the minimum detectable limit and the *in vivo* precision. Two sets of acquisition sequences were therefore studied. The phantoms were placed into the detection system, and spectra were acquired for three 10 s periods (as described before) and then the experiment was repeated but using six 5 s acquisition periods. Both sequences were followed by a 120 s wait period and then a 300 s acquisition. Tables 2 and 3 show the data obtained from the two sets of acquisition sequence. We calculate an inverse variance weighted mean (IVWM) to obtain the final estimate of system performance i.e. the overall MDL, because we believe that it is

Table 2. Phantom detection limits determined from the three different timing segments.

Timing segment (s)	M_{DL} (mg F/g Ca)
0–10	0.5
10–20	0.55
20–30	0.67
M_{DL} inverse variance weighted	0.32

Table 3. Phantom detection limits determined from the six different timing segments.

Timing segment (s)	M_{DL} (mg F/g Ca)
0–5	0.37
5–10	0.45
10–15	0.6
15–20	0.66
20–25	1.06
25–30	1.30
M_{DL} inverse variance weighted	0.23

better, in principle, to place more confidence in estimates with lower uncertainties. The short half-life of fluorine means that there is more signal in the first 10 s and 5 s counts, than in the last 10 s and 5 s counts and thus the measurement uncertainty changes and becomes poorer over the timing sequence. As can be seen from the tables the detection of fluorine is indeed significantly better in the first 5 s as compared to the first 10 s.

Tables 2 and 3 provide the M_{DL} from the IVWM method in different timing segments. When using six 5 s the IVWM M_{DL} provide a lower final detection limit than that three 10 s. The data show that using the different acquisition sequence has improved the MDL by a factor of 1.4.

Increased proton current

It was hypothesized that delivering the neutron dose in a shorter period of time could improve the relative activation of fluorine versus chlorine. The rationale behind this is that activation depends on irradiation time and the half-life of the activation product. The relative amount of activity of the created isotope is

$$A = C(1 - e^{-\lambda t})$$

where A is the activity, t is the time of irradiation, λ is the decay constant of the isotope created through activation, and C is a constant that depends on factors such as mass, neutron absorption cross section and atomic number.

^{20}F and ^{38}Cl have significantly different half-lives: 11.2 s and 37.24 min. In Figure 4, we show the relative activation of ^{20}F and ^{38}Cl versus time of irradiation. As can be seen in the figure, shorter irradiation times should mean more activation of ^{20}F relative to ^{38}Cl and thus potentially an improved detection limit.

The figure would predict that the shorter the irradiation the better. However, limitations of the accelerator and lithium target meant that a maximum current of 600 μA was feasible. In order to achieve the same dose to the phantoms this meant delivering the current for 6 s, as opposed to 370 μA for 10 s. Irradiations were therefore performed at a proton energy of 2.15 MeV with a proton current of 600 μA for 6 s. After irradiation, the hand phantoms were again quickly transferred to the detection system for acquisition for six 5 s timing sequences.

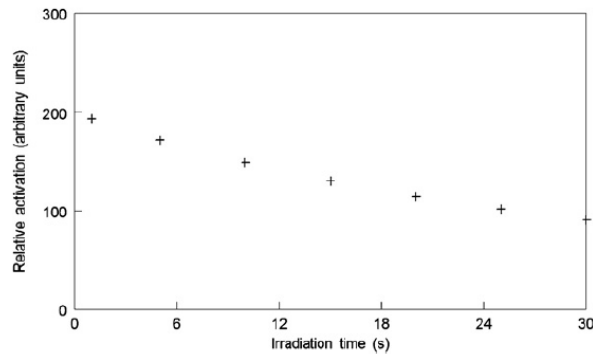


Figure 4. Relative activation of ^{20}F to ^{38}Cl for different irradiation times.

Table 4. Minimum detection limit of phantoms using anticoincidence mode with acquisition using six 5 s timing segments, $600\ \mu\text{A}$ proton current and 6 s accelerator irradiation time.

Timing segment (s)	M_{DL} (mg F/g Ca)
0–5	0.24
5–10	0.42
10–15	0.47
15–20	0.55
20–25	0.71
25–30	0.97
M_{DL} inverse variance weighted	0.17

Increasing the proton current and decreasing the irradiation time was found to improve the MDL improvement by factor of 1.35. The relative activation of ^{20}F and ^{38}Cl would predict an improvement of 1.15 so the experimentally determined value was found to be higher than that predicted. It may be that the slightly better ratio permits better extraction of the ^{20}F signal and so the overall improvement is better than predicted.

Table 4 shows that a minimum detectable limit of 0.17 mg F/g Ca in an anthropomorphic phantom can be achieved. This is a significant improvement compared with our previously published study. This MDL has been improved by a factor of nearly 4 (3.88) compared to the previous measurements performed by Chamberlain *et al* 2012.

We are confident that these data are reproducible. Figure 5 depicts the calculated calibration lines for each of the counting segments. Each calibration line contains measurements taken over a period of several days. During the course of the phantom study, three sets of six phantoms were measured. Phantoms cannot be measured very frequently, as they have to decay for over 48 h after irradiation; the half-life of ^{24}Na being 15 h. The calibration lines for each counting segment are comprised of points from three sets of phantom measurements measured on different days. The point of providing these calibration data is to demonstrate that the measurements are reproducible. The data points from each phantom measurement for a specific fluorine concentration generally lie within two uncertainties of each other. This indicates a good level of measurement reproducibility over a four week period. The intercepts of all the curves were found to be zero within uncertainties, indicating negligible fluorine contamination in the raw materials and some confidence that the mathematical model describing the spectral shape accurately models the background.

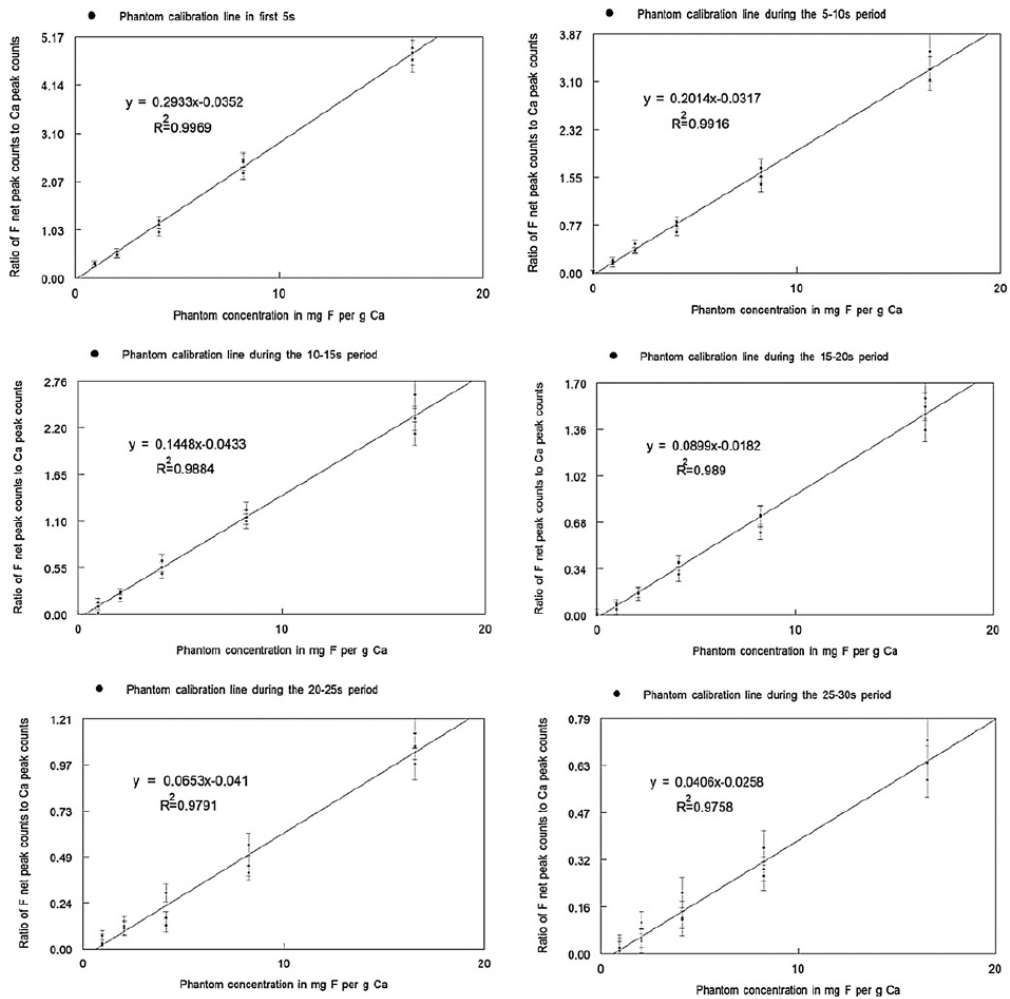


Figure 5. Phantom calibration lines with 2.15 MeV proton energy and 600 μ A for six timing segments.

Alternative detector types: hyperpure germanium detector

The interference in the fluorine and chlorine γ -ray signals observed in sodium iodide detectors led to the hypothesis that there could be an advantage in testing a hyperpure germanium detector. Measurements were therefore performed using a 3500 voltage n-type Pop-Top hyperpure germanium detector (HPGe) photon detector (10% relative efficiency, model GMX-35195-P, ORTEC) and compared against the data from the 4π -NaI(Tl) (detection system). Figure 6 illustrates the HPGe crystal's diameter and the distance from the phantoms that was made to be as close as possible (0.3 cm) to the HPGe window.

A 4π geometry for testing the use of HPGe detectors was not feasible, but the test of a single detector allowed us to calculate any potential improvements in performance. We therefore measured our phantoms under exactly the same irradiation protocols as described earlier and measured with one HPGe detector.

The MDL of fluorine in phantoms with the single HPGe detector was found to be 0.71 mg F/g Ca. This is, of course, a factor of 4.2 poorer than using the 4π NaI (Tl) detector

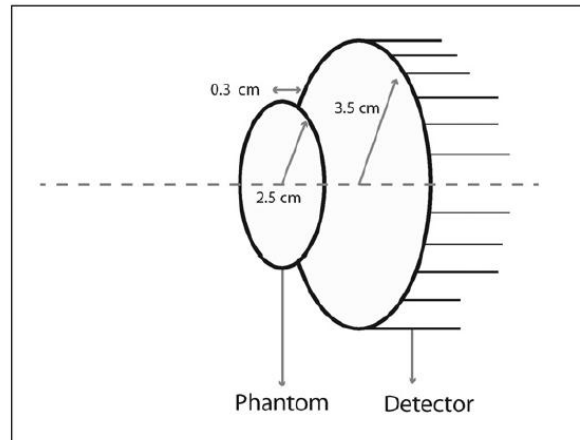


Figure 6. Geometry of HPGe and the distance from the phantoms.

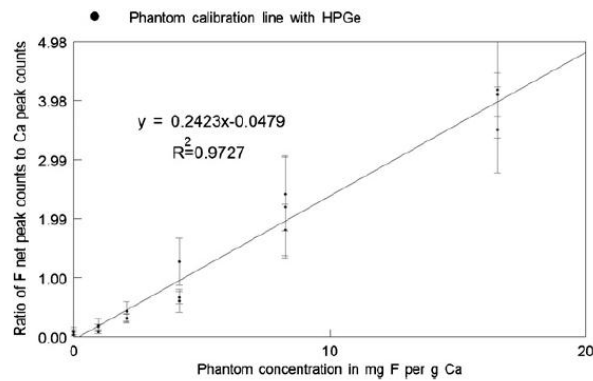


Figure 7. Fluorine phantom calibration line with hyperpure germanium detector.

system. If the overall efficiency could be improved by a factor of 13 to 14 then a hyperpure germanium detector system could be worth adopting. From our geometry the calculated solid angle was 0.3π . It is possible that using a hyperpure germanium detector system with 4π geometry could improve the detection limit. However, this is probably prohibitively expensive to both purchase and operate. Figure 7 illustrates the fluorine phantom calibration line obtained using the single hyperpure germanium detector.

A summary of the factors which were found to improve the detection of fluoride in phantoms are shown in table 5. The series of improvements have led to a reduced detection limit of 0.17 mg F/g Ca. This is an overall improvement in the MDL by factor of 3.88 compared to our previously published study. Previously, we had shown that fluoride could be detected in 95% of volunteers recruited from the geographical area around Hamilton in Southern Ontario (Chamberlain *et al* 2012b). Volunteers were from rural and urban residences and reported drinking city and bottled water. This lowered detection limit will now allow us to test whether individuals with diagnosed dental fluorosis (which occasionally occurs in Canada through the drinking of well water) can be distinguished from the general population using this technique.

Table 5. Summary of the analytical performance for *in vivo* F measurement.

	Proton current (μA)	Proton energy (MeV)	Irradiation time (sec)	Hand dose (μSv)	Counting time (s)	Spectrum analysis	M_{Na} (mg F/g Ca) Using first timing segment	M_{Na} (mg F/g Ca) Using IVWM
Previous study (Chamberlain <i>et al</i> 2012a)	370	2.15	10	35	Three 10 s	Summing detectors	0.92	0.66
This study	600	2.15	6	35	Six 5 s	Anticoincidence mode	0.24	0.17

Conclusions

A series of improvements have been undertaken to a system for the measurement of fluoride in bone *in vivo*. The improvements included

- (1) an improvement in detection limit resulting from adding one more detector to the detection system and the relocation of the equipment of a factor of 1.12;
- (2) the development of better phantoms which improved the MDL by a factor of 1.55;
- (3) the use of anticoincidence counting which improved the MDL by a factor of 1.2;
- (4) the employment of different acquisition timing which improved the MDL by a factor of 1.4;
- (5) the use of higher neutron fluence for a shorter time period which improved the MDL by a factor of 1.35.

Combining these factors has reduced the overall detection limit by a factor of nearly four (3.9). We now intend to perform further studies of human participants to test whether this overall improvement is seen in people. We hope to determine whether the system is capable of distinguishing volunteers who have been diagnosed with dental fluorosis from the general Canadian population who are exposed to low levels of fluoride via water, toothpaste use and tea drinking.

Acknowledgments

Thanks are extended to Justin Bennett, accelerator operator, McMaster University, for his assistance. Funding was provided by the Natural Sciences and Engineering Research Council of Canada.

References

- Aslam, Pejovic-Milić A, Chettle D R, McNeill F E, Pysklywec M W and Oudyk J 2008a A preliminary study for non-invasive quantification of manganese in human hand bones *Phys. Med. Biol.* **53** N371–6
- Aslam, Pejovic-Milić A, McNeill F E, Byun S H, Prestwich W V and Chettle D R 2008b *In vivo* assessment of magnesium status in human body using accelerator-based neutron activation measurement of hands: a pilot study *Med. Phys.* **35** 608
- Aslam, Prestwich W V, McNeill F E and Waker A J 2003 Development of a low-energy monoenergetic neutron source for applications in low-dose radiobiological and radiochemical research *Appl. Radiat. Isot.* **58** 629–42
- Byun S H, Pejovic-Milić A, McMaster S, Matysiak W, Aslam, Liu Z, Watters L M, Prestwich W V, McNeill F E and Chettle D R 2007 Dosimetric characterization of the irradiation cavity for accelerator-based *in vivo* neutron activation analysis *Phys. Med. Biol.* **52** 1693–703
- Byun S H, Pejovic-Milić A, Prestwich W V, Chettle D R and McNeill F E 2006 Improvement of *in vivo* neutron activation analysis of Mn using a 4 π NaI (Ti) detector array *Radioanal. Nucl. Chem.* **269** 615–8
- Chamberlain M, Grafe J L, Aslam, Byun S H, Chettle D R, Egden L M, Orchard G M, Webber C E and McNeill F E 2012a The feasibility of *in vivo* quantification of bone-fluorine in humans by delayed neutron activation analysis: a pilot study *Physiol. Meas.* **33** 243–57
- Chamberlain M, Grafe J L, Aslam, Byun S H, Chettle D R, Egden L M, Webber C E and McNeill F E 2012b *In vivo* quantification of bone-fluorine by delayed neutron activation analysis: a pilot study of hand-bone-fluorine levels in a Canadian population *Physiol. Meas.* **33** 375–84
- Clarke A J, Evans J A, Truscott J G, Milner R and Smith M A 1994 A phantom for quantitative ultrasound of trabecular bone *Phys. Med. Biol.* **39** 1677–87
- ICRP 1975 Report of the Task Group on Reference Man: A Report *ICRP Publication 23* (Oxford: Pergamon)
- Johnson H J E, Kearns A E, Doran P M, Khoo T K and Wermers R A 2007 Fluoride-related bone disease associated with habitual tea consumption *Mayo Clin. Proc.* **82** 719–24
- Kurland E S, Schulman R C, Zerwekh J E, Reinus W R, Dempster D W and Whyte M P 2007 Case report. Recovery from skeletal fluorosis (an enigmatic American case) *J. Bone Miner. Res.* **22** 163–70

-
- Lee S E 1999 *Analyzing Complex Survey Data* vol 22 (New Delhi: Sage) pp 22–39
- Ludlow M, Luxton G and Mathew T 2007 Effects of fluoridation of community water supplies for people with chronic kidney disease *Nephrol. Dial. Transplant.* **22** 2763–7
- Mostafaei F, McNeill F E, Chettle D R, Prestwich W V and Inskip M 2013 Design of a phantom equivalent to measure bone-fluorine in a human's hand via delayed neutron activation analysis *Physiol. Meas.* **34** 503–12
- Pejović-Milić A, Byun S H, Chettle D R, McNeill F E and Prestwich W V 2006 Development of an irradiation/shielding cavity for *in vivo* neutron activation analysis of manganese in human bone *Radioanal. Nucl. Chem.* **269** 417–20
- Yadav A K, Kaushik C P, Haritash A K, Singh B, Raghuvanshi S P and Kansal A 2007 Determination of exposure and probable ingestion of fluoride through tea, toothpaste, tobacco and pan masala *J. Hazard. Mater.* **142** 77–80

Chapter 4

An investigation of the neutron flux in bone-fluorine phantoms comparing accelerator based *in vivo* neutron activation analysis and FLUKA simulation data (Article III)

4.1 Introduction to Article III

The effects of hand position in the cavity and a neutron flux map in and around the irradiation cavity were determined through both Monte Carlo simulation (FLUKA) and experimental methods. A comparison of simulation and experimental methods were found to verify the accuracy of the code, which has not been previously applied in studies of this nature.

The experimental work presented in Article III was performed by the author of this thesis under the supervision of Dr. Fiona McNeill, and with the additional guidance of Dr. David Chettle and Dr. William Prestwich. The simulation code work used input data previously developed by Dr. Witold Matysiak for MCNP studies: the FLUKA input code was developed solely by the author of this thesis. Dr. Chitra Bhatia provided previously unpublished data for comparison tables in the article.

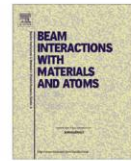
4.2 Contents of Article III

The following article is reproduced with permission. Copyright © 2014, Elsevier.



Contents lists available at ScienceDirect

Nuclear Instruments and Methods in Physics Research B

journal homepage: www.elsevier.com/locate/nimb

An investigation of the neutron flux in bone-fluorine phantoms comparing accelerator based *in vivo* neutron activation analysis and FLUKA simulation data



F. Mostafaei*, F.E. McNeill, D.R. Chettle, W. Matysiak, C. Bhatia, W.V. Prestwich

Medical Physics and Applied Radiation Sciences, McMaster University, Hamilton, ON L8S 4K1, Canada

ARTICLE INFO

Article history:

Received 4 April 2014

Received in revised form 18 September 2014

2014

Accepted 14 October 2014

Available online 7 November 2014

Keywords:

Bone-fluorine

In vivo neutron activation analysis

Accelerator

Phantom

FLUKA

ABSTRACT

We have tested the Monte Carlo code FLUKA for its ability to assist in the development of a better system for the *in vivo* measurement of fluorine. We used it to create a neutron flux map of the inside of the *in vivo* neutron activation analysis irradiation cavity at the McMaster Accelerator Laboratory. The cavity is used in a system that has been developed for assessment of fluorine levels in the human hand. This study was undertaken to (i) assess the FLUKA code, (ii) find the optimal hand position inside the cavity and assess the effects on precision of a hand being in a non-optimal position and (iii) to determine the best location for our γ -ray detection system within the accelerator beam hall.

Simulation estimates were performed using FLUKA. Experimental measurements of the neutron flux were performed using Mn wires. The activation of the wires was measured inside (1) an empty bottle, (2) a bottle containing water, (3) a bottle covered with cadmium and (4) a dry powder-based fluorine phantom. FLUKA was used to simulate the irradiation cavity, and used to estimate the neutron flux in different positions both inside, and external to, the cavity. The experimental results were found to be consistent with the Monte Carlo simulated neutron flux. Both experiment and simulation showed that there is an optimal position in the cavity, but that the effect on the thermal flux of a hand being in a non-optimal position is less than 20%, which will result in a less than 10% effect on the measurement precision. FLUKA appears to be a code that can be useful for modeling of this type of experimental system.

© 2014 Elsevier B.V. All rights reserved.

1. Introduction

We have previously shown that neutron activation analysis (NAA) is a useful technique for the *in vivo* measurement of fluorine [12,11]. We developed a system, which measures the delayed gamma rays emitted following the decay of ^{20}F . This isotope is produced via the neutron capture reaction $^{19}\text{F}(n,\gamma)^{20}\text{F}$. The system is being developed to study people who are commonly exposed to fluorine. The element, fluorine, is found in rocks, clay, coal, water and air and in some areas (often associated with calcium-poor conditions) high levels of fluoride occur naturally in water where substitution of calcium by sodium occurs [17]. In addition, some countries in the world deliberately add fluoride to drinking water and this becomes a source of exposure. Fluoride is added to drinking water because there are many studies which demonstrate that fluoride at specific levels (0.5–1.5 mg F/l) can be useful for the prevention of tooth decay and for enhancing bone formation [17].

However, individuals who have been exposed to high levels of fluoride through drinking water, food and air for extended time periods can suffer from dental and skeletal fluorosis [1,15]. The risk/benefit versus concentration curve for fluoride would therefore appear to be U-shaped, and this has led to some controversy about a 'safe' level of exposure to fluoride. We developed the NAA-based technique to assess fluorine exposures directly, via the assessment of the level of fluorine per unit calcium in bone. Our goal is to apply this technique in studies of population health and thus assist in the determination of the optimal exposure to fluorine. Previously, such studies have had to employ exposure assessments, which are based on water data, and often on self-assessments of the amount people drink, which can be inaccurate. Previously, there has been no non-invasive method available. The limited data in the literature are drawn from biopsies or autopsy measurements [16,18,24,25,40]. We have recently shown however a minimum detection limit for fluoride of 0.17 mg F/g Ca in bone phantoms [31]. This work followed on from earlier studies, which showed that we could detect fluoride in the bone in the majority of adult urban Canadians in a small pilot study of volunteers. We

* Corresponding author.

could measure fluoride with 95% confidence in 33 out of 34 volunteers [11,12].

We employ a system, which uses the McMaster University Tandetron accelerator to irradiate both calibration phantoms and human hands. The system uses an irradiation cavity, which has been described extensively in the literature [3,9,38]. The accelerator produces neutrons via the ${}^7\text{Li}(p,n){}^7\text{Be}$ reaction by irradiating a metallic lithium target with energetic protons. The target is thick, by which we mean protons slow down in the target. The range of proton energies interacting in the target means that a broad neutron energy spectrum is produced from a possible maximum down to thermal energies. Table 1 shows the maximum and mean neutron energy produced for each proton energy incident on the thick lithium target.

The neutrons produced in the target then pass through a 2 cm thick by 30 cm diameter polyethylene moderator, which, through scattering, further reduces the average energy of the emitted neutron spectrum to a region (at thermal to near thermal energies) where the neutron capture cross sections are generally higher for the elements of interest in the hand [10,9,38]. A 2 cm lead filter is positioned to absorb gamma rays created by the ${}^7\text{Li}(p,p'){}^7\text{Li}$ target reaction and to attenuate gamma rays produced from reactions within the polyethylene moderator. Both the neutron moderator and gamma ray filter serve to reduce the gamma and fast neutron dose to the subject's hand, in terms of improving the activation per unit dose, by increasing the thermal neutron flux per emitted neutron [10,9,38]. A 25 cm graphite reflector is employed to scatter neutrons back into the center of the cavity, increasing the thermal flux per incident neutron, making more efficient use of the generated neutrons. The outer 2 cm lead and 1.4 cm boron plastic walls provide further neutron and gamma ray shielding to the subject's body [10,9,38]. Finally, a 30 cm layer of borax, polyethylene and polyester resin was used to cover this box to reduce the neutron flux at the outer surface. A cross sectional drawing of irradiation cavity is shown in Fig. 1.

We have used this experimental arrangement over a period of several years for a series of *in vivo* studies of aluminum, fluorine, manganese and magnesium. Our observations from the work with people encouraged us to determine whether there was a variation in the thermal neutron flux across the interior of the irradiation cavity, and hence whether there was a "optimal" position for the irradiation of the hand in the cavity [2,3,6,7,14]. It was clear to us when measuring volunteers that because people are of different heights and arm lengths, it was sometimes possible for the position of the hand to vary in the cavity. The measurement of fluorine employs a determination of the ratio of fluorine to calcium. We measure the F/Ca ratio for two reasons: (1) the level of fluorine per unit calcium i.e. the level of fluorine in the bone mineral matrix is a good marker of fluoride uptake and (2) the normalization of the F to Ca signals should ideally mean that variations in the thermal flux which may arise from variations in position should not affect the accuracy of the measurement but only the precision. This normalization is based on the assumption that the ratio of the activation of fluorine and calcium should remain constant regardless of whether the thermal flux varies, because it is only thermal neutrons which activate the sample. In this instance, however,

the neutron flux in the cavity is not completely thermalized, so this normalization has limits. The neutron flux in the cavity has a spectrum, which ranges from thermal into the low energy range. In addition, the ${}^{19}\text{F}$ and ${}^{48}\text{Ca}$ isotopes used for the measurement do not have pure $1/v$ neutron cross-sections: there are resonances in the ${}^{19}\text{F}$ cross-section (taken from ENDF). If the neutron spectrum changes it is possible that the relative activation of fluorine to calcium changes. However, we have performed measurements which show that in each case the elemental activation is dominated by thermal neutrons. Table 2 shows the measured proportion of non-thermal activation of Ca and F in the cavity at various incident proton (and thus neutron) energies.

The resonances in the ${}^{19}\text{F}$ neutron cross-section do mean that in our experiments up to 6% of the F signal can arise from non-thermal neutrons, while only 1% of the ${}^{49}\text{Ca}$ arises in this way. However, it can be seen from the data that for the variation from the maximum (as emitted off the target) neutron energy spectrum to the minimum, the activation of F from thermal neutrons varies from 94.5% to 92.3% and for calcium from 98.8% to 98.6%. The relative ratio (for the same level of fluorine) therefore only varies by approximately 2%. Other factors such as changes in current can be far greater than this number. While the normalization is not perfect, it can be applied to within the uncertainties of measurement because the neutron spectrum in the cavity is mostly thermalized. Fig. 2 shows the neutron capture cross-sections for ${}^{48}\text{Ca}$ and ${}^{19}\text{F}$.

We use a detection system composed of nine NaI(Tl) detectors in a nearly 4π geometry. The short fluorine half life of 11.2 s means the detectors have to be placed near the hand irradiation cavity. Transfer from the irradiation cavity to the detection system should ideally take less than one half-life, so ideally less than 10 s in this instance. ${}^{128}\text{I}$ is the main activation isotope that produces significant background in the spectrum in NaI(Tl) detectors if they are subjected to a thermal neutron flux. Determining the best location, i.e. the position with the least potential for activation of the detection system, within the accelerator beam hall, is essential. The 4π NaI(Tl) system with its shielding and built-in stand weighs almost 2000 kg. It must be moved with a crane and each change in position takes a significant amount of time. Moving the system and determining the relative activation of the system was not a reasonable option for us, given that the Tandetron is used by multiple researchers, and beam time can only be booked in short allotments. Time on the Tandetron must be used efficiently.

We performed experiments where we irradiated ${}^{55}\text{Mn}$ wires in a neutron field, and subsequently counted the induced γ -ray activity and used FLUKA [20,32] to simulate the irradiation cavity. Using these data, we had three goals:

1. We wished to determine the variations in the neutron flux in and around the cavity, and assess the code against experimental measurements to see if FLUKA is a reasonable code for this kind of work.
2. Using the Mn experimental and simulation data, we wished to determine the potential effect of 'incorrect' hand positioning.
3. Finally, we wished to determine the best location for our fluorine detection system within the accelerator beam hall in order to decrease potential activation of the detectors in our system.

2. Materials and methods

2.1. Experiment

2.1.1. Irradiation and detection

Samples were irradiated in the irradiation cavity which was mounted on the end of the beam line of the Tandetron accelerator. The spectra from samples were then acquired using a 4π detection system consisting of an array of eight NaI(Tl) detectors (of

Table 1
Maximum and mean neutron energy [29].

Proton energy (MeV)	Maximum neutron energy (keV)	Mean neutron energy (keV)
2	230.6	75.1
2.1	350.4	108.4
2.2	463.4	158.9
2.3	573.1	233.1

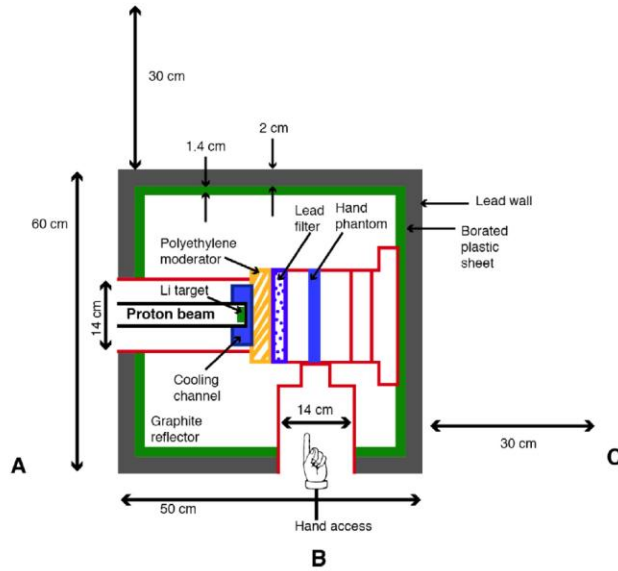


Fig. 1. A cross-section drawing of the target, moderator, filter and irradiation zone.

Table 2
Measured proportion of non-thermal activation of Ca and F.

Proton energy (MeV)	% non-thermal neutron contribution to activation	
	⁴⁸ Ca	¹⁹ F
2.3	1.17	5.46
2.2	1.65	7.73
2.1	1.64	7.68
2	1.41	6.61

dimension 102 × 102 × 406 mm), together with a ninth “plug” detector (of dimensions 102 × 102 × 102 mm). This spectrometer was used in order to enhance the γ -ray detection efficiency [9]. The detector signals can be acquired in several different modes. In ‘singles mode’, the spectrum from the individual photomultiplier tube (PMT) output signals of each detector are fed into a digital signal processor (DSP) and subsequently the master DSP. This, of course, means that the spectra from each detector must

be gain matched. For gain stabilization, every day, before starting measurements all nine detectors are matched by voltage adjustment. This is necessary because the drifts in the detectors can be significant even over a period of a few days.

The detection system is however generally employed in anti-coincidence and coincidence mode amongst all nine detectors simultaneously by adding separate shaping and time pick-off electronics to each detector unit. The time pick-off of each detector unit, which is 1 μ s, is performed by the peak timing method using a digital signal processor (DSP). This technique was originally employed in the system because, for measurements of fluorine, there is an interfering γ -ray from chlorine. Chlorine is, of course, an element that is always present in human tissue. A chlorine γ -ray at $E_\gamma = 1.64$ MeV is not resolved from a fluorine γ -ray at $E_\gamma = 1.63$ MeV. In order to measure fluorine in the body, we have to account for the chlorine signal. Fortunately, chlorine emits two γ -rays partly in coincidence, while fluorine does not. By setting a time window and allocating counts to two spectra, an

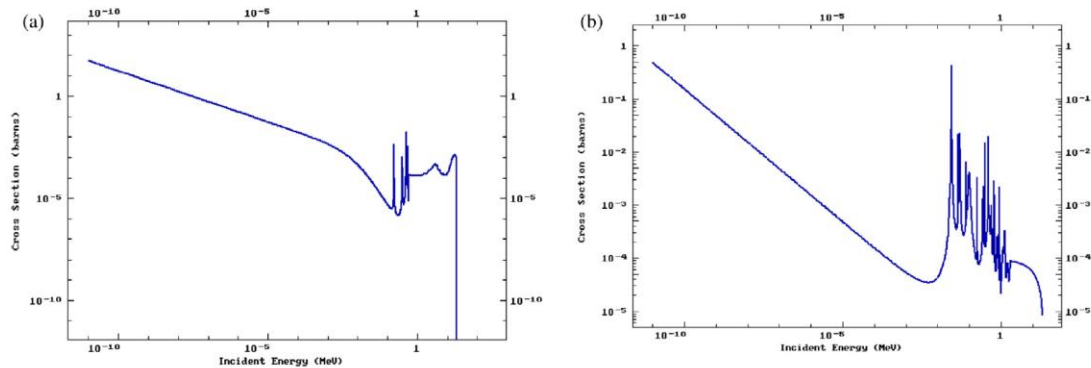


Fig. 2. The capture cross-sections of (a) ⁴⁸Ca and (b) ¹⁹F with neutron energy (taken from ENDF).

'in coincidence' spectrum and an 'in anti-coincidence' spectrum, it was found that the interference of chlorine in fluorine measurements could be significantly reduced. Of course, if the two spectra are added together, they result in the 'singles' spectrum. Our electronics are now set up to record the two coincidence and anti-coincidence spectra. Fig. 3 shows the coincidence and anti-coincidence electronic set-up.

The overall resolution of the spectrum accumulated by the nine summed detectors in anti-coincidence mode was rather poor since three of the detectors had bad resolution. For example the poorest detector had a resolution of 13% at 662 keV while the best detector had a resolution of 7.4% at 662 keV. Fig. 3 also shows the arrangement of the nine NaI(Tl) detectors in 4π geometry.

For measurements of Mn wires, the 4π detection system was located in a separate room at some distance from the Tandemtron irradiation room, to avoid potential activation of the NaI detectors [10]. However, as previously mentioned, when measuring fluorine in people (or phantoms), the half-life of fluorine is so short that the detection system has to be moved and placed in the accelerator beam hall near the irradiation cavity. People cannot be moved quickly enough (i.e. in less than 10 s) from one room to another to measure fluorine.

In addition to the 4π system, a small number of Mn wire measurements were also performed with a hyperpure germanium detector. This permitted the spectra to be studied with better resolution, and allowed the calculation of detection efficiency and hence neutron flux to be performed using a ^{54}Mn standard.

The γ -ray spectra from the irradiated manganese wires were counted and the thermal and above thermal neutron fluxes were back calculated from the measurement of activity. The Mn activity from the sum spectra was used to determine the neutron flux. An example manganese spectrum of an irradiated wire, which was irradiated inside an empty polyethylene bottle, with a detector of 8% resolution, is shown in Fig. 4.

2.2. Monte Carlo simulation

In order to estimate the neutron flux in and around the cavity, Monte Carlo calculations were carried out using the FLUKA code [20]. FLUKA has been previously shown to be an extremely useful tool in the field of radiation physics [33–36]. It is a multipurpose transport Monte Carlo code for calculations of particle transport and interactions with matter, covering an extended range of applications such as proton and electron accelerators. Although FLUKA

can model proton interactions, we have, over the last decade performed significant work in characterizing the neutron spectra produced from targets on our accelerators. We did not therefore model the proton interactions using FLUKA. The lithium target source was represented by a point-source geometry and an input file was instead created which modeled a neutron source at the Li target position with an energy and angular distribution [37]. The neutron flux was scored at various positions by point tallies with three energy groups scoring (0.0000005, 0.01 and 1 eV) and the numbers of histories were chosen to be in the order of millions. The FLUKA neutron flux equivalent was multiplied by an experimentally determined neutron production rate at the Li target since the FLUKA flux is a relative value normalized to the neutron source strength [29,20]. Not every proton as measured by the accelerator produces a neutron; factors such as beam focusing and oxide layers on the target can affect production. In this work we used the experimental neutron production data of Lee and Zhou [29]; we have in other work in our laboratory found similar rates of neutron production per unit current [4,5].

For studies of the center position inside the cavity, the neutron spectra as produced by different incident proton energies (2, 2.1, 2.2 and 2.3 MeV) were studied in the simulation and experiments as the *in vivo* measurements of various elements have been performed previously at these energies [3,9,38]. For further simulations, which included positions both inside and outside the cavity, the neutron spectrum produced by protons of energy of 2.3 MeV was used, and compared with the experimental data.

3. Analysis and results

3.1. Flux determined at different incident proton energies

A series of experiments was performed where manganese wires were placed inside the irradiation cavity via the hand access hole, and were irradiated by the accelerator neutrons produced from 2.00 MeV, 2.10 MeV, 2.20 MeV and 2.30 MeV proton energies on the Li target, respectively. Irradiation was performed with a proton current of 400 μA for 30 s. After irradiation the wires were counted for 120 s in anticoincidence mode in the 4π NaI(Tl) detection system. The neutron flux determined by experiment and FLUKA are compared and shown in Table 3. Neutron flux estimates were determined for a position in the centre of the irradiation cavity.

As can be seen from the Table 3, the experimental estimates are the same as the FLUKA estimates to within uncertainties, although

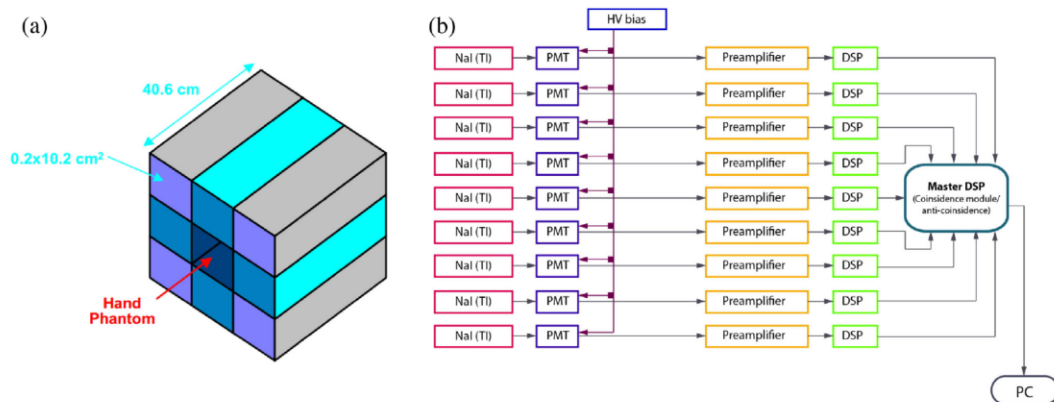


Fig. 3. (a) Arrangement of the nine NaI(Tl) detectors in 4π geometry, (b) block diagram to illustrate the detection in coincidence and anti-coincidence modes.

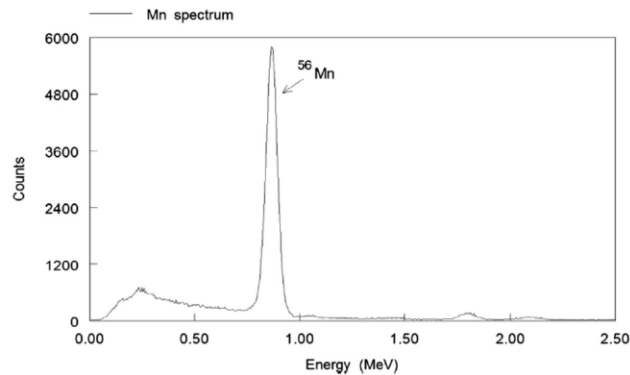


Fig. 4. Manganese wire spectrum inside the empty bottle.

Table 3
Neutron flux with FLUKA & experiments.

Ep [MeV]	Calculated with FLUKA (n/s cm ²)	Calculated from experiment (n/s cm ²)	Ratio experiment to FLUKA
2	$(1.82 \pm 0.05) \times 10^8$	$(1.77 \pm 0.04) \times 10^8$	0.97 ± 0.03
2.1	$(3.13 \pm 0.03) \times 10^8$	$(3.11 \pm 0.03) \times 10^8$	0.99 ± 0.01
2.2	$(5.51 \pm 0.08) \times 10^8$	$(5.43 \pm 0.08) \times 10^8$	0.99 ± 0.02
2.3	$(8.9 \pm 0.09) \times 10^8$	$(8.85 \pm 0.08) \times 10^8$	0.99 ± 0.01

they are admittedly in every case are slightly lower. On average, the experimentally determined estimate is $99 \pm 2\%$ of the FLUKA prediction. There is some slight suggestion ($p = 0.02$) that the experimental data are less than the predicted. This is probably due to the fact that the neutron emission from the target that is used to calculate the FLUKA neutron flux [29] is not a perfect model of the neutron production for our experiment. It is, in fact, a remarkably good match, given the uncertainties, and differences in experimental set-up between the two geographical centres.

These data are also shown in Fig. 5. Error bars are too small to be seen in the figure. The results fall within errors and they do provide confidence in the FLUKA simulation: it is predicting the same pattern of neutron flux as the experiment. A regression of FLUKA on experimentally estimated neutron flux yields a relationship of $Expt = (0.99 \pm 0.006)FLUKA - (4 \times 10^6 \pm 3 \times 10^6)$, $R^2 = 0.999$, ($p < 0.001$). This regression also shows that the experimentally derived slope is 99% of the simulation result. We performed a regression, to determine whether there is a constant systematic offset between the experiment and the simulation, or a different slope. The data show, however, that the offset is not significantly different from zero to within uncertainties, and the FLUKA simulation appears to perform extremely well on a difficult per source neutron test.

3.2. Neutron flux map determined by Monte Carlo simulation

Monte Carlo simulation was also used to calculate the neutron fluxes in a further series of positions inside, and outside of, the irradiation cavity. Table 4 and Fig. 6 show the locations of all of the neutron flux estimates in and around the cavity and the neutron fluxes determined by FLUKA for those positions. To determine the flux incident on the bone-fluorine phantom as if it were in different positions (such as might happen with subject motion during an *in vivo* measurement), the neutron flux at different positions in the hand access hole (7, 9 and 10 cm) was calculated. Fluxes outside of the cavity were also determined as this is of interest

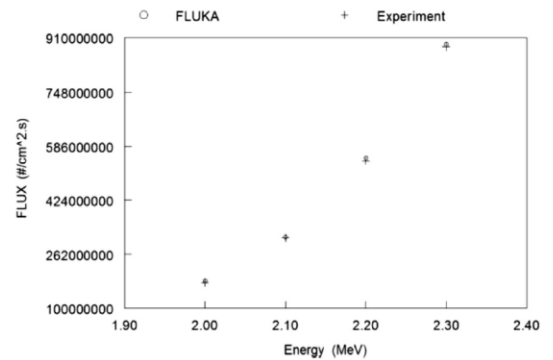


Fig. 5. Comparison between experiment and FLUKA of neutron fluxes for different proton energies.

because of potential activation of the detection system. These positions outside of the box provide important information regarding the neutron flux incident on the detector system.

As can be seen from Table 3 the motion of the phantom inside the hand access hole can change the flux incident on the phantom or hand. If the hand were to be moved to an extreme position, nearly withdrawn from the box, the neutron flux would drop by a factor of 10. However, when a person is irradiated, there is a water shielding system placed around their arm, to shield the torso, which essentially locks their arm in place for the 30 seconds of the *in vivo* measurement. An experimenter stays with the subject during this time. It is unlikely that any hand would be withdrawn this far during the actual measurement. A much more likely scenario is that due to different arm lengths, a subject's hand could be in slightly different positions near the centre of the cavity during the measurement. The neutron flux near the centre of the irradiation box was found to vary from $(9.24 \pm 0.09) \times 10^8$ to $(9.84 \pm 0.1) \times 10^8$ n/cm²/s. This variation of 0.94 in the neutron flux ratio would be expected to change the individual measurement uncertainty by a factor of 0.97. That is, FLUKA predicts that the uncertainty could vary from a best minimum value to an increased uncertainty, by a factor of 1.03, if the hand is not optimally positioned at the centre of the cavity.

3.3. Experimental neutron flux map within the irradiation cavity

In order to simulate different hand positions inside the irradiation box (near the centre of the irradiation box), and compare it

Table 4
Neutron flux in the different position of irradiation box calculated by FLUKA.

Position	Neutron flux (#/cm ² s)	Position	Neutron flux (#/cm ² s)	Position	Neutron flux (#/cm ² s)
1	$(2.16 \pm 0.06) \times 10^7$	14	$(3.74 \pm 0.06) \times 10^6$	27	$(8.7 \pm 0.07) \times 10^6$
2	$(1.8 \pm 0.07) \times 10^7$	15	$(4.52 \pm 0.07) \times 10^6$	28	$(7.78 \pm 0.08) \times 10^7$
3	$(1.22 \pm 0.06) \times 10^7$	16	$(8.1 \pm 0.08) \times 10^6$	29	$(2.12 \pm 0.06) \times 10^6$
4	$(5.62 \pm 0.08) \times 10^8$	17	$(6.53 \pm 0.08) \times 10^7$	30	$(7.3 \pm 0.06) \times 10^5$
5	$(4.3 \pm 0.08) \times 10^8$	18	$(5.73 \pm 0.07) \times 10^7$	31	$(9.1 \pm 0.05) \times 10^5$
6	$(9.63 \pm 0.07) \times 10^7$	19	$(4.41 \pm 0.07) \times 10^7$	32	$(9.24 \pm 0.09) \times 10^8$
7	$(7.79 \pm 0.08) \times 10^7$	20	$(6.41 \pm 0.06) \times 10^6$	33	$(9.84 \pm 0.1) \times 10^8$
8	$(8.9 \pm 0.07) \times 10^7$	21	$(4.32 \pm 0.07) \times 10^6$	34	$(9.63 \pm 0.08) \times 10^8$
9	$(1.38 \pm 0.05) \times 10^6$	22	$(5.84 \pm 0.07) \times 10^6$	35	$(1.71 \pm 0.06) \times 10^6$
10	$(5.26 \pm 0.06) \times 10^6$	23	$(2.54 \pm 0.05) \times 10^5$	36	$(3.91 \pm 0.04) \times 10^4$
11	$(5.79 \pm 0.08) \times 10^7$	24	$(2.15 \pm 0.05) \times 10^5$	37	$(3.64 \pm 0.05) \times 10^4$
12	$(1.6 \pm 0.08) \times 10^8$	25	$(2.68 \pm 0.04) \times 10^5$	38	$(3.52 \pm 0.05) \times 10^4$
13	$(2.43 \pm 0.06) \times 10^6$	26	$(2.8 \pm 0.07) \times 10^7$		

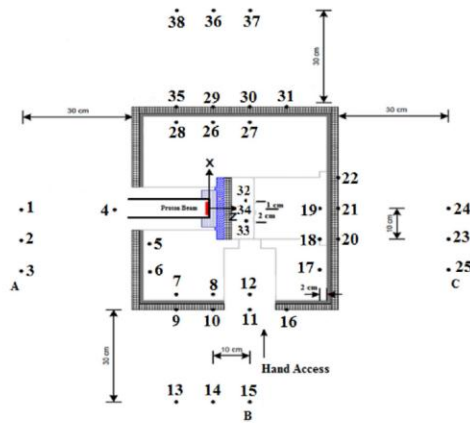


Fig. 6. Neutron flux in the different position of irradiation box calculated by FLUKA.

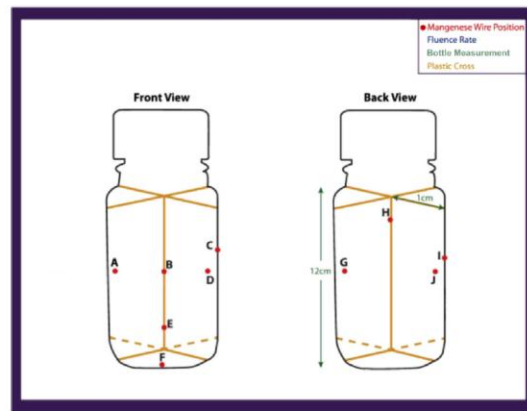


Fig. 7. Neutron flux map inside the empty bottle.

with the hand positions by Monte Carlo simulation, the neutron flux distribution within the irradiation cavity was determined experimentally for a number of different scenarios. Manganese wires were irradiated in (i) an empty Nalgene bottle, (ii) in a bottle containing water, (iii) in a bottle covered with cadmium foil and (iv) in an actual bone-fluorine phantom. The Nalgene polyethylene bottles had been used as the outer container of fluorine bone phantoms in previous *in vivo* studies [12,11]. The Mn wires were positioned in different places inside these Nalgene bottles and were irradiated by placing the bottles inside the irradiation cavity. The manganese gamma rays produced via the $^{55}\text{Mn}(n,\gamma)^{56}\text{Mn}$ reaction were then counted by placing the bottles inside the 4π NaI(Tl) detector system. Irradiation was performed at proton energy of 2.3 MeV with a proton current of 400 μA for 30 s. After irradiation the wires were counted for 120 s in anticoincidence mode. Fig. 7 is an illustration of two views of the bottle, and the fluxes determined at the different positions within the empty Nalgene bottle at which the manganese wires were located.

Table 6 shows a somewhat similar pattern to the results of the simulation, in that there is variation in the neutron flux in the centre of cavity but the experimentally determined variation at the centre of cavity is predicted to be somewhat higher. The neutron flux near the centre of the irradiation box was found experimentally to vary from $(9.1 \pm 0.06) \times 10^8$ to $(9.98 \pm 0.09) \times 10^8$ n/cm²/s. This is a variation of 0.91 ± 0.01 in the neutron flux. Changing the position of the manganese wires inside the bottle does cause a small variation in the flux. The standard deviation of the data would suggest that the neutron flux could vary by up to 9% at different positions.

This would mean the *in vivo* measurement uncertainty could vary by up to 3% at the centre of cavity. The fluxes at specific positions generally agree with FLUKA results. For example, in the middle of the front view the experimentally determined flux is $(9.79 \pm 0.1) \times 10^8$ (n/s cm²), which is comparable with $(9.6 \pm 0.08) \times 10^8$ (n/s cm²) from FLUKA, (previously shown in Table 4).

A Nalgene bottle, filled with water and with the manganese wires in the same positions as used in the empty Nalgene bottle, was irradiated. Irradiation and detection were performed with the same parameters as the empty bottle. Adding water does reduce the neutron flux within the bottle. At different positions, the reduction is of the order of a few percent. Again, this reduction in neutron flux should not affect the accuracy of the measurement, but it is expected to worsen the measurement uncertainty. Water-based phantoms, and by implication, human hands, will have a slightly higher measurement uncertainty than in-air neutron flux measurements would predict.

In order to determine the activation due to neutrons with energies above the thermal range, the cadmium difference technique was employed [26]. Our data show significantly decreased activation when samples were cadmium-wrapped. The eight points used were the same as in the previous experiments, with the outer two points removed because covering the bottle with cadmium changed the wire position. The majority of the in-air activation in the cavity is a consequence of thermal neutrons. For example, at the central position only 2% of Mn activation is from neutrons above thermal energies. The irradiation cavity does a remarkable job of

Table 5
Some data used in above measurements [27].

Nuclear reaction	Cadmium transmission factor F_{Cd}	Effective resonance energy*, E_r (eV)	Half-life (h)	Energy (keV)	Emission probability γ (%)	Self attenuation factor, F_g
$^{55}\text{Mn}(n,\gamma)^{56}\text{Mn}$	1	468 ± 51	2.5789	846.754	98.9	1.010

* $E_{cd} = 0.55$ eV.

Table 6
Comparison of neutron fluxes in the centre of the cavity.

Position	Empty bottle (n/s cm ²)	Bottle with water (n/s cm ²)	Ratio bottle with water to empty bottle	Bottle covered with cadmium (n/s cm ²)	Fluorine phantom (n/s cm ²)
A	$(9.71 \pm 0.08) \times 10^8$	$(9.51 \pm 0.08) \times 10^8$	0.98 ± 0.01	$(1.65 \pm 0.03) \times 10^7$	$(6.36 \pm 0.07) \times 10^8$
B	$(9.79 \pm 0.1) \times 10^8$	$(9.54 \pm 0.09) \times 10^8$	0.97 ± 0.01	$(1.92 \pm 0.04) \times 10^7$	$(7.34 \pm 0.09) \times 10^8$
C	$(9.91 \pm 0.18) \times 10^8$	$(9.21 \pm 0.1) \times 10^8$	0.93 ± 0.02		
D	$(9.63 \pm 0.1) \times 10^8$	$(9.17 \pm 0.08) \times 10^8$	0.95 ± 0.01	$(1.78 \pm 0.05) \times 10^7$	$(7.48 \pm 0.09) \times 10^8$
E	$(9.98 \pm 0.09) \times 10^8$	$(9.01 \pm 0.09) \times 10^8$	0.90 ± 0.01	$(1.88 \pm 0.04) \times 10^7$	
F	$(9.71 \pm 0.08) \times 10^8$	$(9.1 \pm 0.08) \times 10^8$	0.94 ± 0.01	$(2.51 \pm 0.06) \times 10^7$	$(7.77 \pm 0.08) \times 10^8$
G	$(9.66 \pm 0.08) \times 10^8$	$(9.11 \pm 0.07) \times 10^8$	0.94 ± 0.01	$(1.58 \pm 0.04) \times 10^7$	$(8.55 \pm 0.08) \times 10^8$
H	$(9.93 \pm 0.13) \times 10^8$	$(9.25 \pm 0.1) \times 10^8$	0.93 ± 0.02	$(1.77 \pm 0.06) \times 10^7$	
I	$(9.1 \pm 0.1) \times 10^8$	$(8.57 \pm 0.07) \times 10^8$	0.94 ± 0.01		
J	$(9.48 \pm 0.09) \times 10^8$	$(9.18 \pm 0.09) \times 10^8$	0.97 ± 0.01	$(1.77 \pm 0.05) \times 10^7$	$(8.48 \pm 0.08) \times 10^8$

reducing the average neutron energy incident upon a hand as compared to the neutron spectrum emitted at the lithium target.

The effective resonance energy for Mn is 468 eV, the cross-section for this energy was found to be ~ 0.55587 b. Using the Eq. (1) below, with the limits of the integral set as 0.55 eV to 0.496 MeV, (for neutrons produced from a proton energy = 2.3 MeV), the value of integral would be ~ 1.75 b.

$$I = \int \frac{\sigma(E)}{E} dE \quad (1)$$

where $\sigma(E)$ is cross section of selected energy and E is the neutron energy [27,42].

Then the above thermal neutron flux was calculated from Eq. (2), where

$$\phi_{epi} = \frac{A_{epi} F_{Cd} W e^{\lambda t'}}{N_0 \lambda t} \quad (2)$$

ϕ_{epi} is the above thermal neutron flux, A_{epi} is the measured manganese wire activity due to above thermal neutrons, t is the time of exposing to neutron radiation, t' is the time between the end of the neutron exposure and the beginning of the counting in the detector, λ is the decay constant, F_{Cd} is the correction factor for absorption of above thermal neutrons in the cadmium sheets, which retrieved from Table 5, W is an atomic weight (^{55}Mn) and N_0 is an Avogadro's number [27,42].

Measurements were also performed in a fluorine calibration phantom. The phantom was a type used in previous published *in vivo* studies as a calibration standard. It was a mixed dry powder of bone composition material (4.6 g NaNO_3 , 1.78 g NH_4Cl and 37.25 g CaCO_3), with 0.25 g F added [11,12,19,30]. Manganese wires were placed at various positions inside the phantom which was positioned inside the cavity and irradiated as described earlier. The neutron flux determined in different conditions in the centre of cavity are compared and shown in Table 6.

The neutron fluxes inside the fluorine phantom show a similar distribution as in the water phantom. However, the measured thermal neutron flux is significantly lower in the powder phantoms. A fission chamber was used to monitor the beam current, and the fission chamber data for the two sets of data are recorded as being identical. This means the number of neutrons entering the irradiation cavity were the same for both sets of irradiations. At the centre of the phantom, the neutron flux inside the powder phantom (position B) is $23 \pm 1\%$ lower than inside a water phantom. The overall neutron absorption by the two materials is roughly equivalent.

Table 7
Relative thermal neutron capture and neutron scattering rates in fluorine powder and water phantom.

	Total thermal neutron capture	Total neutron scattering
Fluorine powder phantom	1.33	21.11
Water phantom	1.64	414.4

Table 7 shows a calculation of the thermal neutron absorption rate for the two materials, powder phantom and water. As can be seen, the mass averaged reaction rate is such that the expectation was that the water would absorb more neutrons and the measured thermal flux in the centre would be lower. However, we suggest that the difference in thermal neutron flux, which is lower in the powder fluorine phantom than the bottle with water, is perhaps explained by the fact that water is a better neutron scatterer than the powder. The mass averaged relative neutron scattering rate is also shown in Table 7. The previous cadmium data do show that there is a measurable non-thermal neutron flux in the cavity. More of those neutrons may be scattered into the centre of the phantom by the water than by the powder and this may mean that the measured thermal flux inside the water is higher than in the powder.

3.4. The best location for fluorine detection system

In order to confirm the FLUKA simulation results and thus ultimately find the best position for the $4\pi\text{-NaI(Tl)}$ system for *in vivo* studies, a series of experiments was performed at three different positions (A, B and C) around the cavity, as shown in Fig. 1. These positions were chosen because the location of the detection system is limited: the detection system needs to be positioned on the same side of the irradiation cavity as the hand access aperture. It would take more time than the 10 s permitted to move a person from one side of the beam line to the other. A 3500 voltage n-type Pop-Top HPGe photon detector (35% relative efficiency, model GMX-35195-P, ORTEC) was placed in these three positions. This detector was used, because it was much easier to move, and test quickly, than the 2000 kg 4π NaI box. The neutron beam was turned on for a short period of time. The accelerator was then turned back off, and a count on the HPGe detector was started. Activation of the aluminum in the detector canister meant that a signal from the aluminum γ -rays could be detected in the germanium crystal. This

Table 8

The optimal position of experimental measurements around the irradiation cavity.

Detector position	Counts (arbitrary units)
A	394 ± 21
B	297 ± 17
C	110 ± 11

size of this signal was assumed to be proportional to the activation that would result in the NaI detection system. Table 8, shows the experimental gamma-ray signal of aluminum (in arbitrary units) measured in the HPGe detector. These data, combined with the FLUKA neutron flux estimates from Table 4, allowed us to conclude that position “C” is the best place for NaI(Tl) detector system during *in vivo* measurements.

The data suggest that the irradiation cavity effectively reduces the thermal neutron fluxes by three orders of magnitude outside of the box. The data indicate clearly that the detection system should not be placed in line with the beam, behind the box, but should be placed off axis. Since the predicted thermal neutron flux is still significant, 2.5×10^5 n/cm²/s, and there were significant counts in the HPGe detector, the detection system clearly needs an additional layer of borax, polyethylene and polyester resin. These were in fact used in further *in vivo* experiments.

4. Discussion

Our data indicate that FLUKA appears to be a code that can be useful for the modeling of this type of experimental system. The experiment and the Monte Carlo simulated neutron flux results were found to be consistent. This is not surprising: FLUKA has been used in several studies and is validated by various experiments [33–36]. We matched the FLUKA data to experimental results obtained via fairly standard methodology of measurements of neutron fluxes using Mn activation foils as has been performed in multiple studies [23,21,22,43,42,41], and often around accelerators which have been used as a neutron source for therapy purposes [28,13,8,39,27]. We suggest that the match in this instance is remarkably good, given that we were using neutron production rates derived at another centre. Our observations showed that the neutrons within the irradiation cavity are very well thermalized, due to the different layers of moderator, reflector and filter in the irradiation cavity design. There is an optimal position for the hand in the cavity. However, the variation to be expected within the adults we measure should only be of the order of 9%, and this translates to a 3% effect on precision.

5. Conclusion

The previously stated goals of this study were to (i) assess the FLUKA code, (ii) find the optimal hand position inside the cavity and assess the effects on precision of a hand being in a non-optimal position and (iii) to determine the best location for our γ -ray detection system within the accelerator beam hall. We determined that:

- (i) The Monte Carlo code, FLUKA, was found to provide similar results to those obtained from experiments, providing some confidence in the predictions from the FLUKA model.
- (ii) Experiment and simulation both showed that the thermal neutron flux could vary across the inside of the hand irradiation cavity. Overall the variations are predicted to be less than 20% and have a less than 10% effect on the uncertainty estimates of hand fluorine concentration.

- (iii) The best position in the irradiation room for the fluorine detection system was identified. This will be used for future experiments allowing an efficient experimental set-up that makes best use of available Tandatron accelerator beam time.

Acknowledgements

Thanks are extended to Yasaman Shamloo of the Department of Industrial Design, Carleton University, for her kind assistance, designing the images in this study. The authors would also like to thank Justin Bennett, accelerator operator, for his assistance. Funding was provided by the Natural Sciences and Engineering Research Council of Canada.

References

- [1] M. Ando, M. Tadano, S. Asanuma, K. Tamura, S. Matsushima, T. Watanabe, T. Kondo, et al., Health effects of indoor fluoride pollution from coal burning in China, *Environ. Health Perspect.* 106 (5) (1998) 239–244.
- [2] Arnold, F.E. McNeill, I.M. Stronach, A. Pejovic-Milic, D.R. Chettle, A. Waker, An accelerator based system for *in vivo* neutron activation analysis measurements of manganese in human hand bones, *Med. Phys.* 29 (11) (2002) 2718.
- [3] Aslam, A. Pejović-Milić, F.E. McNeill, S.H. Byun, W.V. Prestwich, D.R. Chettle, *In vivo* assessment of magnesium status in human body using accelerator-based neutron activation measurement of hands: a pilot study, *Med. Phys.* 35 (2) (2008) 608.
- [4] Aslam, A. Pejović-Milić, F.E. McNeill, Lithium target performance evaluation for low-energy accelerator-based *in vivo* measurements using gamma spectroscopy, *Appl. Radiat. Isot.* 58 (2003) 321–331.
- [5] Aslam, W.V. Prestwich, F.E. McNeill, A.J. Waker, Investigating the TEPC radiation quality factor response for low energy accelerator based clinical applications, *Radiat. Prot. Dosimetry.* 103 (4) (2003) 311–322.
- [6] Aslam, W.V. Prestwich, F.E. McNeill, A.J. Waker, Monte Carlo simulation of neutron irradiation facility developed for accelerator based *in vivo* neutron activation measurements in human hand bones, *Appl. Radiat. Isot.* 64 (1) (2006) 63–84.
- [7] Aslam, A. Pejović-Milić, D.R. Chettle, F.E. McNeill, M.W. Pysklywec, J. Oudyk, A preliminary study for non-invasive quantification of manganese in human hand bones, *Phys. Med. Biol.* 53 (2008) N371–N376.
- [8] J. Beeck, Neutron flux distribution around the disk-shape source of accelerator type neutron generators, *J. Radioanal. Chem.* 1 (1968) 313–323.
- [9] S.H. Byun, A. Pejović-Milić, S. McMaster, W. Matysiak, Aslam, Z. Liu, L.M. Watters, et al., Dosimetric characterization of the irradiation cavity for accelerator-based *in vivo* neutron activation analysis, *Phys. Med. Biol.* 52 (6) (2007) 1693–1703.
- [10] S.H. Byun, A. Pejović-Milić, W.V. Prestwich, D.R. Chettle, F.E. McNeill, Improvement of *in vivo* neutron activation analysis of Mn using a 4 π NaI (Tl) detector array, *Radioanal. Nucl. Chem.* 269 (3) (2006) 615–618.
- [11] M. Chamberlain, J.L. Grafe, Aslam, S.H. Byun, D.R. Chettle, L.M. Egden, M.G. Orchard, et al., The feasibility of *in vivo* quantification of bone-fluorine in humans by delayed neutron activation analysis: a pilot study, *Physiol. Meas.* 33 (2) (2012) 243–257.
- [12] M. Chamberlain, J.L. Grafe, Aslam, S.H. Byun, D.R. Chettle, L.M. Egden, C.E. Webber, et al., *In vivo* quantification of bone-fluorine by delayed neutron activation analysis: a pilot study of hand-bone-fluorine levels in a Canadian population, *Physiol. Meas.* 33 (2012) 375–384.
- [13] C.N. Culbertson, S. Green, A.J. Mason, D. Picton, et al., In-phantom characterisation studies at the Birmingham Accelerator-Generated epithermal Neutron Source (BAGINS) BNCT facility, *Appl. Radiat. Isot.* 61 (2004) 733–738.
- [14] K. Davis, A. Pejović-Milić, D.R. Chettle, *In vivo* measurement of bone aluminum in population living in southern Ontario, Canada, *Med. Phys.* 35 (11) (2008) 5115.
- [15] B.D. Dinman, M.D. Elder, T.B. Bonney, P.G. Bovard, M.O. Colwell, A 15-years retrospective study of fluoride excretion and bony radiopacity among aluminum smelter workers, *J. Occup. Med.* (1976) 18.
- [16] T.C. Harvey, B.J. Thomas, J.S. McLellan, J.H. Fremlin, Measurement of liver-cadmium concentrations in patients and industrial workers by neutron-activation analysis, *Lancet* 1 (7919) (1975) 1269–1272.
- [17] Health Canada (2010). Guidelines for Canadian Drinking Water Quality Guideline Technical Document, Ottawa.
- [18] G. Henke, H.W. Sachs, G. Bohn, Cadmium determination in the liver and kidneys of children and juveniles by means of neutron activation analysis, *Arch. Toxicol.* 26 (1) (1970) 8–16.
- [19] ICRP 1996 Publication 74, *Ann. ICRP*, Vol. 26, No. 3/4, Elsevier, Amsterdam.
- [20] Ferrari, A., Sala, P.R., Fasso', A., Ranft, J., 2005 CERN-2005-10 (2005), INFN/TC.05/11, SLAC-R-773.
- [21] M. Karadag, H. Yucel, Measurement of thermal neutron cross-section and resonance integral for ¹⁸⁶W(n, γ)¹⁸⁷W reaction by the activation method using a single monitor, *Ann. Nucl. Energy* 31 (2004) 1285–1297.

- [22] M. Karadag, M. Güray Budak, H. Yuçel, Measurement of thermal neutron cross section and resonance integral for the $^{158}\text{Gd}(n, \alpha)^{159}\text{Gd}$ reaction by using a ^{55}Mn monitor, *Ann. Nucl. Energy* 63 (2014) 199–204.
- [23] M. Karadag, H. Yuçel, M. Tan, A. Ozmen, Measurement of thermal neutron cross-sections and resonance integrals for $^{71}\text{Ga}(n, \gamma)^{72}\text{Ga}$ and $^{75}\text{As}(n, \gamma)^{76}\text{As}$ by using ^{241}Am -Be isotopic neutron source, *Nucl. Instrum. Methods Phys. Res. A* 501 (2003) 524–535.
- [24] V. Karlicek, O. Topolcan, Cadmium in kidneys of patients with essential hypertension and renal hypertension, *Cas. Lek. Cesk.* 113 (2) (1974) 41–43.
- [25] V. Karlicek, O. Topolcan, L. Bilkova, J. Kott, J. Sova, Concentration of trace-elements in kidneys of hypertensive patients determined by neutron activation analysis, *Cas. Lek. Cesk.* 110 (32) (1971) 756–761.
- [26] G.F. Knoll, *Radiation Detection and Measurement*, third ed., John Wiley & Sons, Inc., 2000.
- [27] A. Konefal, M. Dybek, W. Zipper, W. Łobodziec, K. Szczucka, Thermal and epithermal neutrons in the vicinity of the Primus Siemens biomedical accelerator, *Nukleonika* 50 (2) (2005) 73–81.
- [28] O.E. Kononov, N.V. Kononov, et al., Optimization of an accelerator-based epithermal neutron source for neutron capture therapy, *Appl. Radiat. Isot.* 61 (2004) 1009–1013.
- [29] C.L. Lee, X. Zhou, Thick target neutron yields for the $^7\text{Li}(p, n)^7\text{Be}$ reaction near threshold, *Nucl. Instrum. Methods Phys. Res. B* 152 (1999) 1–11.
- [30] F. Mostafaei, F.E. McNeill, D.R. Chettle, W.V. Prestwich, M. Inskip, Design of a phantom equivalent to measure bone-fluorine in a human's hand via delayed neutron activation analysis, *Physiol. Meas.* 34 (5) (2013) 503–512.
- [31] F. Mostafaei, F.E. McNeill, D.R. Chettle, W.V. Prestwich, Improvements in an in vivo neutron activation analysis (NAA) method for the measurement of fluorine in human bone, *Physiol. Meas.* 34 (10) (2013) 1329–1341.
- [32] Mughabghab S.F. (2003), *Resonance integrals and G-factors*. International Nuclear Data Committee (INDC), (11376).
- [33] B.J. Patil, S.T. Chavan, S.N. Pethe, R. Krishnan, V.N. Bhoraskar, S.D. Dhole, Design of 6 MeV linear accelerator based pulsed thermal neutron source: FLUKA simulation and experiment, *Appl. Radiat. Isot.* 70 (2012) 149–155.
- [34] B.J. Patil, S.T. Chavan, S.N. Pethe, R. Krishnan, V.N. Bhoraskar, S.D. Dhole, Measurement of angular distribution of neutron flux for the 6 MeV race-track microtron based pulsed neutron source, *Appl. Radiat. Isot.* 68 (2010) (2010) 1743–1745.
- [35] B.J. Patil, S.T. Chavan, S.N. Pethe, R. Krishnan, V.N. Bhoraskar, S.D. Dhole, Simulation of e- γ -n targets by FLUKA and measurement of neutron flux at various angles for accelerator based neutron source, *Ann. Nucl. Energy* 37 (2010) 1369–1377.
- [36] A. Pazirandeh, A. Torkamani, A. Taheri, Design and simulation of a neutron source based on an electron linear accelerator for BNCT of skin melanoma, *Appl. Radiat. Isot.* 69 (2011) 749–755.
- [37] A. Pejović-Milić, M.L. Arnold, F.E. McNeill, D.R. Chettle, Monte Carlo design study for in vivo bone aluminum measurement using a low energy accelerator beam, *Applied radiation and isotopes: including data, instrumentation and methods for use in agriculture, industry and medicine* 53 (4–5) (2000) 657–664.
- [38] A. Pejović-Milić, S.H. Byun, D.R. Chettle, F.E. McNeill, W.V. Prestwich, Development of an irradiation/shielding cavity for in vivo neutron activation analysis of manganese in human bone, *Radioanal. Nucl. Chem.* 269 (2) (2006) 417–420.
- [39] T.B. Ryves, E.B. Paul, The construction and calibration of a standard thermal neutron flux facility at the national physical laboratory, *J. Nucl. Eng.* 22 (1968) 759–775.
- [40] D. Vartsky, K.J. Ellis, N.S. Chen, S.H. Cohn, A facility for in vivo measurement of kidney and liver cadmium by neutron capture prompt gamma ray analysis, *Phys. Med. Biol.* 22 (6) (1977) 1085–1096.
- [41] E. Weigold, Cross sections for the interaction of 14.5 MeV neutrons with manganese and cobalt, *Short Commun.* (1968).
- [42] H. Yuçel, M.G. Budak, M. Karadag, Measurement of thermal neutron cross section and resonance integral for the $^{170}\text{Er}(n, \alpha)^{171}\text{Er}$ reaction by using a ^{55}Mn monitor, *Phys. Rev. C* 76 (2007) 034610.
- [43] H. Yuçel, M. Karadag, Measurement of thermal neutron cross section and resonance integral for $^{165}\text{Ho}(n, \alpha)^{166}\text{Gd}$ reaction by the activation method, *Ann. Nucl. Energy* 32 (2005) 1–11.

Chapter 5

Measurements of fluorine in contemporary urban Canadians: a comparison of the levels found in human bone using *in vivo* and *ex vivo* neutron activation analysis (Article IV)

5.1 Introduction to Article IV

The final paper in this thesis describes the utility of the improved technique in a pilot study of environmentally exposed people. This article has been accepted for publication. In the article fluorine measurements of 35 participants who live in Hamilton, Ontario, Canada are presented. In addition to *in vivo* measurements, a small *ex vivo* study of bone samples was undertaken and is also presented in this paper.

The experimental work presented in Article IV was performed by the author of this thesis under the supervision of Dr. Fiona McNeill, and with the additional guidance of Dr. David Chettle and Dr. William Prestwich. Dr. Bruce Wainman provided access to the anatomy samples and permitted his ethics board approvals to be adapted for the work in this study. Ms. Alice Pidruczny provided access to facilities and assistance for the reactor measurements of the *ex vivo* samples.

5.2 Contents of Article IV

The following article is accepted for publication in Physiological Measurement.

Measurements of fluorine in contemporary urban Canadians: a comparison of the levels found in human bone using *in vivo* and *ex vivo* neutron activation analysis

F. Mostafaei^{1*}, F. E. McNeill¹, D. R. Chettle¹, B. C. Wainman², A. E. Pidruczny³, W. V. Prestwich¹

¹*Medical Physics and Applied Radiation Sciences, McMaster University, Hamilton, Canada*

²*Department of Pathology and Molecular Medicine, McMaster University, Hamilton, Canada*

³*McMaster Nuclear Reactor, McMaster University, Hamilton, ON, Canada*

Abstract

Non-invasive *in vivo* neutron activation analysis (NAA) was used to measure the fluorine concentration in 35 people in Hamilton, Ontario, Canada. Measurement and precision data of this second generation NAA system were determined in 2013, and the results were compared with the performance of a first generation system used in a pilot study of 33 participants from the Hamilton area in 2008. Improvements in precision in line with those predicted by phantom studies were observed, but the use of fewer technicians during measurement seemed adversely to affect performance. We compared the levels of fluorine observed in people between the two studies and found them to be comparable. The average fluorine concentration in bone was found to be 3 ± 0.3 and 3.5 ± 0.4 mg F/g Ca for 2013 and 2008 measurements respectively.

Ten people were measured in both studies; the observed average change in bone fluorine in this subgroup was consistent with that predicted by the observation of the relationship between bone fluorine and age in the wider group. In addition, we observed differences in the relationship between bone fluorine level and age between men and women, which may be attributable either to sex or gender differences. The rate of increase in fluorine content for men was found to be 0.096 ± 0.022 mg F/g Ca per year while the rate of increase for women was found to be slightly less than half that of men, 0.041 ± 0.017 mg F/g Ca per year. A discontinuity in the rate of increase in fluorine content with age was observed in women at around age 50. Bone fluorine content was significantly lower ($p < 0.01$) in women age 50 to 59 than in women age 40 to 49, which we suggest may be attributable to bone metabolism changes associated with menopause. We also observed increased fluorine levels in tea drinkers as compared to non-tea drinkers, suggesting tea may be a significant source of exposure in Canada. The rate of increase in fluorine content of the tea drinkers and the non-tea drinkers were found to be $0.127 (\pm 0.029)$ and $0.050 (\pm 0.009)$ mg F/g Ca per year respectively. Finally, we also obtained twelve bone samples from cadavers' skulls. Neutron activation analysis was used to determine the fluorine levels in these *ex vivo* samples. The rate of increase of fluorine content versus age for *in vivo* and *ex vivo* measurements were found to be 0.078 ± 0.014 and 0.078 ± 0.050 mg F/g Ca per year respectively. Excellent agreement was found between the fluorine levels determined *in vivo* and *ex vivo* using the two separate systems, providing confidence in the fluorine concentration data being measured *in vivo*.

Introduction

Health Canada estimates that as of 2005 approximately 43% of Canadians were provided with fluoridated community drinking water (Health Canada 2010). The fluoridation of some public water supplies began after 1945 in Canada: the main argument for fluoridation was to protect teeth. The incidence of dental caries is reduced in populations who have fluoride added to drinking water (Boivin et al 1989; Khandare et al 2005). Once consumed and absorbed, fluorine is stored in bone as fluoride (Whitford 1994) where it accumulates over time. A measure of fluorine in bone should therefore be a measure of long-term or cumulative exposure to fluoride.

There is some public controversy in North America about the risks of exposure to fluoride, although most health professionals agree that fluoridation of the water supply is, on balance, beneficial (Health Canada 2010). Adding small amounts of fluoride to water and toothpaste can be useful in aiding dental care. Dental fluorosis can occur when a person is exposed to fluoride, although the concerns about this condition are cosmetic rather than health based (WHO, 2006). However, skeletal fluorosis, a sclerosing bone condition, is a serious health condition which can occur when a person is exposed to large amounts of fluoride (Fordyce et al. 2007; Shashi 1992; Tamer et al., 2007; Wang et al., 2007; Prystupa 2011). This condition has rarely been observed in Canada. However, some groups have expressed concerns about potential excess exposure and health effects (Dinman et al 1976). There has been recent discussion in many Canadian municipalities of the issue of fluoridation of the water supply (Schmidt, 2014).

A technique to assess long term exposure to fluoride could be useful in assessing the health risks from exposure to this ion. We have developed, and previously published, articles demonstrating the utility of a low risk technique to measure bone-fluorine, painlessly and non-invasively, *in vivo*, using neutron activation analysis (NAA). In our technique, fluorine in bone is measured via the $^{19}\text{F}(n,\gamma)^{20}\text{F}$ reaction (Chamberlain et al., 2012a; Chamberlain et al., 2012b; Mostafaei et al., 2013a; Mostafaei et al., 2013b). We have performed system changes, which in phantom studies were shown to significantly improve the performance and permit detection of lower levels of fluorine (Mostafaei et al., 2013b).

This paper presents the results obtained from *in vivo* measurements of the fluorine content of the bones of the hand of 36 people living around the City of Hamilton, Ontario, Canada using the improved NAA system. We compare the data on measurement precision, and bone fluorine values, obtained in this study with data from an earlier published study of 33 people (Chamberlain et al., 2012b), also drawn from the greater Hamilton community. Ten people were measured in both studies. We report on the comparison of these ten *in vivo* measurements performed after an interval of approximately five years. Finally, we obtained twelve cadaveric bone samples from the McMaster University anatomy laboratories. We used the McMaster Nuclear Reactor (MNR) to perform an analysis of these *ex vivo* samples using NAA. We compare the data from *ex vivo* and *in vivo* measurements and discuss how this may permit more confidence to be placed on the *in vivo* data.

Materials & Methods

In vivo measurements

Ethics Approval: Prior approval to conduct a study of healthy adult volunteers was obtained from the Hamilton Integrated Research Ethics Board (HIREB) (project approval # 08-312). Thirty-six volunteers (18 male and 18 female), who had no previous history of occupational exposure to fluoride, gave their informed written consent to participate in this study. The mean age of the volunteers was 42.7 ± 16.9 years with a range from 20 to 75 years. Data from one volunteer (a man) was later excluded from this study due to technical problems with their measurement. Data were therefore available for 35 measurements.

Irradiation and counting set-up: The right hand of each of the volunteers was irradiated with neutrons produced on the Tandatron accelerator as described in a number of previous publications (Pejovic-Milic et al 2006, Byun et al 2006, Davis et al, 2008; Aslam et al, 2008a; Aslam et al 2008b; Chamberlain et al., 2012b). Figure 1b shows the irradiation and γ -ray detection arrangement in the accelerator beam hall and control room for the *in vivo* study. The hand was positioned in an irradiation cavity (for reasons of comfort) such that the open palm faced the neutron source (i.e. the accelerator target). The arm was held firmly in place by a water-filled sleeve. This sleeve holds the arm in place, but also serves as a source of neutron shielding, reducing the radiation dose to the radiosensitive tissues of the torso. The person places their arm in the cavity and the sleeve is filled with water until the arm is held firmly but comfortably in place. Figure 5.1a) shows a layout which was used for phantom measurements: we previously published

improvements to the system that were based on phantom measurements in this control room location (Mostafaei et al 2013b). The distance to the control room was too far for volunteers to travel in less than one half-life (11 seconds) so the detection system was re-located to the position near the irradiation cavity shown in Figure 5.1b). Figure 5.2 shows a photograph of a volunteer being measured in the layout shown in Figure 5.1b).

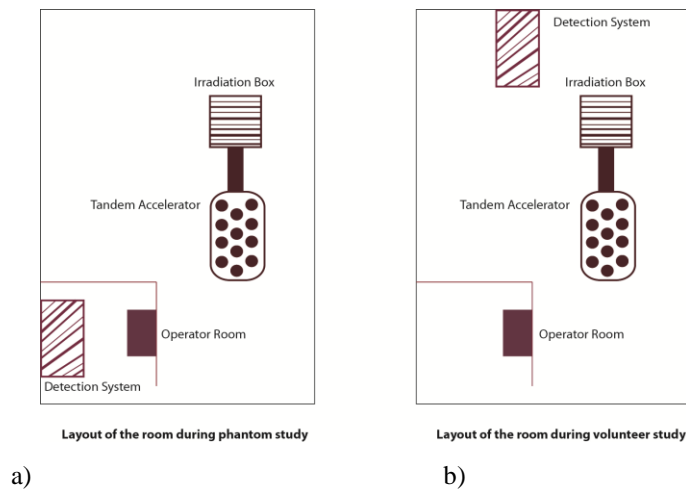


Figure 5.1. a) Experiment layout during the previously published phantom study, b) Experiment layout during this *in vivo* study



Figure 5.2. A volunteer photographed while being irradiated during a fluorine measurement.

Each participant's right hand was irradiated for six seconds. The water sleeve was then deflated quickly using a gravity-draw system. The participant was then asked to take their hand out of the irradiation cavity quickly, and turn and insert their hand into the detection system. The detection system has been described extensively in previous publications (Byun et al., 2007; Byun et al., 2006) so only a brief description will be given here. For fluorine measurements, where the half-life is so short (11.2 seconds) the detection system is placed next to the irradiation cavity at the end of the beam line. Therefore transfer from the cavity to the detectors can ideally take less than one half-life. The detection system (nine NaI(Tl) detectors, eight 102×102×406 mm with a ninth 102×102×102 mm in a quasi-4 π geometry) was covered by concrete blocks and positioned in the area with lowest activation as determined by a previous study using the FLUKA simulation code and experiments (Mostafaei *et al* 2014).

The irradiation protocol, counting set-up and data extraction procedures used for the *in vivo* measurement of fluorine was the same as that described in our published phantom work: 6 seconds of irradiation at a proton energy, E_p , of 2.15 MeV and a beam current of 600 μ A (Mostafaei et al., 2013a, Mostafaei et al., 2013b). This results in an acceptable radiation dose of 30 mSv to the hand and an effective dose of 35 μ Sv.

After the irradiation of the volunteers, they were asked to position their hand into the detection system. Spectra were acquired for six 5 second periods in anticoincidence mode by the MCA followed by a 120 second wait period and then a 300 second count. The purpose of the six 5 second segments is to collect the ^{20}F decay data. The 120 s wait

period allows sufficient time for the ^{20}F to completely decay. This is necessary, because there is interference between ^{20}F and ^{38}Cl in the spectra. Activated ^{38}Cl emits a 1.64 MeV γ -ray which is not resolved from the activated ^{20}F γ -ray at 1.63 MeV. However, they have significantly different half-lives, which allow us to discriminate between the two signals. The half-life of ^{20}F is 11.2 seconds, while the half-life of ^{38}Cl is 37.24 minutes. We count the combined ^{20}F and ^{38}Cl signals in the first sets of six 5 second acquisitions. We then leave the sample to cool and count the ^{38}Cl signal that remains. We can then back-calculate the ^{38}Cl activity and subtract it from the ^{20}F signal. This counting technique is performed in addition to using anticoincidence gating, and thus counting, of the signals to remove the ^{38}Cl signal at 1.64 MeV from the ^{20}F signal at 1.63 MeV. ^{20}F emits a single γ -ray, while ^{38}Cl emits two γ -rays partly in coincidence. By counting in anti-coincidence we remove a considerable portion of the chlorine signal and thus have less to extract using the decay-counting method. Figure 5.3 shows a fluoride-doped phantom spectrum in a) the first five second and b) the 300 second segments.

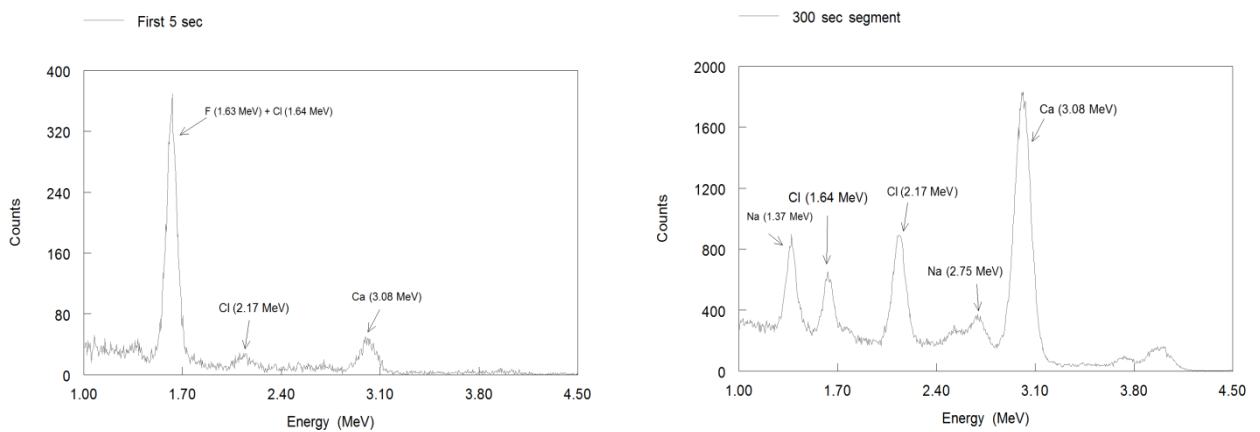


Figure 5.3. Comparison of the first five second and the 300 second spectrum from a fluoride-doped phantom

The 300 second segment also permits us to measure a signal from ^{49}Ca . This allows us to normalize the obtained fluorine data. The goal is to have a robust measurement where the accuracy of the measured fluorine content does not depend on variations in target current, or individual factors such as bone shape, size, mass, tissue overlay thickness or positioning of the hand in the irradiation cavity. (The precision may vary with these factors). The obtained fluorine signal is therefore normalized to the extracted calcium signal. This ideally permits the fluorine to calcium signal to be readily compared among individuals of different ages, sexes, height and weight. The normalization does assume that the ratio of the activation of fluorine and calcium should remain constant regardless of whether the thermal flux varies, and whether the bone shape, size and density vary. This assumes that the fluorine and calcium are co-located in the hand, and only thermal neutrons activate the sample. Fluorine is stored in bone with calcium as calcium fluoride (CaF_2). It displaces the hydroxide (OH^-) functional group in the hydroxyapatite matrix in the bone (Whitford 1994). We know, however, that the neutron flux in the cavity is not 100% thermalized, so this F/Ca normalization is limited in its application. The neutron flux in the cavity has an energy spectrum which ranges from thermal into the low energy range. The ^{19}F and ^{48}Ca do not have pure $1/v$ neutron cross-sections: there are resonances in the F cross-section. However, we have published data illustrating that the elemental activation is dominated by thermal neutrons and the uncertainties introduced by the limits of the normalization are small (at approximately 2%) compared to other sources of uncertainty (Mostafaei et al, 2014).

Questionnaire: Each participant was asked to fill out a short questionnaire which aimed to determine potential factors in a fluoride exposure history. Data were made anonymous for storage: each volunteer was assigned a unique identification number in order to ensure the confidentiality of the information obtained through this study.

Sources of fluoride: None of the participants reported a history of exposure to an acute large dose of fluoride. All of the participants reported using fluoridated toothpaste, and no participants reported swallowing their toothpaste on a regular basis. Because it is well known that teas can contain large amounts of fluoride (Yadav et al., 2007), and because in our previous study (Chamberlain et al., 2012b) we had seen suggestions of differences between tea and non-tea drinkers (the rate of increase in fluorine content for tea and non-tea drinkers were found to be 0.085 ± 0.021 and 0.043 ± 0.019 mg F/g Ca per year respectively), the participants were asked about their tea consumption. Fourteen of the participants reported consuming tea regularly; 21 were non-tea-drinkers. Participants were also asked about their water consumption. We asked participants whether their current source of drinking water was city, bottled or well water and if their past consumption was in these categories. The decision to add fluoride to water is made at the municipal level in Ontario; fluoride is added to tap water in the greater Hamilton area. The City of Hamilton regulates the fluoride level in drinking water to a concentration of 0.6 parts per million (Health Canada 2010). The majority of volunteers reported drinking city water, but some reported drinking bottled water due to the smell and taste of city water. The water in Hamilton is obtained from Lake Ontario. At certain times of year,

there can be algae blooms in the lake. Although the water is perfectly healthy to drink, the algae can lead to a slight odour that some people find off-putting.

***Ex vivo* measurements**

Ethics Approval: In addition to *in vivo* measurements, a small study of *ex vivo* bone samples was undertaken. Prior approval to conduct the cadaver study was obtained from the Hamilton Integrated Research Ethics Board (Project approval # 11-209-T).

Sample collection: Bone samples were collected from the skulls of 12 cadavers prior to embalming from the McMaster University anatomy laboratory. A diamond hole saw with drill bit size of $12.7 \times 11.11 \times 6.35$ mm was used. The samples were collected from the back of the skull (because this was thicker bone with higher bone density) and were sampled all the way through the bone to the periosteum. The samples were all of similar sizes: they were weighed after collection and the average mass of the bone samples was 1.03 ± 0.04 (mean \pm standard deviation) g.

Irradiation and counting: The *ex vivo* bone samples were irradiated with neutrons in the core of McMaster Nuclear Reactor (MNR) using a pneumatic insertion system. The use of the reactor meant that samples were exposed to a neutron flux of approximately 5×10^{13} n.sec⁻¹.cm⁻², permitting the measurement of such low mass samples. This sample mass is not measurable using the Tandatron accelerator system. The air-driven reactor system allows the small samples to be inserted into the reactor core for pre-defined periods of

time. In this case, the samples were irradiated for 20 seconds. Samples were then transferred (again using the pneumatic system) to a hyperpure germanium detector system (30% relative efficiency, model GMX30-70-S, ORTEC) to be counted. Samples were counted for 20 seconds. The average transfer time from the end of the irradiation to start of the count was 7 seconds. The 1.63 MeV fluorine peak was used to assess the fluorine content of the samples, as it had been in the *in vivo* studies. The resolution of the detector system meant that the 1.64 MeV chlorine peak was resolved and no subtraction techniques were required.

The mass of fluorine in the *ex vivo* samples was calculated by comparing the signal from the bone sample, with the signal from irradiated calibration standards. Calibration standards were made by pipetting known volumes of Atomic Absorption standardized solutions, of certified fluorine concentration, into the irradiation vessels. The calibration standards were irradiated and counted under the same conditions as the bone samples. Fluoride standards (77365, SIGMA-ALDRICH, Buchs/Switzerland) and calcium carbonate standards (112205, Fisher Scientific, USA) were used as reference samples for calibration: they contained 1000 and 2000 μ gr F and 0.25, 1 and 2 gr CaCO_3 respectively.

Results

In vivo measurement precision In a previous published study by Mostafaei et al, 2013b, a series of improvements were found to produce a significant improvement of a factor of 2.26 in the phantom minimum detectable limit when compared to the phantom data

previously published by Chamberlain et al, 2012. We had anticipated that this observed improvement in phantoms would be achieved in human measurements.

Table 5.1 provides the mean (\pm standard deviation) and median *in vivo* precisions as determined in this study and the study published in 2012, but performed in 2008.

Table 5.1. Mean and median *in vivo* precisions

	2013 <i>In Vivo</i> Data	2008 <i>In Vivo</i> Data
Mean (\pm SD)	0.32 (\pm 0.15)	0.42 (\pm 0.10)
Median	0.29	0.40

The improvement observed in the mean is a factor of 1.31, while the improvement observed in the median is a factor of 1.38. This is, overall, not as good an improvement as expected.

In order to investigate this further, we looked at the distribution of precisions obtained in both this and the earlier study. Figure 5.4 shows the frequency distribution of the precisions observed in 2008 and 2013.

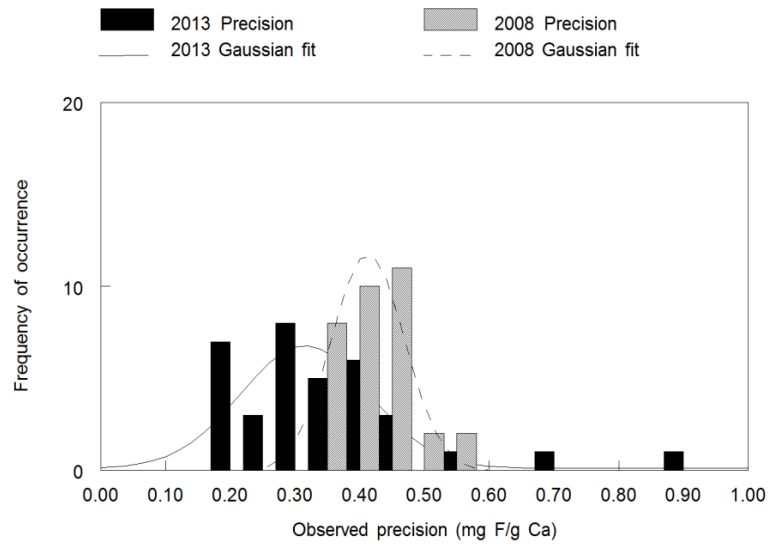


Figure 5.4. Frequency distribution of the precisions observed in 2008 and 2013

The important result that the figure shows is that although much of the data does in fact show an improved precision, there is a much wider spread on the *in vivo* precision results. This, of course, is also suggested by the larger standard deviation on the data obtained in 2013.

We compared the laboratory notebooks from the two *in vivo* studies to try and determine factors which could have led to these obvious differences between the precision distributions. (The lead author on the 2008 study sadly died before publishing his work, so we only have notebooks to rely on for information). We investigated a series of possible factors.

1. The Tandatron accelerator was moved from a large open beam hall to a smaller enclosed room in the time between the two studies.

2. The number of *in vivo* measurements performed per day were significantly increased.

We queried whether these two factors led to an increase in the background detector signal over the course of the day, because of increased activation in the detectors, which could have worsened the precision. Figure 5.5 shows the background signal measured in the 4π spectrometer when it was placed outside of the irradiation hall and in the control room, and when it was placed beside the irradiation cavity. The background spectra were collected at the end of each day. It can be seen, however, that the background magnitude for the location next to the irradiation cavity, while a little poorer, does not explain the differences observed in *in vivo* precisions. It is, at most, a factor of 1.06.

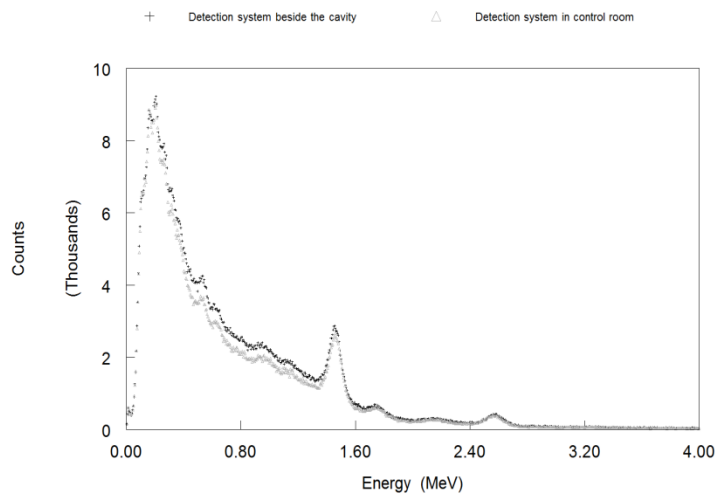


Figure 5.5. Background differences, old and new location

3. We questioned whether the poorer precision was observed in both calibration phantoms and people in the experiment. This could identify whether the issue was

a systematic performance problem with the equipment, or a factor that was confined to human measurements.

The precisions for phantoms measured with the detection system in the beam hall beside the irradiation cavity and in the low background control room area are shown in Table 5.2. It can be seen that the mean and median precisions increased by a factor of 1.33 and 1.60 respectively, when the detection system was located in the beam hall beside the irradiation cavity.

Table 5.2. The precisions for phantoms measured with the detection system in the beam hall beside the irradiation cavity and in the control room area

	Precision in the control room	Precision in the beam hall beside the cavity
Mean (\pm SDM)	0.09 (\pm 0.04)	0.12 (\pm 0.05)
Median	0.07	0.11

It would appear that there are factors which affect the *in vivo* measurements which do not necessarily affect the phantom data.

4. In addition to Faraday cup measurements of the beam current, a fission chamber was used as a back-up system to monitor the beam current. This measures the neutrons produced from the target, rather than the incident current. It does take into account shifts in the beam and melting on the target. Although the current was set to a significant increase to 600 μ A, it was found that the average fission chamber data for *in vivo* measurements was a factor of 2/3 lower than phantom

measurements. This would have resulted in a factor of 1.2 increase (i.e. worsening) in precision in the *in vivo* data.

- The transfer times of each participant were fixed at eight seconds in the first study, but there were a range of transfer times in this study. The average transfer time for volunteers in this study was 10.2 seconds (with a range from 8 to 18 seconds) compared to a consistent 8 seconds for every volunteer for the previous study. To determine whether this is a significant reason for the spread, the precision data were categorized into quartiles from lowest (best) to highest (worst) and the mean and median precision, and mean and median transfer times, calculated (Table 5.3).

Table 5.3. The precision data of mean and median transfer times

Quartile	Median Precision	Mean Precision (\pm SD)	Median Transfer Time (Sec)	Mean Transfer Time (\pm SD)
1	0.19	0.19 (\pm 0.02)	9	8.8 (\pm 0.44)
2	0.28	0.27 (\pm 0.02)	10	10.4 (\pm 3.12)
3	0.34	0.34 (\pm 0.03)	8	9.9 (\pm 3.3)
4	0.44	0.52 (\pm 0.19)	12	11.5 (\pm 2.9)

The data strongly suggest that the range in transfer times has had an effect. The mean transfer time for the quartile with the poorest (i.e., largest) precision is significantly different at the 95% level ($p = 0.03$) from the quartile with the best (i.e., smallest) precision: the poorest precisions had transfer times which were three seconds longer. This is a very small difference in transfer time, but when working with an element with an 11

second half-life, it would appear to have a measurable effect. Also, the extreme 8 s versus 18 s implies a factor of 1.86 more counts and so a factor of 1.36 in precision.

We then investigated how the study in 2008 managed to attain such a consistent transfer time compared with the study conducted in 2013. The largest factor seems to be the number of technical staff supporting the volunteers. In 2008, two technical staff conducted each measurement. One stayed in the room with the patient, and had their dose monitored by an alarming EPD (electronic personal dosimeter). One stayed outside, and entered when the beam was switched off. The person who stayed in the room worked closely with the subject to remove the water sleeve that acts as a radiation shield during the measurement, and helped the volunteer move their position to the detection system. The second person was responsible only for switching on the equipment (starting the counting equipment). This two person system was developed to reduce the total dose to staff during the study. However, health and safety concerns were expressed about having a member of staff entering into the room, especially after the accelerator was moved and the room arrangement involved navigating a bend which was perceived as a trip hazard. At the same time, it was not seen as ideal to have two members of staff in the room with the beam switched on, even though the total dose during the whole study for the technical staff member in the room was low (0.016 mSv). The study in 2013 therefore only used one technician, as opposed to two, and it would appear that this has affected the quality of some of the data.

In the quartile with the mean transfer time that approaches that of the study in 2008, the mean precision was found to be 0.19. If we include the factors that are a result of the lower neutron production per unit current off target (1.2), and the higher background levels (1.06), then this would equate to a precision of 0.15, a factor of 2.8 improvement. It would appear, therefore, that the detection system improvements previously found in phantoms were found to be borne out in people.

In vivo fluorine concentrations as measured by NAA

All 35 subjects were found to have measurable fluorine levels in bone which were significantly different from zero at the 99% confidence level. The average fluorine concentration in bone for this study was found to be 3.0 ± 0.3 mg F/g Ca.

Figure 5.6 shows the hand-bone fluorine content (per unit calcium content) from the 35 participants plotted against age. In our earlier fluorine study, a significant relationship was found between fluorine content with age which is observed in this study. Fluorine is mostly stored in bone as CaF_2 with a long retention time (Shashi et al., 2008; Wilson 1993) and it is expected to accumulate with age. The regression in this case is significant ($p < 0.001$).

The fluorine content of bone in these male and female volunteers was found to increase by 0.078 ± 0.014 mg F/g Ca per year when a linear relationship was fitted. This result agrees with our previous study (Chamberlain et al., 2012b) which was performed in 2008.

In that study, the rate of increase of the linear relationship between bone fluorine content and age was found to be 0.084 ± 0.014 mg F/g Ca per year. The rate of increase observed in 2008 and in 2013 are the same to within uncertainties.

Figure 5.7 shows the comparison of the 2013 and 2008 data in a plot of bone fluorine content versus age. As can be seen, the data from the two studies are comparable. A similar relationship between bone fluorine content and age was observed in both studies.

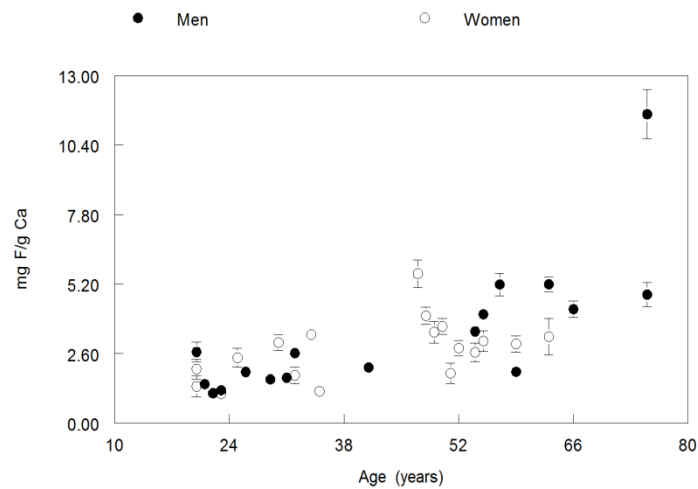


Figure 5.6. Fluorine concentration with age measured in the human hand from 35 participants

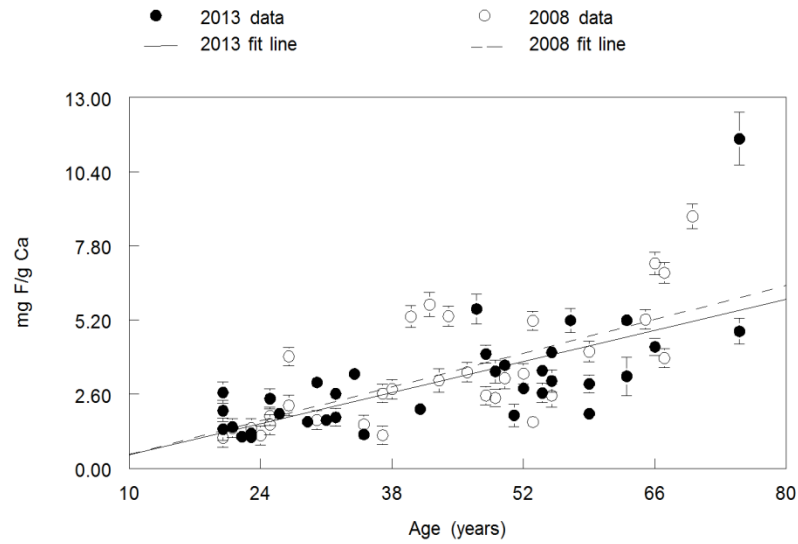


Figure 5.7. Comparison of the 2013 and 2008 data

The data we present above of the increase in bone fluorine content with age is in units of mg F/g Ca per year. We can compare these data with estimates of fluoride consumption in Canada if we convert to units of mg F per day. We make the approximation that the average mass of calcium in the skeleton is 1300g. Thus we estimate that the average retention of fluorine in bone in men and women in the City of Hamilton is $0.079 \times 1300 / 365 = 0.3$ mg per day. Hamilton City water is regulated to a fluoride concentration of 0.6 ppm i.e. $0.6 \mu\text{g F per ml}$ of water. If we further assume that the average person drinks 2.5 – 3.5 liters per day (Burt, 1992), then this would indicate an average consumption of $3000 \times 0.6 \mu\text{g F per day}$ or 1.8 mg F per day. Data suggest that 50% crosses the gastrointestinal tract, and 50% is retained in the body (Ludlow et al 2007; Spencer et al 1970). This would predict an average increase in fluorine in the skeleton of $0.5 \times 0.5 \times 1.8 = 0.45$ mg F per day. These data suggest that our *in vivo* measurements which predict

uptake of 0.3 mg F per day are in line with values predicted from water consumption data.

Sex Differences

In our previous work on lead (Pb), we have shown that men and women have differences in bone metabolism that can lead to sex differences in metal metabolism between menarche and menopause (Popovic et al., 2005). We therefore investigated whether there were observable differences in bone fluorine concentration between men and women. The average fluorine concentration for men was found to be 3.3 ± 0.6 mg F/g Ca, while the average fluorine concentration for women was found to be $2.7 \text{ mg} \pm 0.3 \text{ mg F/g Ca}$. The average age for the groups of men and women were 44 ± 19 and 41.5 ± 14 respectively. There was no significant difference in average fluorine concentration in bone between men and women.

However, regressions of bone fluorine content versus age were then also performed for men and women separately. Figure 5.8 shows the data for a) men and b) women.

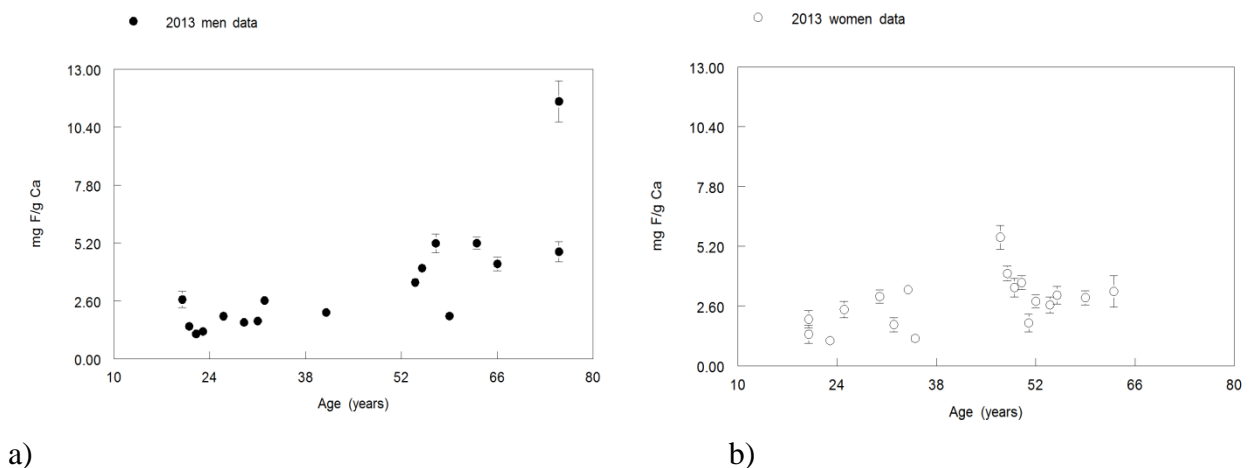


Figure 5.8. The 2013 data for a) men and b) women

Although average bone fluorine levels were found to not be significantly different for men and women, a difference, at greater than the 95% level of confidence ($p=0.034$) was observed for the rate of increase of fluorine content versus age between men and women. The rate of increase for men was found to be 0.096 ± 0.022 mg F/g Ca per year while the rate of increase for women was found to be slightly less than half that of men, 0.041 ± 0.017 mg F/g Ca per year. The difference is a factor of 2.0 ± 1.0 . This could imply either that men ingest more fluoride per unit calcium, or that women retain more calcium per unit fluoride than men. This needs further exploration.

As we have determined that the data of the rate of increase versus age relationship were the same for data collected in 2008 and these data collected in 2013, we combined the two data sets and further investigated the relationship of bone fluorine versus age for men and women separately using the combined data set.

As can be seen from Figure 5.9, the rate of increase for men was found to be 0.095 ± 0.013 mg F/g Ca per year while the rate of increase for women was found to be roughly half that of men, 0.057 ± 0.013 mg F/g Ca per year. The p value was found to be 0.047 for the difference in the two rates of increase of fluorine content versus age.

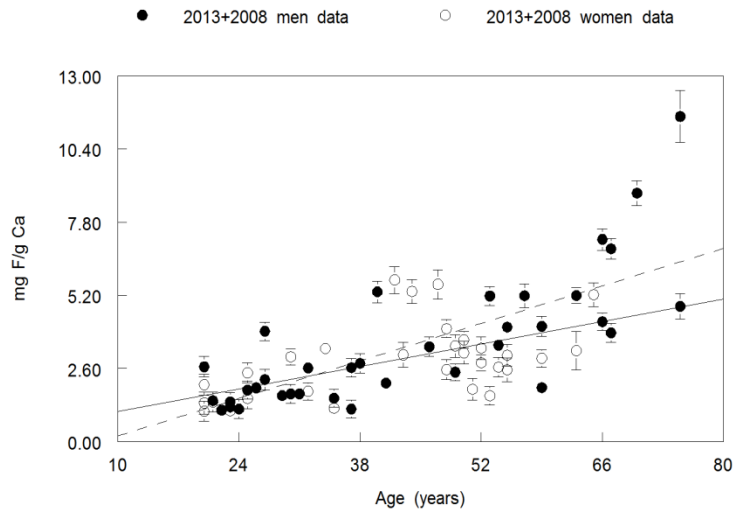


Figure 5.9. Fluorine versus age for women and men using the combined 2013 and 2008 data

Since men and women seem to show a different accumulation in fluorine content with age, and further, since this may be attributable to differences in bone metabolism modulated by estrogen in women, we decided to investigate whether there were differences in accumulation rate into bone that coincide with pre-menopause and post-menopause phases in women. We did not ask the participants about their menopausal status. Instead, we investigated this by using age as a surrogate measure. The average age of menopause in North America is 51 (Utian et al., 1999); this being defined as the age at which women have ceased menstruation for one full year. The age at which, on average, estrogen and progesterone levels have fallen significantly in women in Canada is therefore 50.

Figure 5.10 shows bone fluorine content versus age in women (for the 2008 and 2013 data combined) with women age less than 50 years, and age 50 and older marked

separately. It can be seen that there appears to be a discontinuity in the relationship of fluorine content versus age at age 50 in women. This discontinuity is not seen in men.

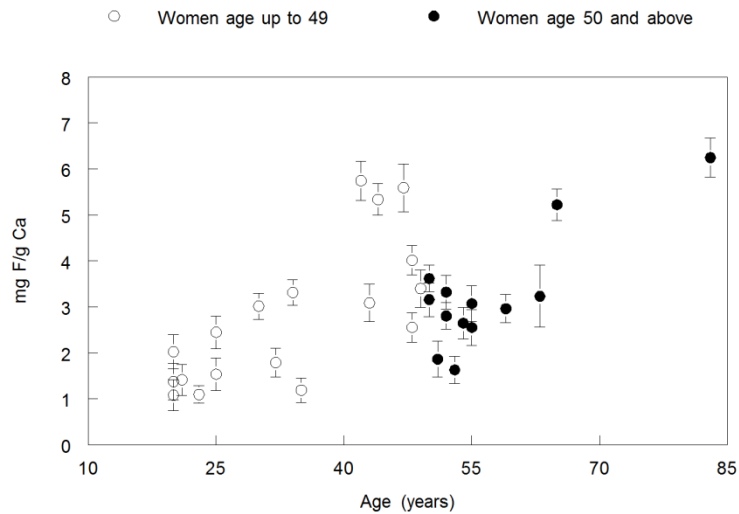


Figure 5.10. Bone fluorine content versus age in women (for the 2008 and 2013 data combined) with women age less than 50 years, and age 50 and older

We performed t-tests on the average bone fluorine content of women ages 40-49, and women ages 50-59. (Ideally, we would have preferred to use smaller age ranges, given that the median perimenopause transition length is 4 years (McKinlay et al., 1992), but the number of data points available here is small). The average (\pm standard error of the mean) bone fluorine content of women age 40-49 was found to be 4.2 ± 0.5 mg F/g Ca, while the average bone fluorine content of women age 50-59 is 2.7 ± 0.2 mg F/g Ca. This is significantly different at the 99% confidence level, $p < 0.01$. Fluorine content appears to have fallen in post-menopausal women as compared to pre-menopausal women. It is not unexpected that bone metabolism changes at menopause. However, these data suggest that fluorine content is lost relative to calcium content, which we suggest is perhaps a

consequence of different re-distribution and re-absorption pathways of different elements released from remodeled bone.

We performed a similar analysis on men. The average (\pm standard error of the mean) bone fluorine content of men age 40-49 is 3.3 ± 0.8 mg F/g Ca, while the average bone fluorine content of men age 50-59 is 4.0 ± 0.5 mg F/g Ca. This is not significantly different, $p=0.45$. Bone fluorine content does not alter at age 50 in men, in the way that the data suggest happens in women.

The data available here are too limited to perform a comprehensive analysis. However, there appears to be evidence that bone fluorine content is altered in women around menopause. This requires further investigation, but may show that this NAA technique can be of use in better understanding both exposure to, and metabolism of, fluoride in people.

Bone fluorine and tea consumption

We also compared the fluorine bone levels of tea-drinkers and non-tea-drinkers in our 2013 data. This is shown in figure 11. The population categorized as 'tea drinking' consisted of individuals whose reported tea consumption varied from one cup per week to a few cups per day. The average age of the regular tea consumers was 41.2 ± 16.9 years, with a range of from 23 to 75 years. The population consisted of six men and eight women. The average age of the non-tea-drinkers was similar, 43.8 ± 17.2 years, with a

range from 20 to 75 years. This population consisted of eleven men and ten women. Figure 5.11 shows that a significant difference was observed in the rates of increase of the tea-drinkers and non-drinkers bone fluorine concentration with age. The rate of increase of the tea drinkers was found to be $0.127 (\pm 0.029)$ mg F/g Ca per year. The rate of increase of the non-tea drinkers was found to be $0.050 (\pm 0.009)$ mg F/g Ca per year. The rate of increase of the tea drinkers' relationship with age is more than twice (2.5 ± 0.7) that of the non-tea drinkers. The difference is significant at the 95% confidence level ($p = 0.016$).

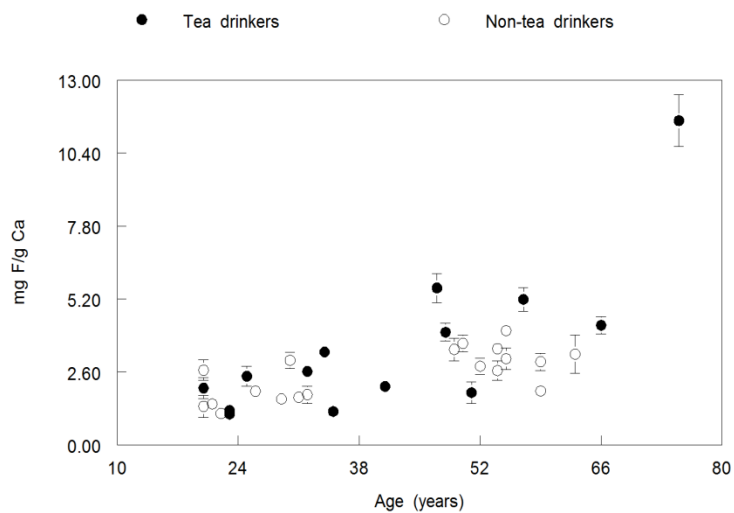


Figure 5.11. Comparison of bone-fluorine concentration in tea-drinkers, and non-tea-drinkers

In the Chamberlain et al study of 2008, the difference between tea and non-tea drinkers was suggestive but not statistically significant. This was thought to be because the number of non-tea drinkers was very small. As with the sex/gender data, where we observed that the relationship between fluorine and age is the same for the two studies, we chose to combine the data sets from 2008 and 2013 to see if the significance of the

difference between tea and non-tea drinkers increased further with an increased sample size. When the data were combined, it was found that the rate of increase of the relationship with age for tea drinkers (n=32) was 0.105 ± 0.015 mg F/g Ca per year while the rate of increase for the non-tea drinkers (n=33) was 0.049 ± 0.008 mg F/g Ca per year. This is shown in figure 5.12. This is a significant difference ($p = 0.004$) in observed fluorine level between tea and non-tea drinkers. The significance of the difference did indeed increase when data from 2008 and 2013 were combined. Tea drinkers living in the greater Hamilton urban area have approximately double the bone fluorine content of non-tea drinkers for a given age group.

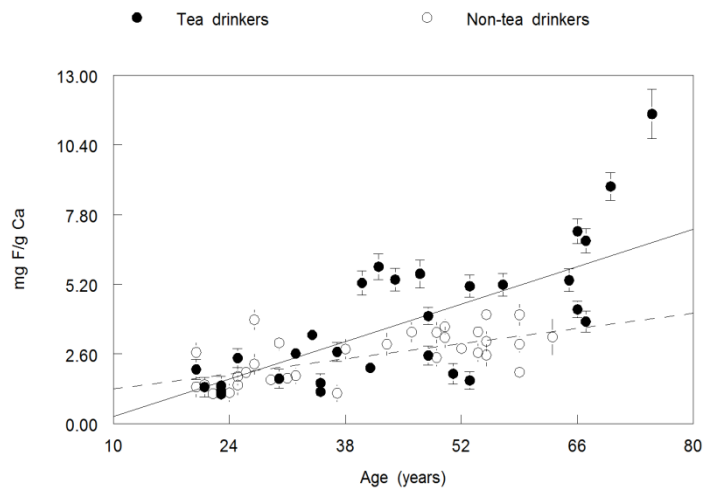


Figure 5.12. Comparison of tea drinkers and non-tea drinkers with data from 2008 and 2013 combined

A similar analysis was conducted for consumption of city water versus bottled water. No differences in bone fluorine content were observed between bottled water consumers and tap water consumers.

Change in fluorine levels over a five year period

Of the thirty-three volunteers measured in 2008 (Chamberlain et al., 2012b) ten people were re-measured after a five year interval. This was prior approved by our human research ethics board. These ten adults should have been exposed to fluoride from water, food, and fluoridated toothpaste over the five year period since the previous study. Figure 5.13 illustrates the change in bone fluorine content observed between the 2008 and 2013 sets of measurements.

The average difference in bone fluorine content of the 10 subjects was found to be 0.66 ± 0.27 mg F /g Ca.

The average difference in bone fluorine content of the 4 tea drinkers was found to be 0.88 ± 0.66 mg F /g Ca.

The average difference in bone fluorine content of the 6 non-tea drinkers was found to be 0.52 ± 0.18 mg F /g Ca.

The rate of increase of the observed relationship between bone fluorine content and age for all 68 subjects should be a measure of the average increase in bone fluorine content per year. That is, we would predict that on average the bone fluorine contents of these ten subjects should increase by $5 \times 0.078 \pm 0.014 = 0.39 \pm 0.07$ mg F /g Ca. Tea drinkers would be predicted to increase by 0.50 while non-tea drinkers would be predicted to increase by 0.25.

We observed that the predicted and measured increases in the bone fluorine contents of these groups are the same to within the uncertainties.

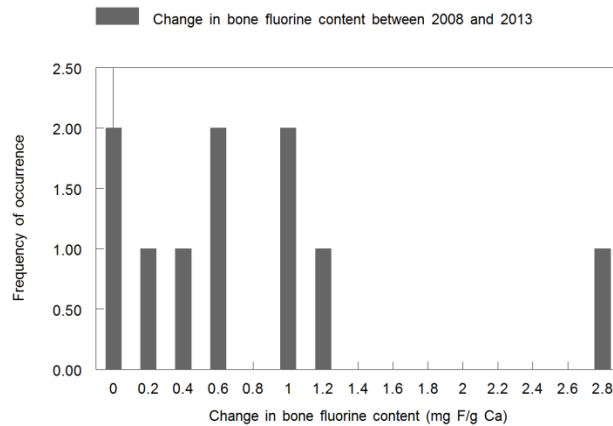


Figure 5.13. Comparison between 2008 & 2013 fluorine measurements

NAA measurements of fluorine concentrations in ex vivo samples

The twelve bone samples obtained from the cadaver skulls were irradiated with neutrons in the McMaster Nuclear Reactor (MNR) using a pneumatic system. Both fluorine and calcium were measured and the resultant measured concentration was expressed in terms of mg F per g of Ca in order to compare with *in vivo* data. Figure 5.14 shows the calibration line used for the *ex vivo* bone fluorine studies. During the course of the cadaver bone sample study, three sets of seven phantoms were measured.

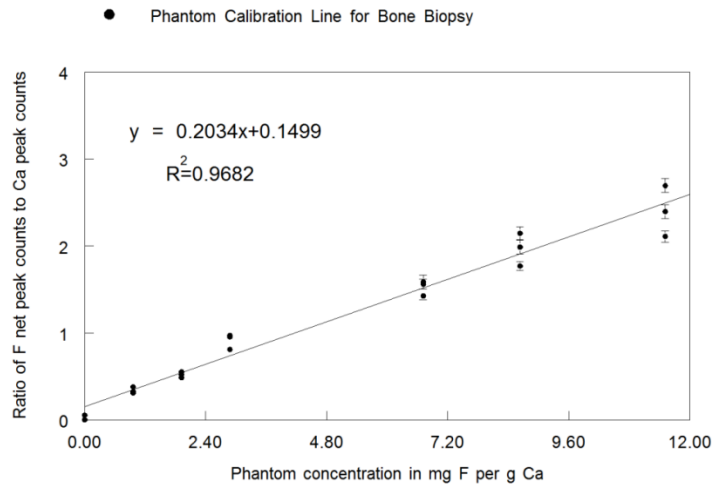


Figure 5.14. Phantom calibration line

Comparison of in vivo and ex vivo data

The F concentrations determined from the *ex vivo* samples were found to range in concentration from 1.02–9.8 mg F/g Ca. The average fluorine concentration in bone was found to be 4.8 ± 0.5 mg F/g Ca for an average age of 81.6 ± 9.3 . Given that the average age of this population is significantly higher than in the *in vivo* study this number seems in line with the *in vivo* data. All 12 samples were found to have measurable fluorine levels in bone i.e. all *ex vivo* samples were found to be significantly different from zero at the 95% confidence level. Figure 5.15 shows the fluorine content per gram of calcium content from the 12 cadavers plotted against age. During the course of the *ex vivo* study, each bone sample was measured three times over a 10 day period. It can be seen from Figure 5.15 that the *ex vivo* measurements were quite reproducible. The average relative uncertainty was $7\% \pm 3\%$. Figure 5.16 shows a plot of the concentration of each *ex vivo* sample (averaged over the three measurements plotted against age on the same graph as the *in vivo* data).

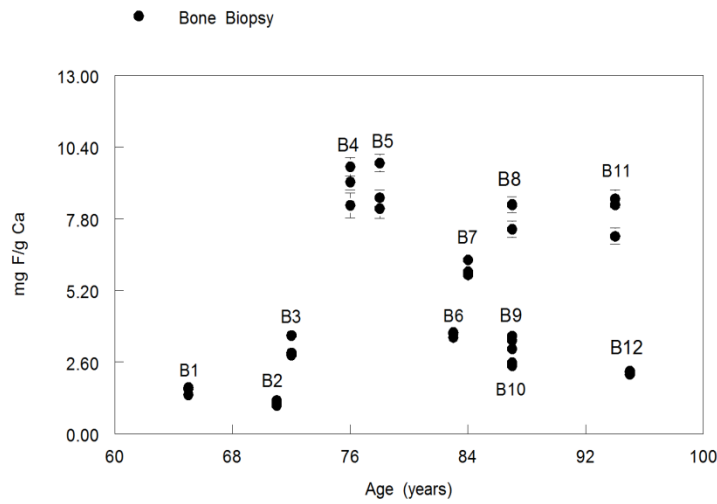


Figure 5.15. Fluorine concentration with age measured in the twelve bone biopsy samples

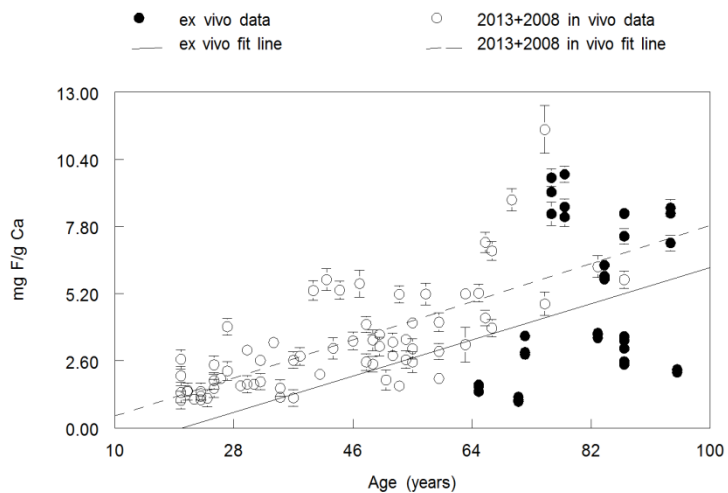


Figure 5.16. A comparison of *in vivo* and *ex vivo* measurement data

The rate of increase of fluorine content versus age for *in vivo* measurements (for men and women and 2008 and 2013 data combined) was found to be 0.078 ± 0.014 mg F/g Ca per year. The rate of increase of fluorine content versus age for *ex vivo* measurements was also found to be 0.078 ± 0.050 mg F/g Ca per year. Although they may look different in Figure 5.16, the intercepts for both the *in vivo* and *ex vivo* data were found to be zero within uncertainties: they were -0.35 ± 0.48 and -1.56 ± 4.43 mg F/g Ca respectively. *Ex*

in vivo measurements of samples from the skull and *in vivo* measurements of a hand therefore show a similar pattern of accumulation of fluorine in the bone matrix, as assessed by calcium content, with age.

Discussion

Comparison of fluorine levels in other published studies

There is evidence in this study that the precision of the *in vivo* measurement of bone fluorine concentrations in volunteers has improved as predicted from previous phantom studies (Mostafaei et al, 2013b) although the use of a single technician performing measurements clearly needs to be re-thought as this has introduced uncertainty into the measurement data. The improvements in precision have, however, meant that even in a small study of 35 volunteers it has been determined that we can measure fluorine concentrations in bone with 99% confidence in 100% of a population of urban Canadians over the age of 20. This means this technique has great potential for assessment the health effects of exposure to fluoride.

A summary of bone fluorine measurements (mostly on autopsy data) with different methods is shown in Table 5.4. Using a conversion factor of 3.68 g dry bone/g Ca (Woodard, 1964), and a conversion factor of 2.5 g bone ash/g Ca (ICRP 1975), this study which measured a Southern Ontario population is comparable to other bone fluorine studies of environmentally exposed subjects from both Canada and other parts of the world. Levels of fluorine measured in patients with fluorosis (Krishnan et al 1985) appear

to be much higher than we observed, which suggests that this *in vivo* technique could be used to identify high exposure patients.

Fordyce published a study in 2011 which divides fluorine concentration in bone into three phases; normal (0.5-1 mg F/g bone ash), preclinical (3.5-5.5 mg F/g bone ash) and clinical phase I (6-7 mg F/g bone ash) (Fordyce et al, 2011). If we use the conversion factor of 2.5 g bone ash/g Ca (ICRP 1975), the range of values determined by us in this study range from 0.4 to 4.6 mg F/g bone ash. Assigning our volunteers into these categories, we can say we observed no people in the 'clinical phase I' of fluoride exposure. Twenty of the volunteer's bone-fluorine concentrations were categorised as 'preclinical phase', while the remaining fifteen were in the 'normal phase'. This may suggest that we either need to re-align these categories taking age into account. A 'high' bone fluorine for a 20-year-old person may be an 'average' or 'normal' bone fluorine for a 60-year-old.

Our data suggest that fluorine metabolism in bone may be different for men and women. This may be due either to sex or to gender. Given that we observe a discontinuity in the relationship of fluorine content with age in women at age 50 in our data, we suggest that sex differences in steroid levels (such as estrogen and testosterone) may account for differences. Steroids are the major contributor responsible for skeletal growth and gain in bone density, helping maintain peak bone density until menopause in women. Steroid production normally decreases at menopause, and leads to relatively rapid bone loss, which occurs in the first 8–10 years after menopause (Clarke et al, 2010). Our previous data on lead in bone (Popovic et al, 2005) showed differences in endogenous release of

lead in pre-menopausal women as compared to men. In post-menopausal women, there was no sex difference observed.

However, there may also be gender differences, such as differences in water, tea or food consumption or use of toothpastes and mouthwashes. However, this is speculation on our part: we merely point out that the observed differences may arise in part both from biological and behavioral factors and further work needs to be performed to unfold this further.

Table 5.4. Comparison of different bone-fluorine published studies

Studies	Location	Bone site	Age	Technique	mg F/g dry bone	mg F/g Ca
Glock et al., 1941	England	Rib bone	0-68	Chemical method	0.24-3.1	0.88-11.4*
Mernagh et al., 1977	Canada	Biopsy sample (osteodystrophy)	N/A	NAA	0.5-1.2	3.2-8.5 (7.6-48.8)
Krishnan et al., 1985	Canada	Biopsy sample (fluorosis patients)	N/A	NAA	N/A	13.4±2.9 (21.5±3.2)
Ebifegha et al., 1986	Canada	Index Finger	N/A	NMR	2.17-5.1	8-18.7*
Fraser Code et al., 1990	Canada	Index Finger	N/A	NMR	0.47-1.1	1.7-4*
McNeill et al., 1991	Canada	Trabecular and cortical bone of the rat	N/A	NMR	N/A	N/A
Ishiguro et al., 1993	Japan	Cortical bone (Human rib)	20-93	Fluoride electrode	0.125-0.75	0.46-2.76*
Samudralwar et al., 1993	USA	Rib (Cortical bone & Trabecular bone)		PIGE (p,p'γ)***	2.074±0.652 1.71±0.632	7.63* 6.29*
Richards et al., 1994	Denmark	Vertebral trabecular	20-91	Fluoride electrode	0.91*	3.34†
Ishiguro et al., 1996	Japan	Trabecular bone Periosteal cortical Endosteal cortical	21-76	Chemical method	0.2-0.6 0.27-1.1 0.23-0.7	0.74-2.21* 0.99-4.05* 0.85-2.58*
Sastri et al., 2001	Turkey and Russia	Iliac crest, rib		PIGE (p,p'γ)***	0.5-1.999	1.84-7.36*
Yildiz et al., 2003	Turkey	vertebra, femur neck, femur trochanter, and Ward's triangle	45-54	DXA**	1.0761±0.179 0.8603±0.1166 0.6821±0.107 0.6527±0.1355	3.96* 3.17* 2.51* 2.4*
Chamberlain et al., 2012	Canada	Hand	20-87	IVNAA	0.3-2.4*	1.1-8.8
This study, 2013	Canada	Hand	23-75	IVNAA	0.3-3.15*	1.1-11.6

* Determined using a conversion factor of 3.68 g dry bone/g Ca (Woodard, 1964)

** Dual X-ray absorptiometry

*** Particle induced gamma-ray emission

† Determined using a conversion factor of 2.5 g bone ash/g Ca (ICRP 1975)

Conclusions

A non-invasive system for measurement of fluorine in the hand was previously developed at McMaster University. This was recently upgraded and improved. There is evidence that the improvement predicted from phantom studies (Mostafaei et al, 2013b) was borne out in humans. However, we have determined that factors such as the number of technicians involved in a measurement have meant that overall the improved precision predicted from phantom studies was not fully observed in people.

This upgraded system was used to perform a pilot *in vivo* study and the data was compared with results from an earlier study performed in 2008. The system of 2013 was found to provide measurements that were compatible with the first generation system of 2008. Both systems showed a consistent increasing relationship between fluorine content of bone mineral and age. In addition, a small study of cadaver data found a relationship between bone fluorine content and age that was also consistent with *in vivo* data. The cadaver data were validated against standard reference material data and thus provides some level of confidence in the results of the *in vivo* data.

The data provided some evidence that fluorine metabolism in bone was different for men and women. There is an observed change in the accumulation rate of fluorine in bone in women at around age 50. This is perhaps not surprising given the role that estrogen plays in bone remodeling between menarche and menopause. However, further studies should be performed to determine whether the differences in fluorine level observed between

men and women are gender differences, i.e. based on behavior, or sex differences, i.e. based on differences in bone metabolism due to differences in sex steroids, the levels of which change in women over time.

There was also evidence that a significant source of fluoride exposure for people living in Southern Ontario is tea drinking. People who reported drinking tea were found to have double the level of fluorine in bone than non-tea drinkers. This is assumed to be because tea is often grown in fluoride rich soils. Further studies to investigate whether particular types of tea are significant sources of exposure are warranted.

Acknowledgments

The authors would like to thank Justin Bennett, the accelerator operator at McMaster University, for his assistance. They also wish to recognize Dave Tucker and Christopher Malcolmson, of McMaster University Health Physics, for providing pertinent radiation safety advice, and assistance with licensing issues. Glen Oomen from the Education Program in Anatomy assisted in collection of the bone specimens. The authors are appreciative of all the volunteers who agreed to participate in the study. Funding was provided by the Natural Sciences and Engineering Research Council of Canada.

References

Aslam, Pejović-Milić A, Chettle D R, McNeill F E, Pysklywec M W and Oudyk J. (2008a) A preliminary study for non-invasive quantification of manganese in human hand bones *Phys. Med. Biol.* 53 N371–6

Aslam, Pejović-Milić A, McNeill F E, Byun S H, Prestwich W V and Chettle D R. (2008b) *In vivo* assessment of magnesium status in human body using accelerator-based neutron activation measurement of hands: a pilot study *Med. Phys.* 35 608

Boivin, G., Chavassieux, P., Chapuy, M. C., Baud, C. a, & Meunier, P. J. (1989). Skeletal fluorosis: histomorphometric analysis of bone changes and bone fluoride content in 29 patients. *Bone*, 10(2), 89–99.

Burt, B.(2002). Fluoridation and social equity. *Journal of public health dentistry*, 62(4), 195-200.

Byun, S. H., Pejović–Milić, A., McMaster, S., Matysiak, W., Aslam, Liu, Z., Watters, L. M., et al. (2007). Dosimetric characterization of the irradiation cavity for accelerator-based *in vivo* neutron activation analysis. *Physics in Medicine and Biology*, 52(6), 1693–1703.

Byun, S. H., Pejović–Milić, A., Prestwich, W. V, Chettle, D. R., & McNeill, F. E. (2006). Improvement of *in vivo* neutron activation analysis of Mn using a 4 π NaI (Tl) detector array. *Radioanalytical and Nuclear Chemistry*, 269(3), 615–618.

Chamberlain, M., Grafe, J. L., Aslam, Byun, S. H., Chettle, D. R., Egden, L. M., Orchard, M. G., et al. (2012a). The feasibility of *in vivo* quantification of bone-fluorine in humans by delayed neutron activation analysis: a pilot study. *Physiological measurement*, 33(2), 243–257.

Chamberlain, M., Grafe, J. L., Aslam, Byun, S. H., Chettle, D. R., Egden, L. M., Webber, C. E. and, et al. (2012b). *In vivo* quantification of bone-fluorine by delayed neutron activation analysis: a pilot study of hand-bone-fluorine levels in a Canadian population. *Physiological Measurement*, 33, 375–384.

Clarke, B.L, Khosla, S., (2010). Female reproductive system and bone. *Archives of Biochemistry and Biophysics*, 503, 118–128.

Davis K, Aslam, Pejović-Milić A and Chettle D R 2008 *In vivo* measurement of bone aluminum in population living in southern Ontario, Canada *Med. Phys.* 35 5115–23

- Dinman, B. D., Elder, M. D., Bonney, T. B., Bovard, P. G., & Colwell, M. O. (1976). A 15-Years Retrospective Study of Fluoride Excretion and Bony Radiopacity Among Aluminum Smelter Workers. *Journal of Occupational Medicine*, 18, 21-23.
- Fordyce, F. M., J. O. Nriagu. (2011). *Fluorine: human health risks Encyclopedia of Environmental Health* vol 2 (Burlington: Elsevier) pp 776–85
- Fordyce, F. M., Vrana, K., Zhovinsky, E., Povoroznuk, V., Toth, G., Hope, B. C., Iljinsky, U. and Baker, J. (2007) A health risk assessment for fluoride in Central Europe. *Environmental Geochemistry and Health. Special Issue Medical Geology in Developing Countries* 29 (2), 83-102
- Glock, G. E., Lowater, F., & Murray, M. M. (1941). The retention and elimination of fluorine in bones. *The Biochemical journal*, 35(10-11), 1235–9.
- Health Canada. (2010). *Guidelines for Canadian Drinking Water Quality Guideline Technical Document*. Ottawa.
- ICRP 1975 *Report of the Task Group on Reference Man* (Oxford: Pergamon) Publication 23
- Ishiguro, K., Nakagaki, H., Eba, H., & Omi, K. (1996). The age relationship of fluoride profiles in trabecular bone endosteal cortical.pdf. *Oral Med Pathol*, 1, 71–76.
- Ishiguro, K., Nakagaki, H., Tsuboi, S., Narita, N., Kato, K., Li, J., Kamei, H., et al. (1993). Distribution of fluoride in cortical bone of human rib. *Calcified tissue international*, 52(4), 278–82.
- Khandare, A L., Harikumar, R., & Sivakumar, B. (2005). Severe bone deformities in young children from vitamin D deficiency and fluorosis in Bihar-India. *Calcified tissue international*, 76(6), 412–8.
- Krishnan S S, Mernagh J R, Hitchman A J W, McNeill K G, Harrison J E. (1985). Measurements of Fluoride in bone biopsies by neutron activation analysis for the clinical study of Osteoporosis. *Nuclear Chemistry*, 95(2), 119–125.
- Ludlow M, Luxton G., and Mathew T. (2007). Effects of fluoridation of community water supplies for people with chronic kidney disease. *Nephrology, dialysis, transplantation*, 22(10), 2763–7.
- McKinlay M S., Brambilla J D, and Posner G J. (1992). The normal menopause transition. *Maturirtrs*. 14, 103-115.

- Mernagh, J. R., Hancock, R., & McNeill, K. G. (1977). Measurement of Fluoride in Bone, *International Journal of Applied Radiation and Isotopes*, 28, 581–583.
- Mostafaei, F., McNeill, F. E., Chettle, D. R., Matysiak, W., Bhatia, C., & Prestwich, W. V. (2015). An investigation of the neutron flux in bone-fluorine phantoms comparing accelerator based in vivo neutron activation analysis and FLUKA simulation data. *Nuclear Inst. and Methods in Physics Research, B*, 342, 249-257.
- Mostafaei, F., McNeill, F. E., Chettle, D. R., Prestwich, W. V., & Inskip, M. (2013a). Design of a phantom equivalent to measure bone-fluorine in a human's hand via delayed neutron activation analysis. *Physiological measurement*, 34(5), 503–512.
- Mostafaei, F., McNeill, F. E., Chettle, D. R., & Prestwich, W. V. (2013b). Improvements in an in vivo neutron activation analysis (NAA) method for the measurement of fluorine in human bone. *Physiological measurement*, 34(10), 1329–1341.
- Pejović-Milić A, Byun S H, Chettle D R, McNeill F E and Prestwich W V. (2006). Development of an irradiation/shielding cavity for *in vivo* neutron activation analysis of manganese in human bone *J. Radioanal.Nucl. Chem.* 269 417–20
- Popovic, M., McNeill, F. E., Chettle, D. R., Webber, C. E., Lee, C. V., & Kaye, W. E. (2005). Impact of Occupational Exposure on Lead Levels in Women. *Environmental Health Perspectives*, 113(4), 478–484.
- Prystupa, J. (2011). Fluorine--a current literature review. An NRC and ATSDR based review of safety standards for exposure to fluorine and fluorides. *Toxicology mechanisms and methods*, 21(2), 103–70.
- Richards, A, Mosekilde, L., & Sogaard, C. H. (1994). Normal age-related changes in fluoride content of vertebral trabecular bone--relation to bone quality. *Bone*, 15(1), 21–6.
- Samudralwar, D. L., & Robertson, J. D. (1993). Determination of major and trace elements in bones by simultaneous PIXE/PIGE analysis. *Journal of Radioanalytical and Nuclear Chemistry Articles*, 169(1), 259–267.
- Sastri, C. S., Iyengar, V., Blondiaux, G., Tessier, Y., Petri, H., Hoffmann, P., Aras, N. K., et al. (2001). Fluorine determination in human and animal bones by particle-induced gamma-ray emission. *Fresenius' journal of analytical chemistry*, 370(7), 924–9.
- Schmidt, D. (2014). Windsor votes to remove fluoride from drinking water. The Windsor star.

- Shashi A (1992) Biochemical effects of fluoride on lipid metabolism in the reproductive organs of male rabbits. *Fluoride* 25:149–154.
- Shashi, A., Kumar, M., & Bhardwaj, M. (2008). Incidence of skeletal deformities in endemic fluorosis. *Tropical doctor*, 38(4), 231–3.
- Spencer, H., Osis, D., Wiatrowski, E., & Samachson, J. (1970). Availability of fluoride from fish protein concentrate and from sodium fluoride in man. *The Journal of nutrition*, 100(12), 1415–24.
- Tamer M N, Kale Koroğlu B, Arslan C, Akdoğan M, Koroğlu M, Cam H, Y. M. (2007). Osteosclerosis due to endemic fluorosis. *The Science of the total environment*, 373(1), 43–8.
- Utian, W H., Boggs, P P. (1999). The North American Menopause Society 1998 Menopause Survey. Part I: Postmenopausal Women's Perceptions about Menopause and Midlife. *The Journal of North American Menopause Society*,6(2), 83-180.
- Wang W, Kong L, Zhao H, Dong R, Li J, et al. (2007). Thoracic ossification of ligamentum flavum caused by skeletal fluorosis. *European spine journal*, 16(8), 1119–28.
- Whitford, G. M. (1994). Intake and Metabolism of Fluoride, *Advances in Dental Research*, 8(1),5-14.
- WHO (2006). *Fluoride in Drinking Water*. London: IWA Publishing.
- Wilson, J. (1993). Endemic Skeleton : Patients Fluorosis Radiographic of the Features. *American Roentgen Ray Society*, 94-98.
- Woodard, H. Q. (1964). The Composition of Human Cortical Bone. *Clinical orthopaedics and related research*, 37, 187–193.
- Yadav A K, Kaushik C P, Haritash A K, Singh B, Raghuvanshi S P, K. A. (2007). Determination of exposure and probable ingestion of fluoride through tea, toothpaste, tobacco and pan masala. *Journal of hazardous materials*, 142(1-2), 77–80.
- Yildiz, M., Akdoğan, M., Tamer, N., & Oral, B. (2003). Bone mineral density of the spine and femur in early postmenopausal Turkish women with endemic skeletal fluorosis. *Calcified tissue international*, 72(6), 689–93.

Chapter 6

Conclusions and Future Work

6.1 Thesis conclusions

The original research in this thesis was presented in four major sections: each was given a Chapter. The significant results, and a summary of each research section follows, where the most significant contributions to the field are noted. A conclusion is provided for each section.

6.1.1 Development of a New Bone-Fluorine Phantom

Chapter 2 detailed the development of a new type of hand-bone simulating phantom for the determination of fluorine concentration by IVNAA. This work was important and was a significant contribution to the field, as it effectively eliminated an observed problem of aluminum contamination.

The phantoms which were used in the early fluoride studies were found to contain a small level of aluminum contamination. This was a problem because the aluminum γ -ray peak interfered with the fluorine γ -ray signal due to energies overlapping within the resolution of the sodium iodide detectors. While this signal could be removed by subtraction, this introduced uncertainties into the measurement. Removing the aluminum from the phantom reduced the measurement uncertainties, improved the calibration line uncertainties, and permitted a significant reduction in the phantom detection limit.

A number of phantoms were tested and after significant number of trial and error experiments a new series of phantoms was developed; and these phantoms were found to have low aluminum contamination. The new phantoms used Mowiol 4-88 an organic anti-fade medium and were found to have non-detectable levels of aluminum. The new phantom's calibration line slope was determined to be comparable with the previously used phantoms.

The use of the new phantoms was found to reduce the MDL by factor of 1.55 and this phantom development is a significant contribution to the field because it permits a better (i.e., more precise) measurement of fluoride. This work will also permit development of better phantoms for researchers wishing to measure aluminum *in vivo*, or any researchers wishing to perform measurements with a low aluminum contaminated medium.

In addition to the conclusions provided in earlier Chapters, an overall conclusion is that calibration phantom development and improvement is an area of research on which it is worth spending time and effort. It is important to have phantoms that are a close match for the organ being measured, but an additional significant challenge for researchers in *in vivo* analysis of trace elements is finding trace free or contaminant free materials. In this case, finding contaminant free materials and preparation methods significantly improved the ability to measure fluoride and was worth the time and effort involved.

6.1.2 Improvements in to the IVNAA Method for Measurement of Fluoride

Chapter 3 detailed improvements to the measurement system. These were performed because although the previous *in vivo* study had been able to measure the fluoride level in the majority of volunteers with confidence, some *in vivo* measurements were below the detection limit. It was decided that lowering the detection limit further, if possible, would make the measurement more applicable in environmental studies. Several improvements to the system were successfully performed. These included changing both the detection mode and the acquisition timing in the γ -ray spectrometry system. By using an anti-coincidence acquisition mode rather than simple summing of nine single detectors together, the minimum detectable limit was lowered by a factor of 1.2. Changing the acquisition time sequence to a series of six 5s steps from a series of three 10s steps lowered the minimum detectable limit by a further factor of 1.4. Increasing the accelerator proton current and reducing the irradiation time at the same time provided a further improvement in minimum detectable limit by a factor of 1.35. Overall, the series of improvements were found to produce a significant improvement of 3.88 in minimum detectable limit, in phantoms, when compared to the previously published data of Chamberlain et al. 2012. The new minimum detectable limit of 0.17 mg F/g Ca was believed to be below the expected F concentration in healthy non-occupationally exposed individuals. The range of fluorine in human bone has been published as being from 300-7000 mg/kg dry tissue (1.1-25.76 mg F/g Ca) (Fordyce, 2011). The minimum detectable limit determined by this particular part of the thesis suggested that the technique should be capable of measuring bone-fluorine *in vivo* in a ‘normal’ or ‘average’ population in

many parts of the world, while delivering an acceptable radiation dose, and eliminating the need for the discomfort and pain of a bone biopsy.

In addition to the information provided in earlier Chapters, a conclusion that can be drawn from this work is that it is worth pursuing a series of relatively small improvements. In the cases presented here, the individual improvement was incremental, not transformative, being, in each case, only of the order of 20% - 40% for each improvement. However, by pursuing a number of these incremental improvements, the overall improvement was ultimately very significant and the phantom detection limit was reduced by nearly a factor of 4.

6.1.3 Monte Carlo Modelling of the Bone Fluoride System

The Monte Carlo code, FLUKA, was used as an additional tool to investigate, and help develop, the neutron activation analysis system for the measurement of fluoride in bone. FLUKA is not a code that has been applied to *in vivo* analysis so there was an interest in testing its performance. The code, as tested using this simulation model, was found to produce comparable data to experimental results and so the work provides some validation that FLUKA can be used for this kind of work. The thermal neutron fluence rate was found to vary by a few percent across the inside of the irradiation cavity. These effects are interpreted to mean that there will be variations in the thermal fluence in the cavity. The activation of F from thermal neutrons varies from 94.5% to 92.3% and for calcium from 98.8% to 98.6%. Therefore the balance of the activation comes from epithermal or resonance neutrons with a relative ratio varying by approximately 2%.

While the normalization of F to Ca is not perfect, it can be applied to within the uncertainties of measurement because the neutron spectrum in the cavity is mostly thermalized. This will mean variations in the measurement precision from person to person, but should not affect the accuracy of a fluorine measurement.

In addition, the use of the modelling, and comparison of simulation and experimental data, allowed us to predict the best position in the irradiation room for the detection system for *in vivo* measurements. Figure 6.1 illustrates the actual location of the detection system for the series of *in vivo* measurements which was predicted by a combination of experimental and with FLUKA simulation.



Figure 6.1. The detection system best position beside the irradiation cavity

An overall conclusion from this work is that FLUKA is a code that has some utility for investigation of *in vivo* analysis. As with all simulation codes, some combination of experiment and simulation is required to validate the code, but the resulting information can significantly assist in the design of the system.

6.1.4 Measurements of Fluoride in Bone in Urban Canadians: a Study of Volunteers from the City of Hamilton

The series of incremental improvements to the system had been shown to result in a significant reduction in minimum detectable limit in phantoms. The system was therefore used in a pilot *in vivo* study of the measurement of fluoride in the hand bones of volunteers recruited from Hamilton, Ontario. The measurement subjects were a convenient sample of volunteers drawn mostly from the McMaster community. They were assumed to not be heavily exposed to fluoride from either industrial or environmental sources. They were assumed to be a ‘normal’ population representing the average exposure in Southern Ontario. We performed fluorine measurements in human bone with the newly improved non-invasive method on 35 participants.

In Chapter 3, a series of improvements were found to produce a significant improvement in the phantom minimum detectable limit when compared to the phantom data previously published by Chamberlain et al, 2012. The improvement observed in the volunteer’s measurements were not as good an improvement as expected. Some reasons which were affected the precision are: 1) two technical staff conducted each measurement in 2008

compare with one technician in this study (which resulted in a lower transfer time in 2008), 2) lower neutron production per unit current off the target, and 3) the higher background levels.

Bone fluoride was measurable in all 35 subjects at the 95% confidence level. We found a significant correlation between bone fluoride content and subject age: fluoride is accumulating in bone with a long retention time. The average fluorine concentration in bone was found to be 3 ± 0.3 and 3.5 ± 0.4 mg F/g Ca for 2013 and 2008 measurements respectively. Differences in the relationship between bone fluoride level and age between men and women were observed, which may be attributable either to sex or gender differences. The slope for women was found to be slightly less than half that of men.

In addition, we found that there was a significant difference in bone fluoride level (as determined by the slope of the regression of bone fluoride versus age, $p = 0.001$) between individuals who drink tea regularly as compared to non-tea drinkers, suggesting tea may be a significant source of exposure. The slope of the tea drinkers' relationship with age is more than twice that of the non-tea drinkers. The difference is significant at the 95% confidence level ($p = 0.016$). This is not surprising as tea is known to contain significant amounts of fluoride.

Tea becomes an important source of fluoride in areas of the globe where it is considered a common drink (Duckworth et al., 1978). The concentration of fluoride in tea may vary based on the way it is handled, generally natural tea leaves contain fluoride levels as high as 400 mg/kg (Duckworth et al., 1978). But when it is brewed with deionized water it can

range from 0.1 to 4.2 mg/L, the overall average can be 3 mg/L (Duckworth et al., 1978).

Table 6.1 shows the levels of fluoride measured in teas from different parts of the world.

Table 6.1. Measured levels of fluoride in tea as reported by researchers from different countries

Studies	Country	Number of cups per day	Tea-fluoride concentrations (mg F/liter)
(Gulati et al., 1993)	India	2-6	1.55-3.21
(Chan et al., 1996)	USA	4-5	0.34-3.71
(Fung et al., 2000)	China	N/A	1.6-7.34
(Lung et al., 2003)	Taiwan	N/A	5.37-25.7
(Gardner et al., 2007)	UK	≥3	Insufficient evidence
(Lung et al., 2008)	Taiwan	N/A	1.97-8.64
(Malinowska et al., 2008)	Poland	5	1.5-2.5
(Joshi et al., 2011)	UK	6	7.6

In addition to the *in vivo* measurements, we also performed a small *ex vivo* study of bone samples. We collected twelve bone samples from the skulls of cadavers: the subjects were assumed to be non-exposed and ‘normal’ subjects representing the average exposure to fluoride in Southern Ontario. The McMaster Nuclear Reactor (MNR) pneumatic neutron activation analysis system was used to determine the fluoride levels. This small study of cadaver bone data found levels in bone and a relationship between bone fluoride content and age that was consistent with *in vivo* data. *Ex vivo* samples were found to be significantly different from zero at the 95% confidence level. Excellent agreement was found between the fluoride levels determined *in vivo* and *ex vivo* using the two separate systems. These data provided some confidence that the *in vivo* data are an accurate measurement of bone fluoride content.



Figure 6.2. Volunteer's hand irradiation at MAL for IVNAA measurements.

An overall series of conclusions can be drawn from this *in vivo* study. First and foremost, it is important to note that this result shows that data from phantom studies cannot always be directly extrapolated to the actual *in vivo* situation. While it was found that there were some improvements in detection limits in humans, the results from the measurement of phantoms were not completely borne out in the measurements of people. Phantom data do not include human factors, such as challenges in positioning people, or dealing with a person, while also trying to switch on electronics. Results from phantom studies therefore need a series of caveats placed on the interpretation of data.

Secondly, the data show that fluoride level correlates with age. A conclusion that can be drawn from these data is that there is evidence that fluoride levels in bone are a marker of long term or cumulative fluoride exposure. *In vivo* neutron activation analysis fluoride

bone measurements are therefore likely to be very useful as an exposure measure in studies of the health effects of exposure to fluoride. This is a significant finding of this thesis. However, studies will need to take sex and gender into account as there is some evidence of sex and/or gender differences in exposure levels.

6.2 Future work

There are a number of future studies that could be performed to improve this system further and ensure that it can be applied in studies of the health effects of fluoride.

6.2.1 Transfer times

Given the results of the *in vivo* data, the first piece of future work that needs to be performed is an analysis of how to ensure that short transfer times can be consistently performed. Some suggestions are:

- 1- Using an easy removal water sleeve, which is tightened around the volunteer's arm. In this thesis work, we have had a problem with the water sleeve's zipper being stuck in some cases.
- 2- Using a pump to remove water from the sleeve instead of the gravity-draw method
- 3- Explaining the procedure in more detail to the volunteers, and helping them to understand the situation better in order to prevent confusion after irradiation.

6.2.2 Future *in vivo* studies

The data determined by the *in vivo* measurement technique were found to be consistent with results from *ex vivo* studies. As mentioned in the last section, this suggests that the data demonstrate that this low risk non-invasive diagnostic technique will permit the assessment of long term fluoride exposure and has potential application in the study of clinical fluoride induced bone-related diseases. Future investigations in the following areas are suggested:

1. Apply the neutron activation technology to a larger scale study of volunteers and improve the environmental exposure questionnaire to look at possible effects of tea drinking, toothpaste use, bottled and tap water exposure. Questions that unfold the effect of sex and gender are warranted, and information on the menstrual status of women participants should be requested, as it is known that estrus and menopause affect bone turnover. A wider sample of volunteers could allow the effect of factors such as, geographical area in Ontario and Canada, ethnicity and cultural background, and occupation on bone fluoride level to be assessed.
2. The use of a 4π hyperpure germanium detector (HPGe) as a detection system. In this thesis work, nine NaI(Tl) detectors in a nearly 4π array were used for this PhD study. They proved to have near 100 % efficiency and were studied in both coincidence and anti-coincidence mode. The detector has shown a high performance for our

measurements in that studies in humans are possible. However, NaI detectors have a poor energy resolution compared to other detector types. Given that this system has issues with interferences from chlorine and aluminum, investigating detectors which may reduce interferences could be useful. The testing of hyperpure germanium detectors (HPGe) could be important. The feasibility of buying several hyperpure germanium detectors (HPGe) to build a 4π shape will be challenging. Each detector costs roughly \$30,000, so a 4π system would cost over one million dollars. The study performed in Chapter 3 with a single detector showed a feasibility and predictive analysis, and illustrated that perusing the technique is warranted.

3. Recruit patients who have been diagnosed with skeletal or dental fluorosis or sclerosing bone conditions to determine if the system has a potential clinical application i.e. determine if the system can discriminate between normal and raised fluorine exposures. The volunteers that were measured in this thesis were all healthy adults with no previous diagnosis of raised fluoride exposure. Healthy adults would seem to follow a predictable pattern of increasing mass fraction, or concentration or possibly accumulation with age. However, a limitation of the technique at the moment is that it is not known whether the system would be able to determine if people who show clinical symptoms (including dental effects) would be found to have levels that lie outside the confidence limits of 'normal' exposure. Future studies should test this method by measuring levels in patients who suffer from skeletal or dental fluorosis or sclerosing bone conditions and seeing if there levels are significantly different. If this can be shown in an individual, the system will have clinical utility.

4. Investigate the fluoride content of different tea brands available in Canada using the McMaster Nuclear Reactor and incorporate tea consumption levels into the exposure questionnaire. Previous studies and Health Canada's report of 2010 indicated that tea is one of the main sources of fluorine exposure in Canada. This was borne out by the studies reported in this thesis: drinking tea appears roughly to double an individual's exposure to fluoride. Since a large number of people in Canada drink tea regularly, and it is a source of exposure, investigating different tea brands and the method of preparing tea, in order to assess fluoride exposure, could be important. Canada imports various kinds of tea such as tea leaves and teabags from different countries. China and India are the two main tea producers in the world, and they are countries which happen to have the highest concentration of fluorine in underground water. In order to measure the amount of fluorine concentration in tea consumed by Canadian citizens, future studies could analyse each tea brand and type using the pneumatic NAA system in the McMaster Nuclear Reactor. Other than measuring the tea type, different preparation styles could also be studied. Since different people from different cultures have their own method for tea preparation, adding a questionnaire to future *in vivo* studies, asking how individuals prefer their tea is suggested (e.g. using a pot or a boiler). This could be linked to a study of exposure from types of tea. The data gathered from this type of measurement can result in recommendations for individuals in choosing the type of tea they consume and the style they brew their tea.

Due to a series of improvements and repeated measurements on volunteers, using the Tandem accelerator for measuring fluoride *in vivo* is promising. It was shown to be a

reliable system for measuring fluorine concentration in bone for people who have been exposed to low levels of fluoride. It is now possible to measure the exposure of people to fluoride in Canada.

References

- Ad Hoc Subcommittee on Fluoride (1991). Review of fluoride benefits and risks. Ad Hoc Subcommittee on Fluoride of the Committee to Coordinate Environmental Health and Related Programs, Public Health Service, United States Department of Health and Human Services, Research Triangle Park, NC, February.
- Alhava, E. M. Olkkonen, H. Kauranen, P. Tarja Kari (1980). The effect of drinking water fluoridation on the fluoride content, strength and mineral density of human bone, *Acta orthop. scand* 51, 413–420.
- Ando, M., Tadano, M., Asanuma, S., Tamura, K., Matsushima, S., Watanabe, T., Kondo, T., et al. (1998). Health effects of indoor fluoride pollution from coal burning in China. *Environmental health perspectives*, 106(5), 239–44.
- Aslam, Pejović–Milić, A., McNeill, F. E., Byun, S. H., Prestwich, W. V. and, & Chettle, D. R. (2008). In vivo assessment of magnesium status in human body using accelerator-based neutron activation measurement of hands: A pilot study. *Medical Physics*, 35(2), 608-616.
- ATSDR (2003). Toxicological profile for fluorides, hydrogen fluoride, and fluorine. Agency for Toxic Substances and Disease Registry, Public Health Service, United States Department of Health and Human Services, Atlanta, Georgia, September. Available at: www.atsdr.cdc.gov/toxprofiles/tp11.html.
- Augenstein, W.L., Spoerke, D.G., Kulig, K.W., Hall, A.H., Hall, P.K., Riggs, B.S., Saadi, M.E. and Rumack, B.H . (1991). Fluoride ingestion in children: a review of 87 cases. *Pediatrics*, 88: 907–912.
- Bevington, P. R. (2003). *Data Reduction and Error Analysis for Physical Sciences.pdf* (Third Edit.). New York: McGraw-Hill.
- Boivin, G., Chavassieux, P., Chapuy, M. C., Baud, C. a, & Meunier, P. J. (1989). Skeletal fluorosis: histomorphometric analysis of bone changes and bone fluoride content in 29 patients. *Bone*, 10(2), 89–99.
- Boivin G, Chavassieux P, Chapuy MC, Baud CA, Meunier PJ. (1986). Profil histomorphométrique de la fluorose osseuse induite par l'ingestion prolongée d'eau de Vichy Saint-Yorre. Comparaison avec le taux de fluoroséux. *Pathol Biol*. 34:33–9.
- Brown LJ, Wall TP, Lazar V. (2000). Trends in untreated caries in primary teeth of children 2 to 10 years old. *J Am Dental Assoc* 131:93-100.

- Bryson, C. (2004). *The Fluoride Deception*. A seven stories press, first edition.
- Burt B A. (1985). The future of the caries decline. *J Public Health Dentistry* 45:261-9.
- Burt BA. (1992). The changing patterns of systemic fluoride intake. *J Dent Res*.71:1228–37.
- Burt, B. (2002). Fluoridation and social equity. *Journal of public health dentistry*, 62(4), 195–200.
- Byun, S. H., Pejović–Milić, A., McMaster, S., Matysiak, W., Aslam, Liu, Z., Watters, L. M., et al. (2007). Dosimetric characterization of the irradiation cavity for accelerator-based in vivo neutron activation analysis. *Physics in Medicine and Biology*, 52(6), 1693–1703.
- Byun, S. H., Pejović–Milić, A., Prestwich, W. V, Chettle, D. R., & McNeill, F. E. (2006). Improvement of in vivo neutron activation analysis of Mn using a 4 π NaI (Tl) detector array. *Radioanalytical and Nuclear Chemistry*, 269(3), 615–618.
- Chachra, D., Vieira, A. P. G. F., & Grynypas, M. D. (2008). Fluoride and mineralized tissues. *Critical reviews in biomedical engineering*, 36(2-3), 183–223.
- Chamberlain, M., Gräfe, J. L., Aslam, Byun, S.-H., Chettle, D. R., Egden, L. M., Webber, C. E., et al. (2012). In vivo quantification of bone-fluorine by delayed neutron activation analysis: a pilot study of hand-bone-fluorine levels in a Canadian population. *Physiological measurement*, 33(3), 375–84.
- Charen, J., Taves, D. R., Stamm, J. W., & Parkins, F. M. (1979). Clinical Investigations Bone Fluoride Concentrations Associated with Fluoridated Drinking Water, *Clacified tissue international*, 99, 95–99.
- Chettle, D. R. (2006). Occupational nuclear medicine : Trace element analysis of living human subjects, *Journal of Radioanalytical and Nuclear Chemistry*, 268(3), 653–661.
- Chettle, D. R., & Fremlin, J. H. (1984). Techniques of in vivo neutron activation analysis. *Physics in medicine and biology*, 29(9), 1011–43.
- Chlubek D, Grucka-Mamczar E, Birkner E, Polaniak R, Stawiarska-Pieta B, Duliban H (2003) Activity of pancreatic antioxidative enzymes and malondialdehyde concentrations in rats with hyperglycemia caused by fluoride intoxication. *J Trace Elem Med Biol* 17:57–60.

Dean, H. T. (1942). The investigation of physiological effects by the epidemiological method. In Mouton, R. F. (ed.) *Fluorine and Dental Health*. Washington: American Association for the Advancement of Science 19, 23-31.

Department of National Health and Welfare (1983). Recommended nutrient intakes for Canadians. Health Protection Branch, Ottawa.

Department of National Health and Welfare (1990). Nutrition recommendations. The report of the Scientific Review Committee. Supply and Services Canada, Ottawa. p.160.

Dinman, B. D., Elder, M. D., Bonney, T. B., Bovard, P. G., & Colwell, M. O. (1976). A 15-Years Retrospective Study of Fluoride Excretion and Bony Radiopacity Among Aluminum Smelter Workers. *Journal of Occupational Medicine*, 18, 21-23.

Drinking Water Atlas of China. (1990). China Cartographic Publishing House, Beijing, pp. 91-92.

Duckworth, S.C., Duckworth, R., (1978). The ingestion of fluoride in tea. *British Dent. J.* 153, 64-66.

Eble, D. M., Deaton, T. G., Wilson, F. C., & Bawden, J. W. (1992). Fluoride concentrations in human and rat bone. *Journal of public health dentistry*, 52(5), 288-91.

Edmunds, W. M. and Smedley P. M. (2005). Fluoride in natural waters. In Selinus, O. (ed.) *Essentials of Medical Geology*. London: Elsevier, 301-330.

Ekstrand, J., Alvan, G., Boreus, L.O. and Norlin, A. (1977). Pharmacokinetics of fluoride in man after single and multiple oral doses. *Eur. J. Clin. Pharmacol.*, 12: 311-317.

Fawell, J. (2003). Contaminants in drinking water. *British Medical Bulletin*, 68(1), 199-208.

Fisher, J.R., Sievers, M .L., Takeshita, R.T. and Caldwell, H. (1981). Skeletal fluorosis from eating soil. *Ariz. Med.*, 38(11): 833-835.

Flaitz, C.M., Hill, E.M. and Hicks, M .J. (1989). A survey of bottled water usage by pediatric dental patients: implications for dental health. *Quint. Int.*, 20: 847-852.

Fluoridation Census, (1988), Centers for Disease Control, U.S. Public Health Service, 1985.

- Fordyce, F. M., Vrana, K., Zhovinsky, E., Povoroznuk, V., Toth, G., Hope, B. C., Iljinsky, U. and Baker, J. (2007) A health risk assessment for fluoride in Central Europe. *Environmental Geochemistry and Health. Special Issue Medical Geology in Developing Countries* **29** (2), 83-102.
- Fordyce, F. M. (2011). Fluorine-Human Health Risks. *Encyclopedia Of Environmental Health, Elsevier*, 2, 776–785.
- Fung, K. F., Zhang, Z. Q., Wong, J. W. C., & Wong, M. H. (2000). Fluoride contents in tea and soil from tea plantations and the release of fluoride into tea liquor during infusion, *104*, 197–205.
- Gardner, E. J., Ruxton, C. H. S., & Leeds, a R. (2007). Black tea--helpful or harmful? A review of the evidence. *European journal of clinical nutrition*, *61*(1), 3–18.
- Glock, G. E., Lowater, F., & Murray, M. M. (1941). The retention and elimination of fluorine in bones. *The Biochemical journal*, *35*(10-11), 1235–9.
- Gulati, P., Singh, V., Gupta, M. K., Vaidya, V., Dass, S., & Prakash, S. (1993). Studies on the leaching of fluoride in tea infusions. *The Science of the total environment*, *138*(1-3), 213–21.
- Grucka-Mamaczar E, Birkner E, Kasperczyk S, Kasperczyk A, Chlubek D, Samujło D, Cegłowski A (2004) Lipid balance in rats with fluoride- induced hyperglycemia. *Fluoride* *37*(3):195–200.
- Haftenberger, M ., Viergutz, G., Neumeister, V. and Hetzer, G . (2001). Total fluoride intake and urinary excretion in German children aged 3–6 years. *Caries Res.*, *35*: 451–457.
- Health Canada. (2010). *Guidelines for Canadian Drinking Water Quality Guideline Technical Document*. Ottawa.
- Health Canada. (2009). *Guidelines for Canadian Drinking Water Quality Guideline Technical Document*. Ottawa.
- Hedlund LR, Gallagher JC. (1989). Increased incidence of hip fractures in osteoporotic women treated with sodium fluoride. *J Bone MinerRes.* *4*:223-225.
- Hodge HC, Smith FA. (1963). Hard tissue metabolism of fluoride. In: Simons JH, editor. *Fluorine chemistry*. New York: Academic Press; p. 517–682.
- Inkovaara J, Hekinheimo R, Jarnen K, Kosurlnen V, Hanhijarvi H, Lisolo E. (1975). Prophylactic fluoride treatment and aged bones. *Br MedJ.* *3*:73-74.

ICRP 2002, "Basic anatomical and physiological data for use in radiological protection: reference values. A report of age- and gender-related differences in the anatomical and physiological characteristics of reference individuals. ICRP Publication 89", *Annals of the ICRP*, vol. 32, no. 3-4, pp. 5-265.

IPCS (2002). Fluorides. International Programme on Chemical Safety, World Health Organization, Geneva (Environmental Health Criteria 227).

Ishiguro, K., Nakagaki, H., Eba, H., & Omi, K. (1996). The age relationship of fluoride profiles in trabecular bone endosteal cortical.pdf. *Oral Med Pathol*, 1, 71–76.

Ishiguro, K., Nakagaki, H., Tsuboi, S., Narita, N., Kato, K., Li, J., Kamei, H., et al. (1993). Distribution of fluoride in cortical bone of human rib. *Calcified tissue international*, 52(4), 278–82.

Jenkins, G. N. (1990). Trace Metal and fluoride in bones and teeth. *Direct all inquiries to CRC press*. Chapter 6. p 141-167.

Johnson H J E, Kearns A E, Doran P M, K. T. K. and W. R. A. (2007). Fluoride-related bone disease associated with habitual tea consumption. *Mayo Clinic proceedings*. *Mayo Clinic*, 82(6), 719–724.

Joshi, S., Hlaing, T., Whitford, G. M., & Compston, J. E. (2011). Skeletal fluorosis due to excessive tea and toothpaste consumption. *Osteoporosis international : a journal established as result of cooperation between the European Foundation for Osteoporosis and the National Osteoporosis Foundation of the USA*, 22(9), 2557–60.

Kaminsky, L. S., Mahoney, M. C., Leach, J., Melius, J., & Miller, M. J. (1990). Fluoride: Benefits and Risk of Exposure, *Oral Biology and Medicine*, 261-281(1).

Kaplan GA. (1996). People and places: contrasting perspectives on the association between social class and health. *Int J Health Services* 26:507-19.

Khandare, a L., Harikumar, R., & Sivakumar, B. (2005). Severe bone deformities in young children from vitamin D deficiency and fluorosis in Bihar-India. *Calcified tissue international*, 76(6), 412–8.

Kiritsy MC, Levy SM, Warren JJ, Guha-Chowdhury N, Heilman JR, Marshall T. (1996). Assessing fluoride concentrations of juices and juice-flavored drinks. *J Am Dent Assoc* 127:895-902.

Krishnamachari, K.A.V.R. (1987). Fluorine. *Trace Elem. Hum. Anim. Nutr.*, 1: 365–415.

- Krishnan S S, Mernagh J R, Hitchman A J W, McNeill K G, Harrison J E. (1985). Measurements of Fluoride in bone biopsies by neutron activation analysis for the clinical study of Osteoporosis. *Nuclear Chemistry*, 95(2), 119–125.
- Kurland E S, Schulman R C, Zerwekh J E, Reinus W R, Dempster D W, and Whyte M P. (2007). Case Report. *Journal of bone and mineral research*, 22(1), 163–170.
- Kurtio, P., Gustavsson, N., Vartiainen, T., & Pekkanen, J. (1999). Exposure to natural fluoride in well water and hip fracture: a cohort analysis in Finland. *American journal of epidemiology*, 150(8), 817–24.
- Levy, S.M., Chankanka, O. and Nair, R. (2006). A review of fluoride intake relevant to Canadian water fluoride discussions. Unpublished report. University of Iowa College of Dentistry, Iowa City, Iowa.
- Levy, S.M. (1994). Review of fluoride exposures and ingestion. *Community Dent. Oral Epidemiol.*, 22(3): 173–180.
- Li, Y., Liang, C., Slemenda, C. W., Ji, R., Sun, S., Cao, J., Emsley, C. L., et al. (2001). Effect of long-term exposure to fluoride in drinking water on risks of bone fractures. *Journal of bone and mineral research*, 16(5), 932–9.
- Limeback, H. (1999). A re-examination of the pre-eruptive and post-eruptive mechanism of the anti-caries effects of fluoride: is there any anti-caries benefit from swallowing fluoride? *Community dentistry and oral epidemiology*, 27(1), 62–71.
- Lindsay R. (1990). Fluoride and bone--quantity versus quality. *N Engl J Med.* 322:845-846.
- Ludlow M, Luxton G., and Mathew T. (2007). Effects of fluoridation of community water supplies for people with chronic kidney disease. *Nephrology, dialysis, transplantation*, 22(10), 2763–7.
- Lung, S.-C. C., Cheng, H.-W., & Fu, C. B. (2008). Potential exposure and risk of fluoride intakes from tea drinks produced in Taiwan. *Journal of exposure science & environmental epidemiology*, 18(2), 158–66.
- Lung, S.-C. C., Hsiao, P.-K., & Chiang, K.-M. (2003). Fluoride concentrations in three types of commercially packed tea drinks in Taiwan. *Journal of exposure analysis and environmental epidemiology*, 13(1), 66–73.
- McIvor, M.E. (1990). Acute fluoride toxicity: pathophysiology and management. *Drug Saf.*, 5: 79–85.

- Maguire, A., Moynihan, P.J. and Zohouri, V. (2004). Bioavailability of fluoride in drinking water—a human experimental study. Report for the United Kingdom Department of Health.
- Mamell N, Meunier PJ, Duson R, et al. (1988). Risk-benefit ratio of sodium fluoride treatment in primary vertebral osteoporosis. *Lancet*. 2:361-365.
- Mernagh, J. R., Hancock, R., & McNeill, K. G. (1977). Measurement of Fluoride in Bone, *International Journal of Applied Radiation and Isotops*, 28, 581–583.
- Nair, K. R., Manji, F. & Gitonga, J. N. (1984). The occurrence and distribution of fluoride in groundwaters of Kenya. Challenges in African Hydrology and Water Resources. Proceedings of the Harare Symposium. International Association of Hydrological Sciences Publication No. 144.
- NRC (1993). Health effects of ingested fluoride. Report of the Subcommittee on Health Effects of Ingested Fluoride, National Research Council. National Academy Press, Washington, DC.
- Parkins, F. M. Tinanoff, N. Moutinho, M. Anstey, M. B. and Waziri. M. H. (1974). Relationships of Human Plasma Fluoride and Bone Fluoride to Age. *Calcif. Tiss. Res.* 16, 335-338
- Pejović–Milić, A., Byun, S. H., Chettle, D. R., McNeill, F. E., & Prestwich W. V. (2006). Development of an irradiation / shielding cavity for in vivo neutron activation analysis of manganese in human bone. *Radioanalytical and Nuclear Chemistry*, 269(2), 417–420.
- Phipps KR. (1996). Fluoride. In: Ziegler EE, Filer LJ, Jr, Present knowledge in nutrition. 7th ed. Washington, DC: ILSI Press; p.329–33.
- Rao, G.S., (1984). Dietary intake and bioavailability of fluoride. *Ann. Rev. Nutr.*, 4: 115–136.
- Riggs BL, Hodgson SF, O'Fallon W, et al. (1990). Effect of fluoride treatment on the fracture rate in postmenopausal women with osteoporosis. *N EngI J Med.* 322:802-809.
- Rupal AV, Dhritigna RK, Krutika LB, Narasimhacharya AVRL (2010) Therapeutic benefits of glibenclamide in fluoride intoxicated diabetic rats. *Fluoride* 43(2):141–149.
- Richards, A, Mosekilde, L., & Sjøgaard, C. H. (1994). Normal age-related changes in fluoride content of vertebral trabecular bone--relation to bone quality. *Bone*, 15(1), 21–6.

- Saleh, M. A., Ewane, E., Jones, J., & Wilson, B. L. (2001). Chemical Evaluation of Commercial Bottled Drinking Water from Egypt. *Journal of Food Composition and Analysis*, 14(2), 127–152.
- Sampaio, F. C., Fehr, F. R. Von Der, & Gigante, D. P. (1999). Dental fluorosis and nutritional status of 6- to 11-year-old children ... *ProQuest Nursing & Allied Health Source*, 33(1), 66-73.
- Samudralwar, D. L., & Robertson, J. D. (1993). Determination of major and trace elements in bones by simultaneous PIXE/PIGE analysis. *Journal of Radioanalytical and Nuclear Chemistry Articles*, 169(1), 259–267.
- Sastri, C. S., Iyengar, V., Blondiaux, G., Tessier, Y., Petri, H., Hoffmann, P., Aras, N. K., et al. (2001). Fluorine determination in human and animal bones by particle-induced gamma-ray emission. *Fresenius' journal of analytical chemistry*, 370(7), 924–9.
- Shashi A (1992) Biochemical effects of fluoride on lipid metabolism in the reproductive organs of male rabbits. *Fluoride* 25:149–154.
- Shanthakumari D, Srinivasalu S, Subramanian S (2004) Effect of fluoride intoxication on lipid peroxidation and antioxidant status in experimental rats. *Toxicol* 204:219–228.
- Shivarajashankara YM, Shivashankara AR, Gopalakrishna BP, Rao HS (2003) Lipid peroxidation and antioxidant systems in the blood of young rats subjected to chronic Fluoride toxicity. *Indian J Exp Biol* 41:857–860.
- Shivashankara, A.R., Shankara, Y.M.S., Rao, S.H. and Bhat, P.G. (2000). A clinical and biochemical study of chronic fluoride toxicity in children of Kheru Thanda of Gulbarga district, Karnataka, India. *Fluoride*, 33: 66–73.
- Shulman, ER. and Vallejo, M. (1990). Effect of gastric contents on the bioavailability of fluoride in humans. *Pediatr. Dent.* Jul-Aug; 12(4): 237–240.
- Sidhu, K.S. and Kimmer, R.O. (2002). Fluoride overfeed at a well site near an elementary school in Michigan. *J. Environ. Health*, 65: 16–21, 38.
- Simard PL, Lachapelle D, Trahan L, Naccache H, Demers M, Brodeur JM. (1989). The ingestion of fluoride dentifrice by young children. *ASDC J Dent Child*.56:177–81.
- Slooff, W. (Eds.). (1988). *Basisdocument-uoriden*, Report no. 758474005. National Institute of Public Health and Environmental Protection, Bilthoven, Netherlands.
- Spencer, H., Lewin, I., Wistrowski, E. and Samachson, J. (1970). Fluoride metabolism in man. *Am. J. M ed.*, 49: 807–813.

- Spencer, H., Osis, D. and Lender, M. (1981). Studies of fluoride metabolism in man: a review and report of original data. *Sci. Total Environ.*, 17: 1–12.
- Susheela AK (2007). Fluorosis: Indian Scenario. In: A treatise on Fluorosis. Fluorosis Research and Rural Development Foundation, Delhi, India
- Shashi, A., Kumar, M., & Bhardwaj, M. (2008). Incidence of skeletal deformities in endemic fluorosis. *Tropical doctor*, 38(4), 231–3.
- Spencer, H., Osis, D., Wiatrowski, E., & Samachson, J. (1970). Availability of fluoride from fish protein concentrate and from sodium fluoride in man. *The Journal of nutrition*, 100(12), 1415–24.
- Suarez-Almazor, M. E., Flowerdew, G., Saunders, L. D., Soskolne, C. L., & Russell, A. S. (1993). The fluoridation of drinking water and hip fracture hospitalization rates in two Canadian communities. *American journal of public health*, 83(5), 689–93.
- Susheela, A. K., Bhatnagar, M., & Vig, K. (2005). EXCESS FLUORIDE INGESTION AND THYROID HORMONE DERANGEMENTS IN CHILDREN LIVING IN DELHI , INDIA, *International Society for Fluoride Research* , 38(2), 98–108.
- Tamer M N, Kale Koroğlu B, Arslan C, Akdoğan M, Koroğlu M, Cam H, Y. M. (2007). Osteosclerosis due to endemic fluorosis. *The Science of the total environment*, 373(1), 43–8.
- Tate, W.H. and Chan, J.T. (1994). Fluoride concentrations in bottled and filtered waters. *Gen. Dent.*, 42(4): 362–366.
- Tilley, D. R., Cheves, C. M., Kelley, J. H., Raman, S., & Weller, H. R. (1998). Energy levels of light nuclei. *Nucleonics*, 636, 249–364.
- Torra, M., Rodamilans, M., & Corbella, J. (1998). Serum and urine fluoride concentration: relationships to age, sex and renal function in a non-fluoridated population. *The Science of the total environment*, 220(1), 81–5.
- Trautner, K. and Einwag, J. (1989). Influence of milk and food on fluoride bioavailability from NaF and Na₂FPO₃ in man. *J. Dent. Res.* 68(1): 72–77.
- Turner, C H, Boivin, G., & Meunier, P. J. (1993). A mathematical model for fluoride uptake by the skeleton. *Calcified tissue international*, 52(2), 130–8.
- Turner, C.H., Hasegawa, K., Zhang, W., Wilson, M., Li, Y., & Dunipace, A. J. (1995). Fluoride Reduces Bone Strength in Older Rats. *Journal of Dental Research*, 74(8), 1475–1481.

- U.S. Environmental Protection Agency. (1985) ,Ambient water quality criteria 1984. U.S. EPA, Office Water Regulations and Standards, Washington, DC.
- Vasant, R. A, & Amaravadi V R L, N. (2013). A multigrain protein enriched diet mitigates fluoride toxicity. *Journal of food science and technology*, 50(3), 528–34. doi:10.1007/s13197-011-0367-3
- Vargas CM, Crall JJ, Schneider DA. (1998). Sociodemographic distribution of pediatric dental caries: NHANES III, 1988-1994. *J Am Dent Assoc* 129:1229-38
- Van Winkle, S., Levy, S.M., Kiritsy, M .C., Heilman, J.R., Wefel, J.S. and Marshall, T. (1995). Water and formula fluoride concentrations: significance for infants fed formula. *Pediatr. Dent.*, 17(4): 305–310.
- Villa, A., Anabalón, M. and Cabezas, L. (2000). The fractional urinary fluoride excretion in young children under stable fluoride intake conditions. *Community Dent. Oral Epidemiol.*, 28: 344–355.
- Wang W, Kong L, Zhao H, Dong R, Li J, et al. (2007). Thoracic ossification of ligamentum flavum caused by skeletal fluorosis. *European spine journal*, 16(8), 1119–28.
- Wang, X.C., Kawahara, K. and Glio, X.-J. (1999). Fluoride contamination of groundwater and its impacts on human health in Inner Mongolia area. *J. Water Supply Res. Technol. – Aqua*, 48: 146–153.
- Whelton, H. P., Ketley, C. E., McSweeney, F., & O’Mullane, D. M. (2004). A review of fluorosis in the European Union: prevalence, risk factors and aesthetic issues. *Community dentistry and oral epidemiology*, (5), 9–18.
- Whitford, G. M. (1994). Intake and Metabolism of Fluoride, *Advances in Dental Research*, 8(1),5-14.
- Whitford GM. (1989). The metabolism and toxicity of fluoride. Basel, Switzerland: Karger
- Whitford, G.M. (1990). The physiological and toxicological characteristics of fluoride. *J. Dent. Res.*, 69: 539–549.
- Whitford, G. (1996). The metabolism and toxicity of fluoride. 2nd rev. edition. Karger, Basel. 156 pp. (Monographs in Oral Science, Vol. 16).
- WHO (2003). The world oral health report 2003. Global Oral Health Programme, World Health Organization, Geneva. 38 pp.

WHO (2006). *Fluoride in Drinking Water*. London: IWA Publishing.

Whyte, M .P., Essmyer, K., Gannon, F.H. and Reinus, W.R. (2005). Skeletal fluorosis and instant tea. *Am. J. Med.*, 118: 78–82.

Wilson, J. (1993). Endemic Skeleton : Patients Fluorosis Radiographic of the Features. *American Roentgen Ray Society*, 94-98.

Woodard, H. Q. (1964). The Composition of Human Cortical Bone. *Clinical orthopaedics and related research*, 37, 187–193.

Wright, J. A, Cronin, A., Okotto-Okotto, J., Yang, H., Pedley, S., & Gundry, S. W. (2013). A spatial analysis of pit latrine density and groundwater source contamination. *Environmental monitoring and assessment*, 185(5), 4261–72.

Yadav A K, Kaushik C P, Haritash A K, Singh B, Raghuvanshi S P, K. A. (2007). Determination of exposure and probable ingestion of fluoride through tea, toothpaste, tobacco and pan masala. *Journal of hazardous materials*, 142(1-2), 77–80.

Yildiz, M., Akdoğan, M., Tamer, N., & Oral, B. (2003). Bone mineral density of the spine and femur in early postmenopausal Turkish women with endemic skeletal fluorosis. *Calcified tissue international*, 72(6), 689–93.

Zipkin, I., McCaps, F. J., & Lee, W. A. (1960). Relation of the fluoride content of human bone to its chemical composition. *Archives of oral biology*, 2, 190–5.

Zohouri, F.V. and Rugg-Gunn, A.J. (2000). Total fluoride intake and urinary excretion in 4-year-old Iranian children residing in low-fluoride areas. *Br. J. Nutr.*, 83: 15–25.